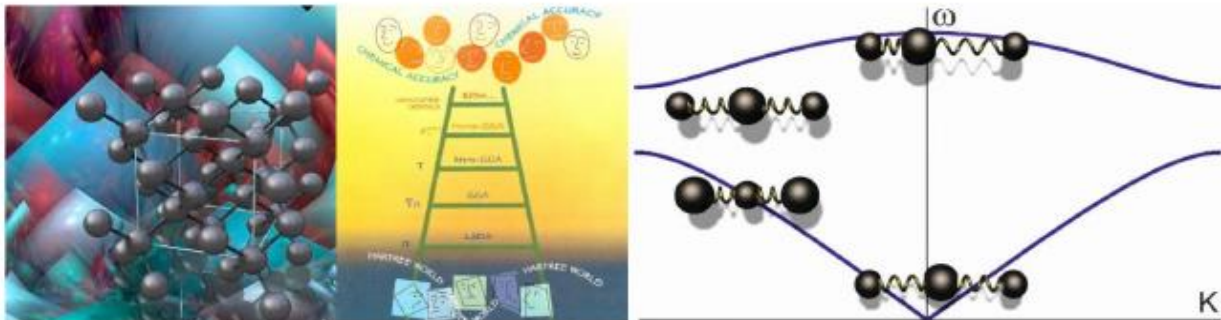


Skoltech

Skolkovo Institute of Science and Technology



Advanced Materials Modeling

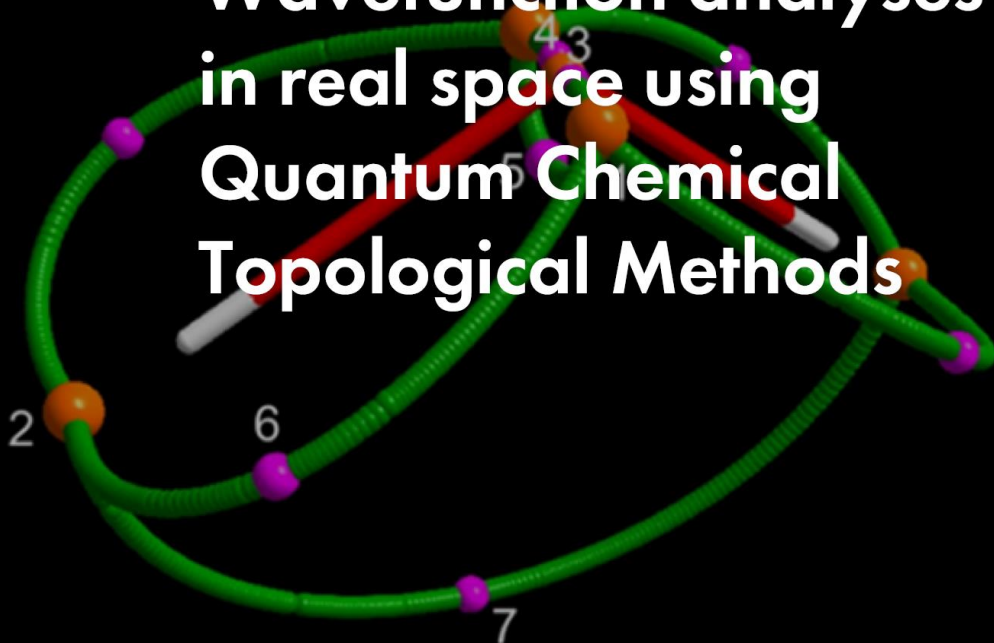
Carlo Gatti

CNR-SCITEC, Istituto di Scienze e Tecnologie
Chimiche, "Giulio Natta", Milano, Italy

Seminar
May 20
17:00

Online

Wavefunction analyses in real space using Quantum Chemical Topological Methods



Consiglio Nazionale
delle Ricerche





~ 100 researchers

CNR-SCITEC, Istituto di Scienze e Tecnologie Chimiche «Giulio Natta»



CHIMICA
VERDE



CHIMICA
PER
L'ENERGIA



CHIMICA E
SALUTE



MATERIALI
AVANZATI



CHIMICA
PER I BENI
CULTURALI



CHIMICA
COMPUTA-
ZIONALE



Milano, 73

Roma, 9



Perugia, 10

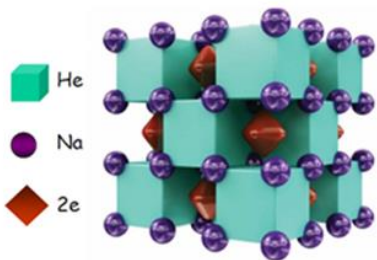
Genova, 6



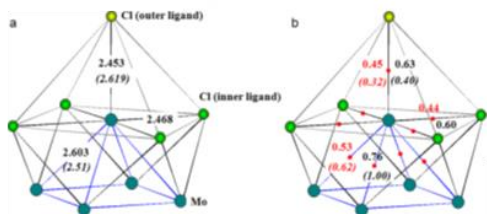
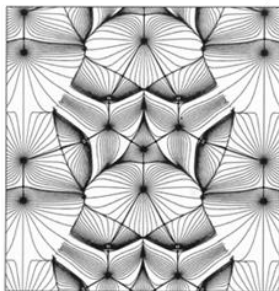


Carlo Gatti

A.R. Oganov,
Skoltech Institute
Moscow, Russia



S. Casassa, B. Civalleri, A.
Erba Univ. Torino, Italy



My general expertise

Chemical bonding

High pressure evolution of structure and bonding

Li, Na batteries
Organic electrodes;
Phase-change materials

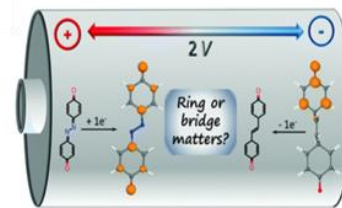
Molecular Recognition in HPLC

New Chemical descriptors:
SF for SD, EP,
SD topology

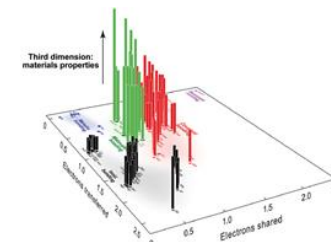
Modern Pauling's Bond Valence Model
Me-Me bonds

E. Levi, D. Aurbach
Bar-Ilan University, Israel

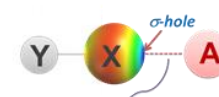
B.B. Iversen, CMC project,
Aarhus Univ. Denmark



C. Frayret, Jules Verne
Univ. Amiens, France

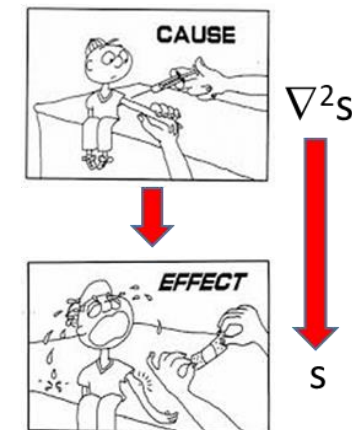
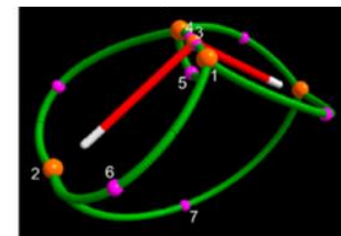
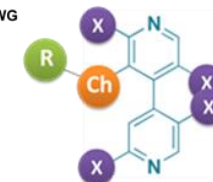


M. Wuttig, RWTH,
Aachen, Germany



A = Lewis base (O, N, S, halogen, π -donor, anion); Y = EWG

P. Peluso, CNR-ICB,
Sassari, Italy
V. Mamane,
Strasbourg University
France



Outline

- Retrieving chemical bonding information from the wf: compresses the information contained in the wf by using its probabilistic interpretation ➡ reduced densities
- Bond descriptors from reduced densities (ρ and related quantities; first and second order matrices)
- How to analyse reduced densities. Pros and cons of deformation densities ➡ **topology**
- The theory of *Gradient dynamical systems* ➡ partitioning of the molecular space ➡ topological features/study of the scalar associated to the gradient field
- QTAIM as a specific very important case (topological basin ➡ topological atom ↔ quantum atom)
- Some important hints on QTAIM chemical bonding classification and on the use of the density Laplacian
- Didactic example on the use of QTAIM to detect packing effects (urea crystal)



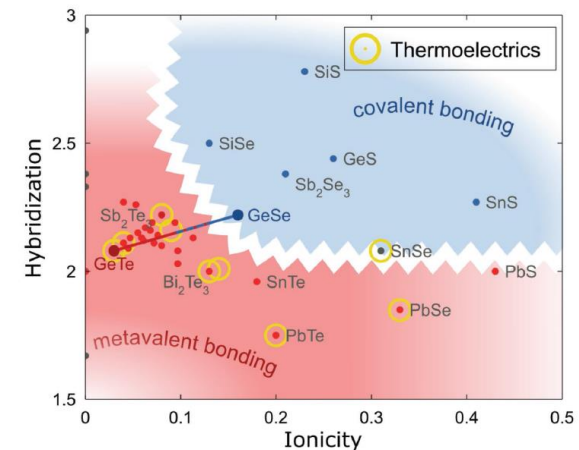
- Spin density topology
- Electrostatic potential Source Function (applied to enantioseparation outcome in HPLC)
- Do the peculiar physical properties of phase change materials entail unusual chemical bonding features? (LI and DI application)

Why retrieving chemical (bonding) information from the model wavefunction of a material? (or, in general, of any investigated system of some fundamental and/or practical interest?)

- Thoughtful searches for more and more performing materials or of materials with novel properties and functions require a profound understanding of their structure-property relationships
- The detailed knowledge of the **structure** of a material, either through experimental and/or *in silico* approaches, is a necessary and fundamental prerequisite for its study.
- Yet the geometrical, electronic and (magnetic) structure of a material is ultimately related to its **chemical bonding features**, which are just a function of its chemical composition/stoichiometry, and of external constraints (applied P, T and external fields)

Material's properties are determined by **chemical bonding**

GeSe: orthorhombic, **poor** thermoelectrics \Rightarrow covalent bonding (2c-2e)
GeTe: almost cubic, **good** thermoelectrics \Rightarrow *metavalent* bonding (1c-2e)

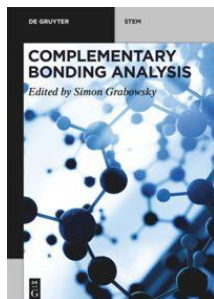


How retrieving chemical (bonding) information from wavefunctions?

The amount of information stored in a wavefunction becomes soon so large with increasing number of electrons that it escapes human comprehension → an information compression technique is needed
Vleck JHV. Phys Rev. 1932;49:232

Two main strategies:

- ❑ **A.** Take advantage of the models/approximations used to solve Schrödinger's equation. In HF, e.g., ψ is written as a Single Determinant (SD) constructed from one-electron functions or orbitals ϕ → mean-field (MF) approach: e^- move in the average potential created by the rest of the particles (e^- and n) of the system → Knowledge and manipulation of the N (number of e^-) 3D ϕ of a system is much easier than that of the full wf. However, this simplification **comes at the expense of several problems and caveats:** (a) ψ is invariant to unitary transformations of orbitals → orbital interpretations are method (MO, VB, etc.) dependent; (b) when the MF is abandoned and electron correlation is taken into account, the pristine SD orbital concept vanishes and (MC approaches) many more than N partially occupied functions appear
- ❑ **B.** compress the information contained in the wavefunction by using its probabilistic interpretation



Ángel Martín Pendás and Carlo Gatti,
Chapter 3: Quantum theory of atoms in molecules and the AIMAll software in *Complementary Bonding Analysis*, S. Grabowsky Ed, De Gruyter 2021



G. Saleh, D. Ceresoli, G. Macetti and C. Gatti*,
Chapter 5: Chemical Bonding Investigations for Materials, in *Computational Materials Discovery*, A.R. Oganov, G. Saleh, A.G. Kvashnin Eds., RSC 2019

From wavefunctions to chemical bond descriptors

Forget about the behavior of all e^- but 1 or 2 and get the density of finding e^- or e^- pairs at given positions of R^3 or R^6 . These **reduced densities** are QM observables (experimentally accessed in principle), invariant under orbital transformations  do not depend on models of computational methods, and have clear-cut interpretations

$$\Psi_{el}(\mathbf{r}, \mathbf{r}_2, \dots, \mathbf{r}_N; \mathbf{R})$$

System of N_{el} and M nuclei; Ψ_{el} : stationary *wf* for fixed nuclear space coordinates (BO approx.) \mathbf{R} : ensemble of nuclear coordinates for the M nuclei

$$\Psi_{el}(\mathbf{r}_1, \mathbf{r}_2, \dots, \mathbf{r}_N; \mathbf{R}) \cdot \Psi_{el}^*(\mathbf{r}_1, \mathbf{r}_2, \dots, \mathbf{r}_N; \mathbf{R}) d\mathbf{r}_1 d\mathbf{r}_2, \dots, d\mathbf{r}_N$$

Born's interpretation of the *wf*

$$\rho(\mathbf{r}_1) d\mathbf{r}_1$$

probability of finding any of its electrons at \mathbf{r}_1 regardless of the exact position of the other e^-

where the corresponding *probability density* is the *position electron density* (ED) $\rho(\mathbf{r})$

$$\rho(\mathbf{r}) = N \int \Psi_{el}(\mathbf{r}, \mathbf{r}_2, \dots, \mathbf{r}_N; \mathbf{R}) \cdot \Psi_{el}^*(\mathbf{r}, \mathbf{r}_2, \dots, \mathbf{r}_N; \mathbf{R}) d\mathbf{r}_2, \dots, d\mathbf{r}_N$$

Density matrices are a convenient mathematical device for evaluating the expectation values of operators corresponding to physical observables, $\langle \Psi_{el} | O | \Psi_{el} \rangle$

$$\gamma_p(\mathbf{r}_1 \mathbf{r}_2 \dots \mathbf{r}_p; \mathbf{r}'_1 \mathbf{r}'_2 \dots \mathbf{r}'_p) = \binom{N}{p} \int \Psi_{el}(\mathbf{r}_1 \mathbf{r}_2 \dots \mathbf{r}_p \mathbf{r}_{p+1} \dots \mathbf{r}_n) \Psi_{el}^*(\mathbf{r}'_1 \mathbf{r}'_2 \dots \mathbf{r}'_p \mathbf{r}'_{p+1} \dots \mathbf{r}'_n) d\mathbf{r}_{p+1} \dots d\mathbf{r}_n$$

A numerical value is assigned to γ_p by two sets of indices. γ_p may be seen as an element of a matrix and $\gamma_p(\{\mathbf{r}\}; \{\mathbf{r}'\})$ as the corresponding matrix with infinite elements. The diagonal elements ($\mathbf{r}_1 \equiv \mathbf{r}'_1$) of this matrix, correspond to the probability of finding p electrons with given space coordinates and regardless of those of the remaining $(N-p)$ electrons. This is a p -particles density, motivating why $\gamma_p(\{\mathbf{r}\}; \{\mathbf{r}'\})$ is called a *density matrix*

$\binom{N}{p}$ is a binomial coefficient ensuring proper normalization

$$\gamma_2(\mathbf{r}_1 \mathbf{r}_2; \mathbf{r}'_1 \mathbf{r}'_2) = \frac{N(N-1)}{2} \int \Psi_{el}(\mathbf{r}_1 \mathbf{r}_2 \mathbf{r}_3 \dots \mathbf{r}_n) \Psi_{el}^*(\mathbf{r}'_1 \mathbf{r}'_2 \mathbf{r}'_3 \dots \mathbf{r}'_n) d\mathbf{r}_3 \dots d\mathbf{r}_n$$

$$\gamma_1(\mathbf{r}_1; \mathbf{r}'_1) = N \int \Psi_{el}(\mathbf{r}_1 \mathbf{r}_2 \dots \mathbf{r}_n) \Psi_{el}^*(\mathbf{r}'_1 \mathbf{r}'_2 \dots \mathbf{r}'_n) d\mathbf{r}_2 \dots d\mathbf{r}_n$$

Since only one- and two-body interactions take place among electrons, we need just γ_1 and γ_2

$$\gamma_1(\mathbf{r}_1; \mathbf{r}'_1) = N \int \psi_{el}(\mathbf{r}_1 \mathbf{r}_2 \dots \mathbf{r}_n) \psi_{el}^*(\mathbf{r}'_1 \mathbf{r}'_2 \dots \mathbf{r}'_n) d\mathbf{r}_2 \dots d\mathbf{r}_n$$

First order density matrix (DM)

$$\gamma_2(\mathbf{r}_1 \mathbf{r}_2; \mathbf{r}'_1 \mathbf{r}'_2) = \frac{N(N-1)}{2} \int \psi_{el}(\mathbf{r}_1 \mathbf{r}_2 \mathbf{r}_3 \dots \mathbf{r}_n) \psi_{el}^*(\mathbf{r}'_1 \mathbf{r}'_2 \mathbf{r}'_3 \dots \mathbf{r}'_n) d\mathbf{r}_3 \dots d\mathbf{r}_n$$

Second order DM

The expectation value of any one- and two-electron operators may be expressed as

$$\langle \hat{O}_1 \rangle = \left\langle \sum_i^N O_1(\mathbf{r}_i) \right\rangle = \int_{\mathbf{r}_1 = \mathbf{r}'_1} O_1(\mathbf{r}_1) \gamma_1(\mathbf{r}_1; \mathbf{r}'_1) d\mathbf{r}_1$$

$$\langle \hat{O}_2 \rangle = \left\langle \sum_{i,j}^N O_2(\mathbf{r}_i \mathbf{r}_j) \right\rangle = \int_{\mathbf{r}_1 = \mathbf{r}'_1; \mathbf{r}_2 = \mathbf{r}'_2} O_2(\mathbf{r}_1 \mathbf{r}_2) \gamma_2(\mathbf{r}_1 \mathbf{r}_2; \mathbf{r}'_1 \mathbf{r}'_2) d\mathbf{r}_1 d\mathbf{r}_2$$

using the convention that the operators act only on functions of the unprimed variables and that \mathbf{r}' is put equal to \mathbf{r} after operating with the operators but before completing the integration

All 1-electron and all 2-electron properties may be obtained from the first and second order DMs

From wavefunctions to chemical bond descriptors

$$\Psi_{el}(\mathbf{r}, \mathbf{r}_2, \dots, \mathbf{r}_N; \mathbf{R})$$

$$\gamma_1(\mathbf{r} = \mathbf{r}') \equiv \rho(\mathbf{r}) \quad \rho(\mathbf{r}) = N \int \Psi_{el}(\mathbf{r}, \mathbf{r}_2, \dots, \mathbf{r}_N; \mathbf{R}) \cdot \Psi_{el}^*(\mathbf{r}, \mathbf{r}_2, \dots, \mathbf{r}_N; \mathbf{R}) d\mathbf{r}_2, \dots, d\mathbf{r}_N$$

Derived from the ED ρ :

$\rho, \nabla^2 \rho$, ESP, EF, SF, RDG, etc.

SF Source Function; ESP Electrostatic Potential; EF Electric Field, RDG Reduced Density Gradient

$$\gamma_1(\mathbf{r}_1; \mathbf{r}'_1) = N \int \Psi_{el}(\mathbf{r}_1 \mathbf{r}_2 \dots \mathbf{r}_n) \Psi_{el}^*(\mathbf{r}'_1 \mathbf{r}'_2 \dots \mathbf{r}'_n) d\mathbf{r}_2 \dots d\mathbf{r}_n$$

Derived from $\gamma_1(\mathbf{r}_1; \mathbf{r}'_1)$:

G, V, H, LOL, ELF, etc.

G, V, H : kinetic, potential and energy densities, ELF : Electron Localization Function

Derived from $\gamma_2(\mathbf{r}_1 \mathbf{r}_2; \mathbf{r}'_1 \mathbf{r}'_2)$:

$$\rho_2(\mathbf{r}_1, \mathbf{r}_2) \equiv \gamma_2(\mathbf{r}_1, \mathbf{r}_2; \mathbf{r}_1, \mathbf{r}_2)$$

$\rho_2(\mathbf{r}_1, \mathbf{r}_2)$ Pair density

LI, DI, DAFH, ELI's family...

LI/DI: local/deloc indices; DAFH
Domain Average Fermi Hole, ELI,
Electron Localizability Indicators

From wavefunctions to chemical bond descriptors: LI and DI

$\rho_2(\mathbf{r}_1, \mathbf{r}_2) \equiv \gamma_2(\mathbf{r}_1, \mathbf{r}_2; \mathbf{r}_1, \mathbf{r}_2)$ Pair Density : all information on the correlated motion of electrons

$$\rho_2(\mathbf{r}_1, \mathbf{r}_2) = \frac{1}{2}[\rho(\mathbf{r}_1)\rho(\mathbf{r}_2) - \rho_{2,xc}(\mathbf{r}_1, \mathbf{r}_2)]$$

LI, DI, DAFH, ELI's family...

$$\rho_{2,xc}(\mathbf{r}_1, \mathbf{r}_2)$$

It is the so called *exchange-correlation density*, which incorporates all non classical effects and measures to which degree the density is excluded at \mathbf{r}_2 because of the presence of an electron at \mathbf{r}_1 .

$\rho_{2,xc}(\mathbf{r}_1, \mathbf{r}_2)$ integrates to N, so that integration of $\rho_2(\mathbf{r}_1, \mathbf{r}_2)$, $\frac{1}{2}(N^2 - N) = \frac{1}{2} N(N-1)$, yields the total number of distinct pairs, $\frac{1}{2} N(N-1)$

The probability of finding one electron at \mathbf{r}_1 and another one at \mathbf{r}_2 deviates from the purely classical description of a product of independent EDs because of Coulomb and Fermi correlation of e^- motions

$$\lambda(A) = \int \int_A \rho_{2,xc}(\mathbf{r}_1, \mathbf{r}_2) d\mathbf{r}_1 d\mathbf{r}_2$$

$\lambda(A)$ Electron localization index, **LI**

$$\delta(A, B) = 2 \cdot \int \int_{A B} \rho_{2,xc}(\mathbf{r}_1, \mathbf{r}_2) d\mathbf{r}_1 d\mathbf{r}_2$$

$\delta(A, B)$ Electron delocalization index, **DI**

A and B are "atomic" basins (to be defined)

$$N(A) = \lambda(A) + \frac{1}{2} \sum_{B \neq A} \delta(A, B)$$

Source of information

Coherent elastic

$$\rho(\mathbf{r}) \equiv \rho_1(\mathbf{r}, \mathbf{r}) \longrightarrow \nabla^2 \rho, \text{ESP, EF, SF, RDG, etc.}$$

Only indirect information on electron correlation

C. Gatti, PJ Mac Dougall and RFW Bader, Effect of electron correlation on the topological properties of molecular charge distributions, *J. Chem. Phys.* 88, 3792 (1988)

wavefunction & inelastic scattering

$$\rho_1(\mathbf{r}, \mathbf{r}') \longrightarrow G(\mathbf{r}), V(\mathbf{r}), H(\mathbf{r}), \text{LOL, ELF,}$$

$$\rho_2(\mathbf{r}_1, \mathbf{r}_2) \equiv \rho_2(\mathbf{r}_1, \mathbf{r}_2; \mathbf{r}_1, \mathbf{r}_2)$$

Pair Density : all information on the correlated motion of electrons

$$\rho_2(\mathbf{r}_1, \mathbf{r}_2) = \frac{1}{2}[\rho(\mathbf{r}_1)\rho(\mathbf{r}_2) - \rho_{2,xc}(\mathbf{r}_1, \mathbf{r}_2)]$$

$$\lambda(A) = \int_A \int_A \rho_{2,xc}(\mathbf{r}_1, \mathbf{r}_2) d\mathbf{r}_1 d\mathbf{r}_2 \quad \text{Electron localization index, LI}$$

$$\delta(A, B) = 2 \cdot \int_A \int_B \rho_{2,xc}(\mathbf{r}_1, \mathbf{r}_2) d\mathbf{r}_1 d\mathbf{r}_2 \quad \delta(A, B) \text{ Electron delocalization index, DI}$$

$$\%loc(A) = [\lambda(A)/N(A)] \cdot 100$$

$$\%deloc(A) = \sum_{A \neq B} [0.5 \cdot \delta(A, B)/N(A)] \cdot 100$$

How to analyse reduced densities

- Reduced densities, are dominated by the nuclear positions

It was thus clear from the beginning that a theory of chemical bonding based on electron densities (or functions derived thereof) should focus on density differences, i.e. on how electrons redistribute in chemical processes



$$\Delta\rho = \rho - \rho_{\text{ref}}$$

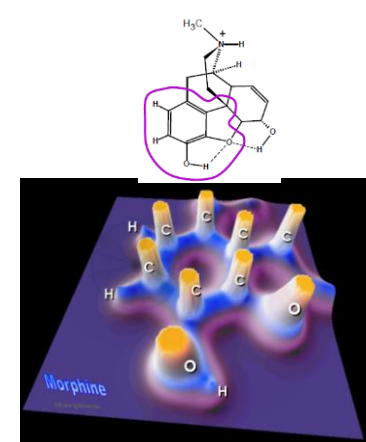
- Yet, the "arbitrary choice of the reference density can completely alter the interpretation



- Analyse the density **itself**



- Examine its **topology**. If we want to study the behavior of a scalar function without recourse to an external reference, only its value and that of its derivatives are available (Paul Mezey).



CF Matta, HDR thesis,
Nancy 2009

Deformation densities: pros and cons

$$\Delta\rho(\mathbf{r}; \mathbf{X}) = \rho(\mathbf{r}; \mathbf{X}) - \rho_{\text{ref}}(\mathbf{r}; \mathbf{X})$$

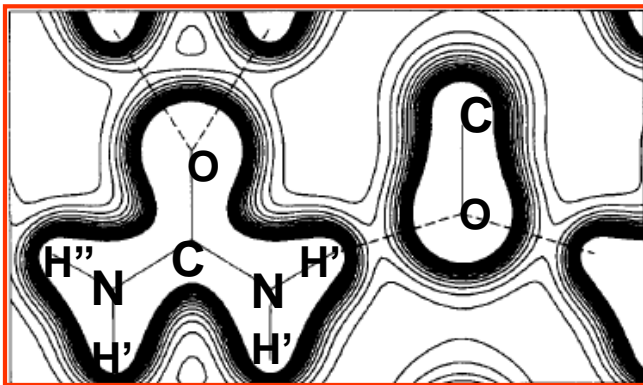
$\Delta\rho$ standard deformation electron density

ρ total electron density, either ρ_{th} or $\rho_{\text{exp,MM,static}}$

ρ_{R} reference density

molecules → promolecular density
crystals → procystal density

$\rho_{\text{ref}} = \sum_{\text{atoms}} \rho_{\text{a}}(\mathbf{r}-\mathbf{R}_{\text{a}})$ where ρ_{a} is the ground state spherically averaged atomic electron density

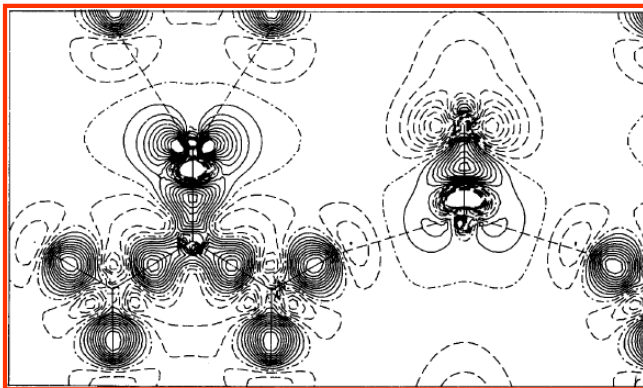


Total electron density

ρ , urea crystal

0.01 au contour intervals

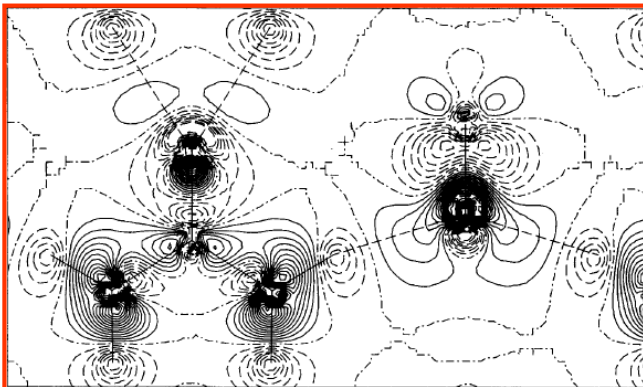
Dovesi et al., JCP 92, 7402 (1990)



Deformation electron density

$\Delta\rho$ (bulk minus atoms)

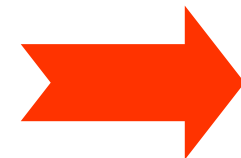
0.01 au cont. int.



Interaction electron density

$\Delta\rho$ (bulk minus molecular superposition) **0.002** au cont. int.

Useful! Yet DD may have
serious drawbacks.....

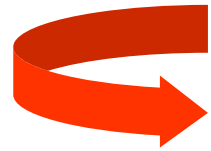
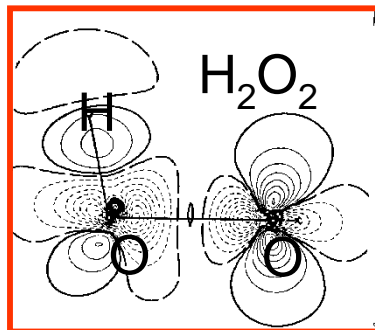
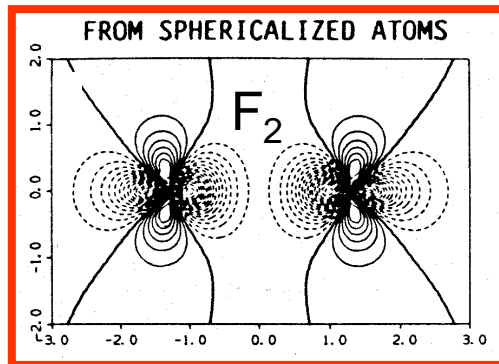


■ $\rho_{\text{ref}}(\mathbf{r}; \mathbf{X})$ is a non physical quantity: the antisymmetry requirement is only fulfilled separately by each ρ_a

■ $\rho_{\text{ref}}(\mathbf{r}; \mathbf{X})$ is not unique

In the case of an atom with spatially degenerate or nearly degenerate GS (e.g. atoms with an open valence shell, like B, C, O or F) many alternative ρ_a may be chosen.

$\Delta\rho$

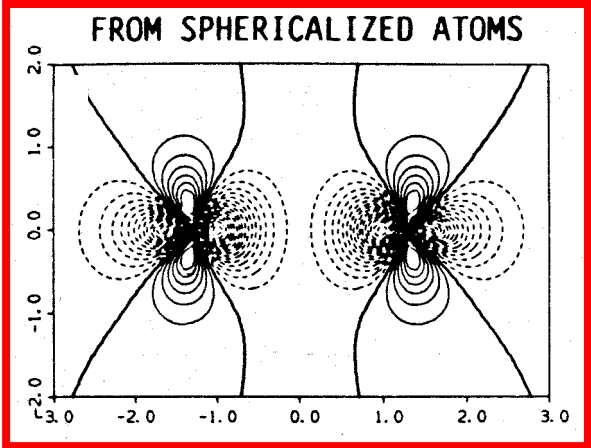
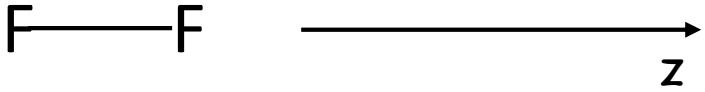


Orientational freedom exists for degenerate atomic GSs

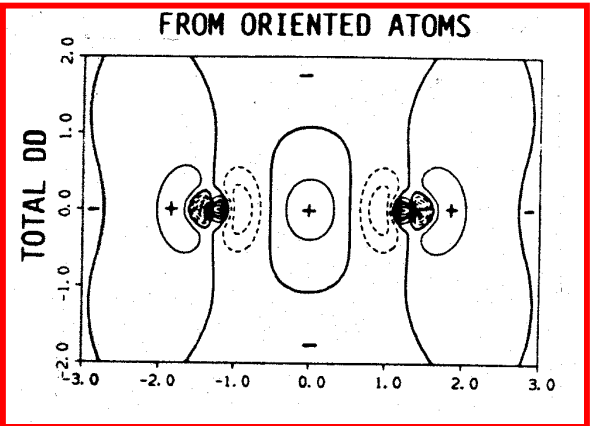
The spherically averaged density might not be the best reference choice to give insight on the way an atom is bonded to other atoms

Some covalent bonds do not show the expected accumulation of the electron density along the internuclear axis

$\Delta\rho$ in F_2

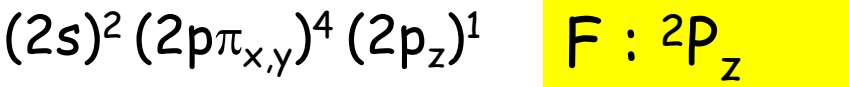


..... Depletion; interval 0.04 au
 ——— Accumulation

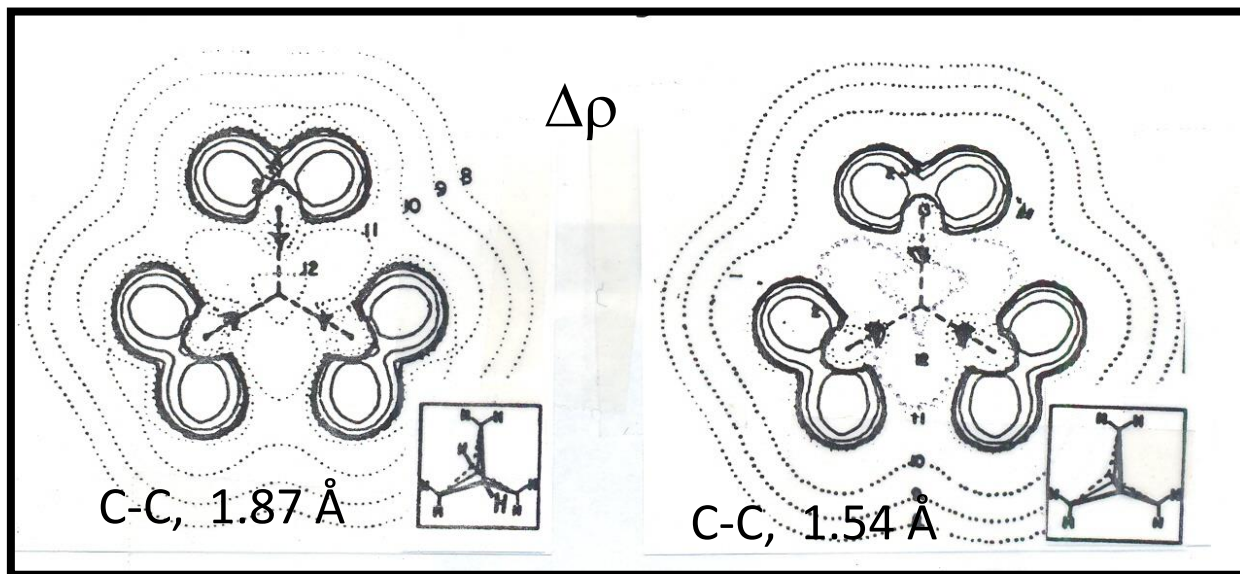


$2p_\sigma : 5/3 e^-$ for each F
 $10/3 e^-$ in the promolecule
 $2p_\sigma$ M.O. $2e^-$ in the molecule
 $2 - 10/3 e^- = -4/3 e^-$

In the p_σ region there are globally $4/3 e^-$ less than for the promolecule \longrightarrow depletion in the internuclear region (typical behaviour for atoms with more than half-filled valence shells)



$2 - 2 e^- = 0 e^- \longrightarrow$ accumulation and depletion along z ($\Delta\rho_b=0.05$ au; $\Delta\rho_{\text{lone pair maximum}}=0.07$ au)

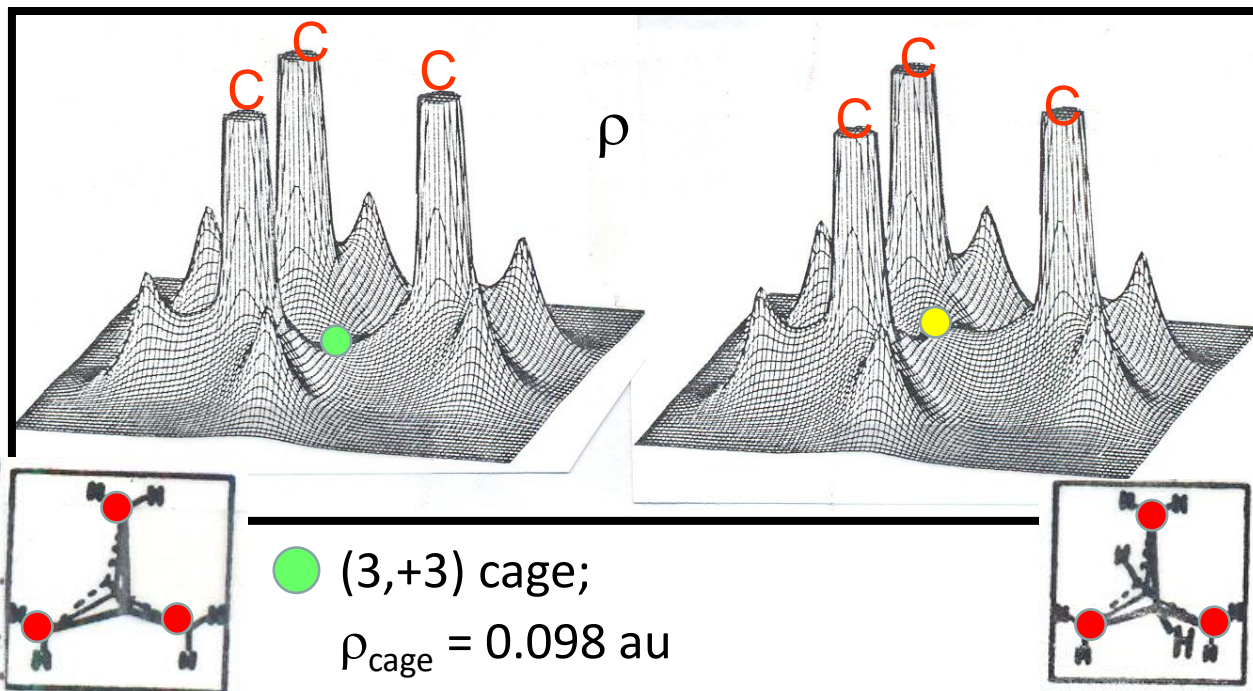


Bicyclo [1.1.1] pentane

1.1.1 propellane

$\Delta\rho$ and total ρ in strained hydrocarbons

Jackson J, Allen, LC
JACS, 106, 591 (1984)



● (3,+3) cage;
 $\rho_{\text{cage}} = 0.098 \text{ au}$

Wiberg KB, Bader RWF et al., JACS, 109, 985 (1987)

● (3,-1) saddle;

$\rho_b = 0.203 \text{ au} \cong 4/5$ of a normal CC bond
(in this plane is a local maximum)

The theory of gradient dynamical systems and scalar field topology

R. H. Abraham, C. D. Shaw *Dynamics: The Geometry of Behavior*; Addison Wesley: Redwood City, CA, 1992; (b) R. H. Abraham, J. E. Marsden, *Foundations of Mechanics*, Addison Wesley: Redwood City, CA, 1994.

□ \mathbf{y} differentiable vector field

Let's introduce a fictitious time coordinate t and the system of equations

$$d\mathbf{r}/dt = \mathbf{y} \quad (\text{this trick transforms the field into a } \textit{gradient dynamical system})$$

□ Solution of this system of equations defines the **trajectories or field lines** of $\mathbf{r}(t)$ and the **theory of dynamical systems** allows us to fully classify their properties

□ Let's turn to R^3 and take a scalar function f (carrying the physical or chemical information, for instance it may be the ED, the ELF, etc) and define an associated vector field through its gradient ∇f

$$d\mathbf{r}/dt = \nabla f$$

an explicit form for the field (or flux) lines of the gradient field is given by:

$$\mathbf{r}(t) = \mathbf{r}(t_0) + \int_{t_0}^t \nabla f(\mathbf{r}(s)) ds$$

which is simply interpreted as a temporal movement guided by the gradient field ∇f at the position reached at the (fictitious) time t

$$\mathbf{r}(t) = \mathbf{r}(t_0) + \int_{t_0}^t \nabla f(\mathbf{r}(s)) ds$$

- ❑ Except that at special points (Critical Points, CPs)
 - a) Only one gradient line passes through each point \mathbf{r}
 - b) ∇f is tangent to the trajectory at every point
 - c) the trajectories are orthogonal to isoscalar surfaces of the field at any point
- ❑ every line must begin and end where $\nabla f(\mathbf{r}) = 0$. All other points are *wandering* points
- ❑ The points \mathbf{r}_c where $\nabla f(\mathbf{r}_c) = 0$ are the so called Critical Points (CPs) of the field f . Their number and properties characterize its global structure (**or topology**)
- ❑ CPs are classified in terms of rank and signature

Hessian matrix $H(\mathbf{r}_c) = \begin{bmatrix} \frac{\partial f(\mathbf{r}_c)}{\partial x^2} & \dots & \frac{\partial f(\mathbf{r}_c)}{\partial x \partial z} \\ \vdots & \ddots & \vdots \\ \frac{\partial f(\mathbf{r}_c)}{\partial z \partial x} & \dots & \frac{\partial f(\mathbf{r}_c)}{\partial z^2} \end{bmatrix}$ H Diagonalization \longrightarrow Eigenvalues λ_i Eigenvectors \mathbf{v}_i ($i=1,3$)

CP(**RANK**, **SIGNATURE**)

RANK: number of non zero λ_i **SIGNATURE:** difference between the number of positive and negative curvatures λ_i

NON DEGENERATE CPs : (**3**, **-3**), (**3**, **-1**), (**3**, **+1**) and (**3**, **+3**)

□ Behaviour of the trajectories of the field along each eigendirection v_i depends on the sign of its associated λ_i value. Either they start or end at the CP when $\text{sgn } \lambda_i$ is positive or negative, respectively

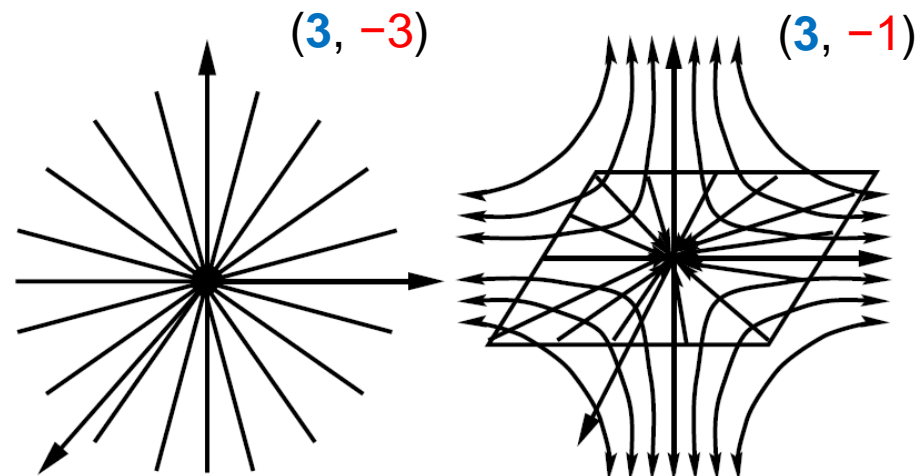
□ Ordering λ_i such that $\lambda_1 \leq \lambda_2 \leq \lambda_3$:

a) all $\lambda_i < 0$, $(\mathbf{3}, -\mathbf{3})$ *sink or attractor*: all trajectories converge toward the CP

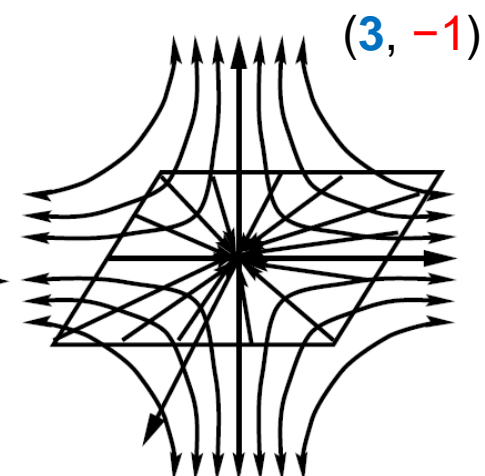
b) λ_1 and $\lambda_2 < 0$, $\lambda_3 > 0$, $(\mathbf{3}, -\mathbf{1})$ *saddle point of the first kind*; in the plane defined by v_1 and v_2 the gradient lines approach the CP, in the orthogonal direction v_3 direction escape from it

c) $\lambda_1 < 0$, λ_2 and $\lambda_3 > 0$, $(\mathbf{3}, +\mathbf{1})$ *saddle point of the second kind*; in the plane defined by v_2 and v_3 the gradient lines escape from the CP, while approach the CP in the orthogonal direction v_1

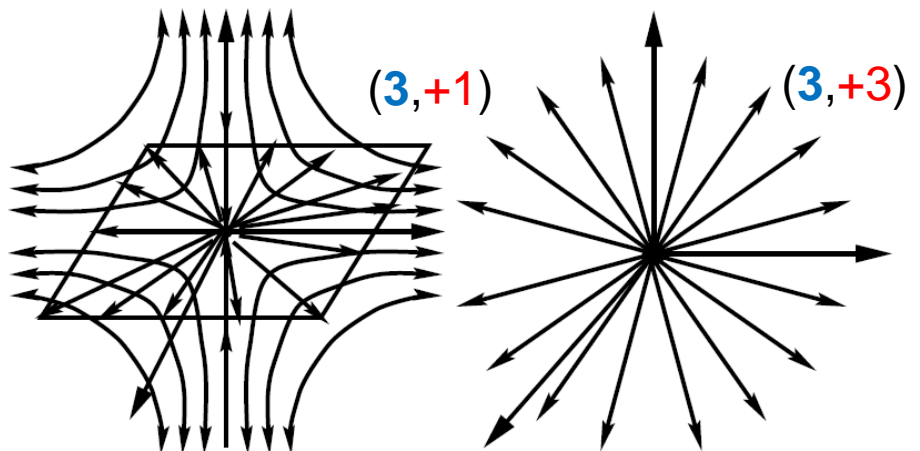
d) all $\lambda_i > 0$, $(\mathbf{3}, +\mathbf{3})$ *source or repellor*: every field line escapes the CP in all directions



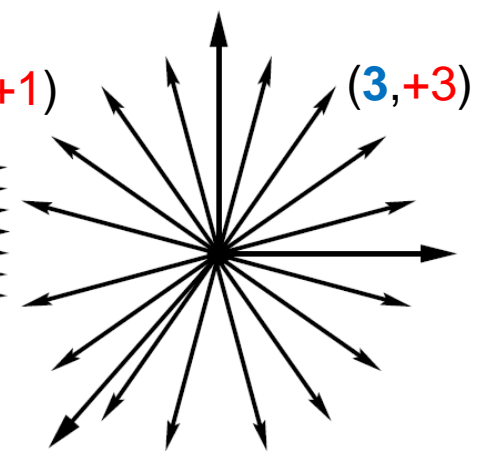
(a) Sink critical point



(b) Saddle of the first kind.



(c) Saddle of the second kind.



(d) Source.

Figure 3.1: The four types of CPs of a 3D scalar field.

□ Either the attraction basins of the (3,-3) CPs or the repulsion basins of the (3,+3) CPs are 3D regions. So, e.g., the union of all the (3,-3) attraction basins of the field is the full R^3 space, except a null measure set formed by the 2D surfaces or 1D lines which correspond to the attraction basins of the other CPs.

□ The attraction (or repulsion) basins of a field induce a topology in R^3 , i.e. an exhaustive partition into disjoint regions

$$R^3 \equiv \bigcup_A \Omega_A \quad , \quad A \text{ runs over all the attraction (repulsion) basins}$$

□ Surfaces that separate the basins are called separatrices. At all their points ∇f is parallel to the surface, so :

$$\text{Separatrices are local zero-flux surfaces of } \nabla f: \quad \nabla f(\mathbf{r}_s) \cdot \mathbf{n}_s = 0$$

□ The theory of gradient dynamical systems leads to a space partitioning analogous to the well-known partition made in hydrology in river basins delimited by watersheds.

□ In our case the space is that of an *in vacuo* system or of the unit cell of a periodic system.



- ❑ Number and type of CPs of a given scalar field is limited through topological invariants, which depend only on the intrinsic properties of the space in which the field is defined
- ❑ In R^3 , the space where we embed finite molecules, the Euler-Poincaré or Morse invariant (Morse M. Trans Am Math Soc. 1931;33:72–91) reads:

$$n(3,-3) - m(3,-1) + i(3,+1) - k(3,+3) = 1$$

(n, m, i, k, being the number of CPs with signatures -3, -1,+1 and +3)

- ❑ For 3D periodic systems (e.g. crystal), the space in which the unit cell is embedded is not R^3 , but a 3D torus, S^3 , since each spatial direction is equivalent to a closed line or circumference. The invariant (Morse relations) reads:

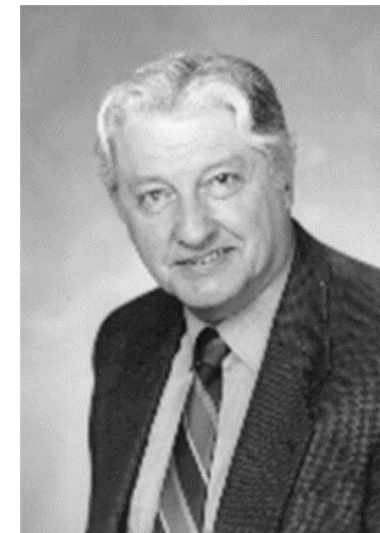
$$n(3,-3) - m(3,-1) + i(3,+1) - k(3,+3) = 0$$

- ❑ Those Wyckoff positions of the space group that have three fixed coordinates must contain a critical point of the crystal structure (For more details see: C. K. Johnson, M.M. Burnett and W. D. Dunbar, “Crystallographic Topology and Its Applications <https://digital.library.unt.edu/ark:/67531/metadc675925/> and A. Martín Pendás, A. Costales, V. Luaña, PRB 55, 4275 (1997))
- ❑ In a periodic 3D crystal, $k \geq 1, i \geq 3, m \geq 3, n \geq 1$, so at least 8 CPs

Quantum Theory of Atoms in Molecules (QTAIM) and crystals (QTAIMC)

- ❑ Uses as scalar f the total ρ as an information source from which to (re)formulate chemical concepts
- ❑ Provides a bridge between chemistry and QM and shows that all chemistry is already hidden in ρ (no need to invoke any arbitrary reference density)
- ❑ QTAIM goes far beyond a simple topological study of ρ .

It provides a full consistent QM framework for the definition of the atoms or groups of atoms in a molecule or crystal and for the treatment of the mechanics of their interaction



Richard Bader

Topological study of $\rho(r;X)$

$$\nabla\rho = \mathbf{i}\frac{d\rho}{dx} + \mathbf{j}\frac{d\rho}{dy} + \mathbf{k}\frac{d\rho}{dz}$$

● $\nabla\rho(\mathbf{r}_c) = 0$ $\mathbf{r}_c = \text{Critical Point, CP}$

1) find CPs

H $H_{12} = \partial^2\rho/(\partial x\partial y)$

H $\equiv \nabla\nabla\rho =$

Hessian matrix

$$\begin{pmatrix} \frac{\partial^2\rho}{\partial x^2} & \frac{\partial^2\rho}{\partial x\partial y} & \frac{\partial^2\rho}{\partial x\partial z} \\ \frac{\partial^2\rho}{\partial y\partial x} & \frac{\partial^2\rho}{\partial y^2} & \frac{\partial^2\rho}{\partial y\partial z} \\ \frac{\partial^2\rho}{\partial z\partial x} & \frac{\partial^2\rho}{\partial z\partial y} & \frac{\partial^2\rho}{\partial z^2} \end{pmatrix}$$

● Diagonalize H at \mathbf{r}_c

Allows to find a rotation of the coordinate axes to a new set such that all of the off-diagonal elements vanish \longrightarrow eigenvectors and eigenvalues:

principal axes of curvatures and curvatures

$$\begin{pmatrix} \frac{\partial^2\rho}{\partial x'^2} & 0 & 0 \\ 0 & \frac{\partial^2\rho}{\partial y'^2} & 0 \\ 0 & 0 & \frac{\partial^2\rho}{\partial z'^2} \end{pmatrix}_{\mathbf{r}'=\mathbf{r}_c} = \begin{pmatrix} \lambda_1 & 0 & 0 \\ 0 & \lambda_2 & 0 \\ 0 & 0 & \lambda_3 \end{pmatrix}$$

$$(\nabla\nabla\rho)\mathbf{v}_i = \lambda_i\mathbf{v}_i ; i=1,2,3$$

● Get its eigenvalues λ_i (curvatures)

- Get H matrix eigenvalues λ_i (curvatures)

$$\lambda_3 \geq \lambda_2 \geq \lambda_1$$

2) Classify CPs by (RANK, SIGNATURE)
the CP of ρ in \mathbb{R}^3

- Non degenerate CPs (rank 3) \longrightarrow

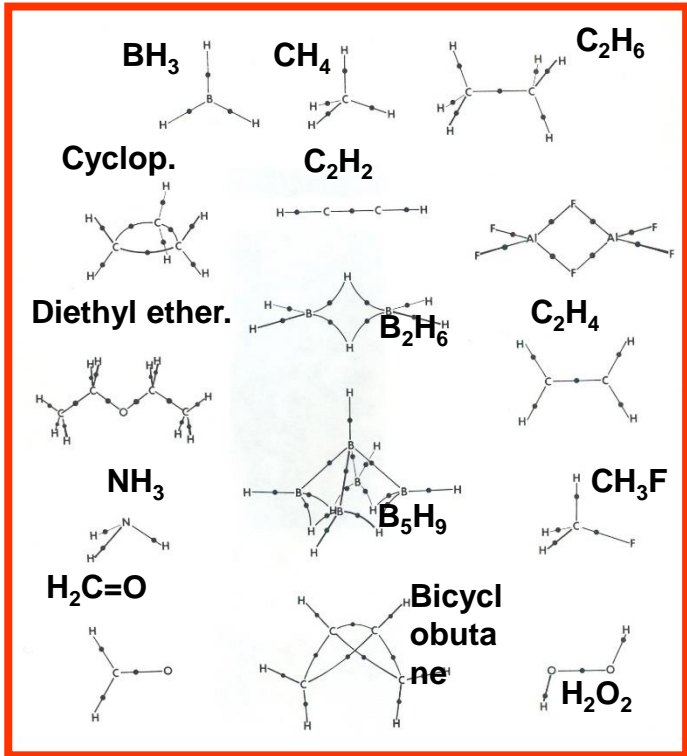
(3, -3) \longrightarrow NUCLEI (and in special cases NNA)

(3, -1) \longrightarrow BONDED ATOMS (\in "chemical bonds")

(3, +1) \longrightarrow RING

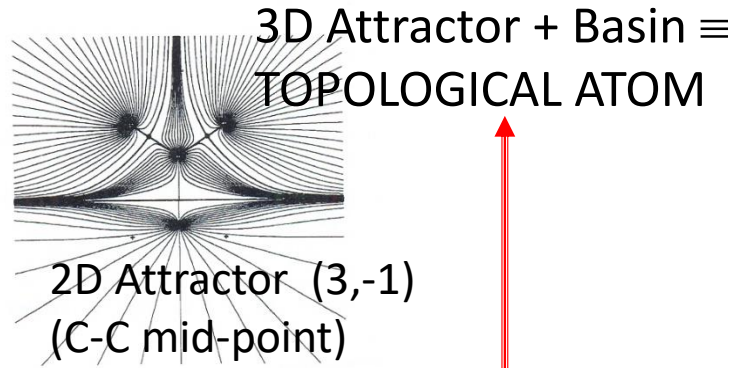
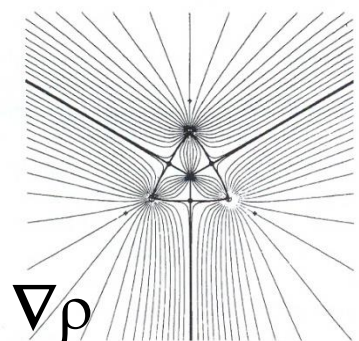
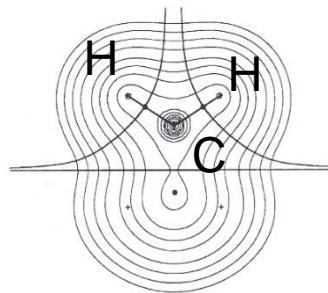
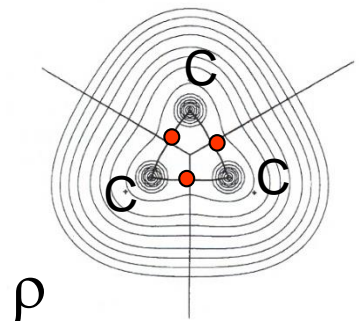
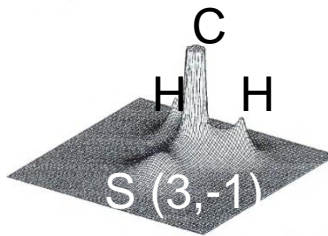
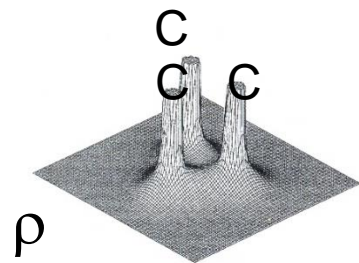
(3, +3) \longrightarrow CAGES

Name	Acronym	λ_1	λ_2	λ_3	(rank,signature)
Nuclear attractor	NA	-	-	-	(3, -3)
Bond Critical Point	BCP	-	-	+	(3, -1)
Ring Critical Point	RCP	-	+	+	(3, +1)
Cage Critical Point	CCP	+	+	+	(3, +3)



“Molecular graphs”
Molecular structure

Bond paths
● Bcp, $\nabla\rho=0$



$\nabla\rho(\mathbf{r}_c) = 0$ $\mathbf{r}_c =$ Critical Point 1) Find

\mathbf{H} $H_{12} = \partial^2\rho/(\partial x\partial y)$ 2) Classify

H eigenvalues λ_i and eigenvectors $\lambda_3 \geq \lambda_2 \geq \lambda_1$ Non degenerate CPs (rank 3)

(3, -3) - - - - -> NUCLEI

(3, -1) - - - - -> BONDED ATOMS (“chemical bonds”)

(3, +1) - - - - -> RING

(3, +3) - - - - -> CAGES

Classify by (RANK, SIGN) the CP of ρ in \mathbb{R}^3

“QUANTUM” ATOM

The $\nabla\rho$ vector field and the definition of the molecular structure

• $dr(s)/ds = \nabla\rho[r(s); \mathbf{X}]$ for a given $r(0) \equiv r_0$

• $r(s) = r_0 + \int \nabla\rho[r(t); \mathbf{X}] dt$ Gradient Paths

3D, (3,-3) • $\nabla\rho$ attractors

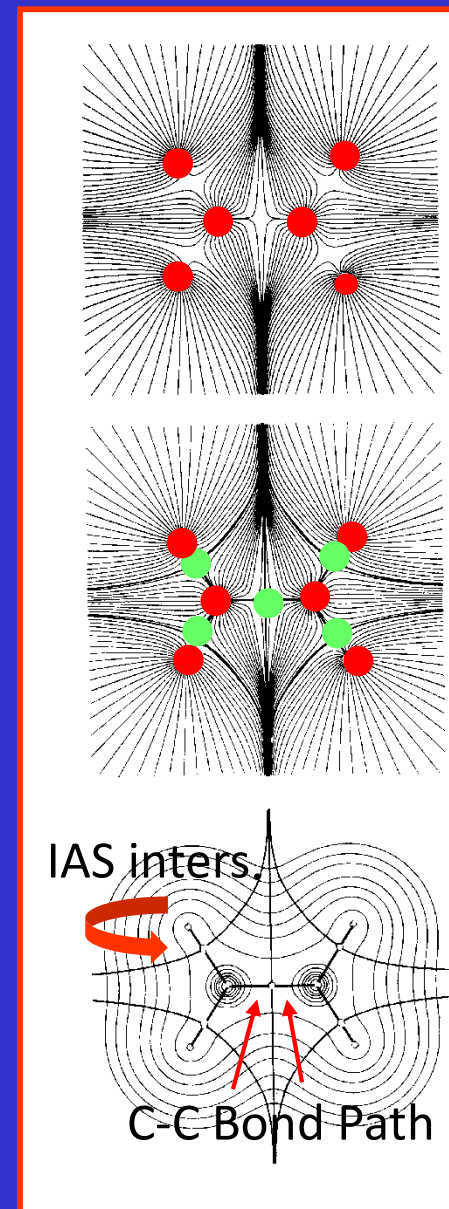
3D, (3,-3) •

+ $\nabla\rho$ attractors

2D (3,-1) •

ρ contours + $\nabla\rho$ lines of 2D attractors :
molecular graph (BPs) and intersections
of IAS

Basin + 3D attractor \equiv topological atom



Atomic properties

$$\langle \hat{O} \rangle_{molecule} = \sum_i \left(N \int_{\Omega_i} \left\{ \int \frac{1}{2} [\Psi^* \hat{O} \Psi + (\hat{O} \Psi)^* \Psi] d\tau' \right\} d\mathbf{r} \right)$$

$$= \sum_i \left(\int_{\Omega_i} \rho_O d\mathbf{r} \right) = \sum_i O(\Omega_i)$$

$\int d\tau'$ integration over the coordinates of all electrons but one and summation over all spins

Any molecular property O which can be expressed in terms of a corresponding property density in space $\rho_O(\mathbf{r})$ can be written as a sum of atomic contributions

Atomic kinetic energy

Many alternative formulas for the kinetic energy density

$$K(\mathbf{r}) = N k \int d\tau' [[\Psi^* \nabla^2 \Psi + (\nabla^2 \Psi)^* \Psi]$$

$$k = -\hbar^2 / (16\pi^2 m_e)$$

In terms of the Laplacian operator

$$G(\mathbf{r}) = N \frac{1}{2} k \int d\tau' \nabla \Psi^* \bullet \nabla \Psi$$

In terms of the dot product of the moment operator

$$K(\mathbf{r}) - G(\mathbf{r}) = k \nabla^2 \rho(\mathbf{r})$$

The local zero flux condition enables to define a kinetic energy for the atom $\equiv -E(\Omega)$ \rightarrow virial fragment, as is for the whole system

$$\int_{\Omega} [K(\mathbf{r}) - G(\mathbf{r})] d\tau = K(\Omega) - G(\Omega) = k \int_{\Omega} \nabla^2 \rho(\mathbf{r}) d\tau = k \int_{\Omega} \nabla \cdot \nabla \rho(\mathbf{r}) d\tau = \oint_{S(\Omega)} \nabla \rho \cdot \mathbf{n}(\mathbf{r}_s) ds \equiv 0$$

TOPOLOGICAL ATOM \equiv "QUANTUM" ATOM

Divergence theorem

Atomic electron population and net charge

$$N(\Omega) = \int_{\Omega} \rho(\mathbf{r}) d\tau$$

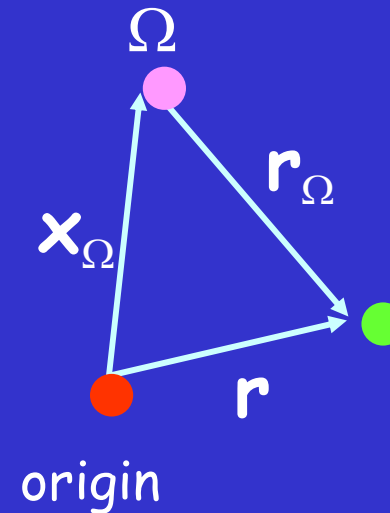
$$q(\Omega) = Z_{\Omega} - N(\Omega)$$

Atomic moments

$$M_j(\Omega) = - \int_{\Omega} d\tau \rho(\mathbf{r}) r_{j\Omega}; j = 1-3$$

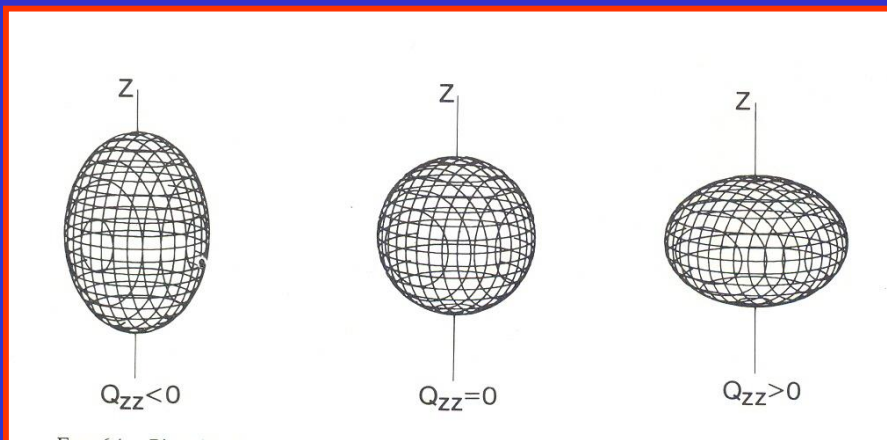
Atomic dipole

$$Q_{ij}(\Omega) = - \int_{\Omega} d\tau \rho(\mathbf{r}) (3r_i r_j - r^2_{\Omega} \delta_{ij}); i, j = 1-3$$



Atomic quadrupole moment tensor (traceless)

Real symmetric matrix which can be diagonalized



Atomic volumes

$$V(\Omega) = \int_{\Omega} d\tau$$

$$\sum_{\Omega \text{ of all cell}} V(\Omega) = V_{\text{cell}}$$

Generally infinite in the molecular case; always finite in the crystalline case

Normally the atomic volume is however defined as the region of space enclosed by the intersection of the atomic zero-flux surface and a particular envelope of ρ

$$V_{0.001}(\Omega) \equiv V1 = \int_{\Omega^*} d\tau ; \quad \Omega^*: \forall \mathbf{r} \in \Omega \text{ where } \rho \geq 0.001 \text{ au}$$

$V_{0.001}$ yields molecular sizes in agreement with those determined from the analysis of the kinetic theory data for gas-phase molecules (van der Waals volumes)

$$V_{0.002}(\Omega) \equiv V2 = \int_{\Omega^{**}} d\tau ; \quad \Omega^{**}: \forall \mathbf{r} \in \Omega \text{ where } \rho \geq 0.002 \text{ au}$$

$V_{0.002}$ yields molecular sizes compatible with the closer packing found in the solid state

$\nabla^2\rho$ and the local contributions to the energy

$$\frac{1}{4}\nabla^2\rho(\mathbf{r}) = 2G(\mathbf{r}) + V(\mathbf{r})$$

Local expression of quantum virial theorem

- $V(\mathbf{r})$ electronic potential energy density, ≤ 0 always

$$\int_{\Omega} V(\mathbf{r}) = V(\Omega) = 2E_e(\Omega)$$

- $G(\mathbf{r})$ positive definite kinetic energy density, ≥ 0 always

$$\int_{\Omega} G(\mathbf{r}) = T(\Omega) = -E_e(\Omega);$$

- $2T(\Omega) + V(\Omega) = -2E(\Omega) + 2E_e(\Omega) = 0$; virial theorem

- Regions where $\nabla^2\rho < 0$, $V(\mathbf{r})$ dominates over $G(\mathbf{r})$
- Regions where $\nabla^2\rho > 0$, $G(\mathbf{r})$ dominates over $V(\mathbf{r})$

$$G(\mathbf{r}) = \frac{1}{2}(\nabla \cdot \nabla') \Gamma(1)(\mathbf{r}, \mathbf{r}') \big|_{\mathbf{r}=\mathbf{r}'} \approx$$

Using semiclassical Thomas-Fermi equation
 $T_{\infty} \rho(\mathbf{r})^{5/3}$ with the total form of Kirzhnitz's
 gradient quantum corrections

$$G(\mathbf{r}) \approx (3/10)(3\pi^2)^{2/3} \rho(\mathbf{r})^{5/3} + (1/72)[\nabla \rho(\mathbf{r})]^2 / \rho(\mathbf{r}) + (1/6)\nabla^2 \rho(\mathbf{r})$$

Yu A. Abramov, Acta
 Cryst. **A53** 264 (1997)

$\equiv 0$ at bcp

Assuming that the multipole derived electron distributions obey
 the local virial theorem (though they don't), one gets also $V(\mathbf{r})$

$$\frac{1}{4} \nabla^2 \rho(\mathbf{r}) = 2 G(\mathbf{r}) + V(\mathbf{r})$$

Relatively accurate description in the medium-range behaviour (1-4 a.u.
 from the atomic nucleus) of $G(\mathbf{r})$

Agreement with "exact" $G(\mathbf{r})$ values nearly quantitative for closed-shell
 interactions (bcps at large distances from nuclei)

Agreement only qualitative and often rather poor ($\Delta > 300\%$) for typical
 shared interactions

The dichotomous classification based on the sign of $\nabla^2\rho$

Bader, R.F.W.; Essén, H., J. Chem. Phys. 80 (1984) 1943

Local expression of quantum virial theorem

$$\frac{1}{4} \nabla^2\rho(\mathbf{r}) = 2G(\mathbf{r}) + V(\mathbf{r})$$

$$\nabla^2\rho_b$$

$$G(\mathbf{r}) > 0$$

$$V(\mathbf{r}) < 0$$

Chemical Interactions

shared

Closed-shell

$$\nabla^2\rho_b < 0$$

$V(r_b)$ in local excess
respect to the average
 $2G(\Omega) = -V(\Omega)$

$$\nabla^2\rho_b > 0$$

$G(r_b)$ in local excess
respect to the average
 $2G(\Omega) = -V(\Omega)$

The dichotomous classification based on the sign of $\nabla^2\rho$

Property	Shared shell, $\nabla^2\rho_b < 0$ Covalent and polar bonds	Closed-shell, $\nabla^2\rho_b > 0$ Ionic, H- bonds and vdW molecules
λ_I	$\lambda_{1,2}$ dominant ; $ \lambda_{1,2} / \lambda_3 > 1$	λ_3 dominant; $ \lambda_{1,2} / \lambda_3 \ll 1$
VSCC	The VSCCs of the two atoms form one continuous region of CC	$\nabla^2\rho > 0$ over the entire interaction region. The spatial display of $\nabla^2\rho$ is mostly atomic-like
ρ_b	Large	Small
Energy Lowering	By accumulating ρ in the interatomic region	Regions of dominant $V(r)$ are separately localized within the boundaries of interacting atoms
Energy components	$2G_b < V_b $; $G_b/\rho_b < 1$; $G_{b } \ll G_{b\perp}$; $H_b < 0$	$2G_b > V_b $; $G_b/\rho_b > 1$, $G_{b } \gg G_{b\perp}$; H_b any value

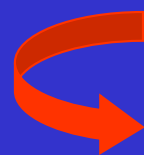
Electron sharing is decreasing
(and polarity increasing)



Electron sharing (covalency) is
increasing (and polarity decreasing)

The classification based on the adimensional $|V_b|/G_b$ ratio
 Espinosa, E. *et al.*, J. Chem. Phys. 117 (2002) 5529

Shared shell (SS) $ V_b /G_b > 2$	Transit region, incipient covalent bond formation $1 < V_b /G_b < 2$	Closed-shell (CS) $ V_b /G_b < 1$
$H_b < 0; \nabla^2 \rho_b < 0$	$H_b < 0; \nabla^2 \rho_b > 0$	$H_b > 0; \nabla^2 \rho_b > 0$
Bond degree (BD) = $H_b/\rho_b \equiv$ Covalence degree (CD) BD large and negative The larger is $ BD $ the more covalent is the bond	$BD \equiv CD$ BD negative and smaller in magnitude than for SS interactions BD Approaching zero at the boundary with CS region	$BD \equiv H_b/\rho_b \equiv$ Softness degree (SD) SD positive and large The larger is SD the weaker and closed- shell in nature is the bond

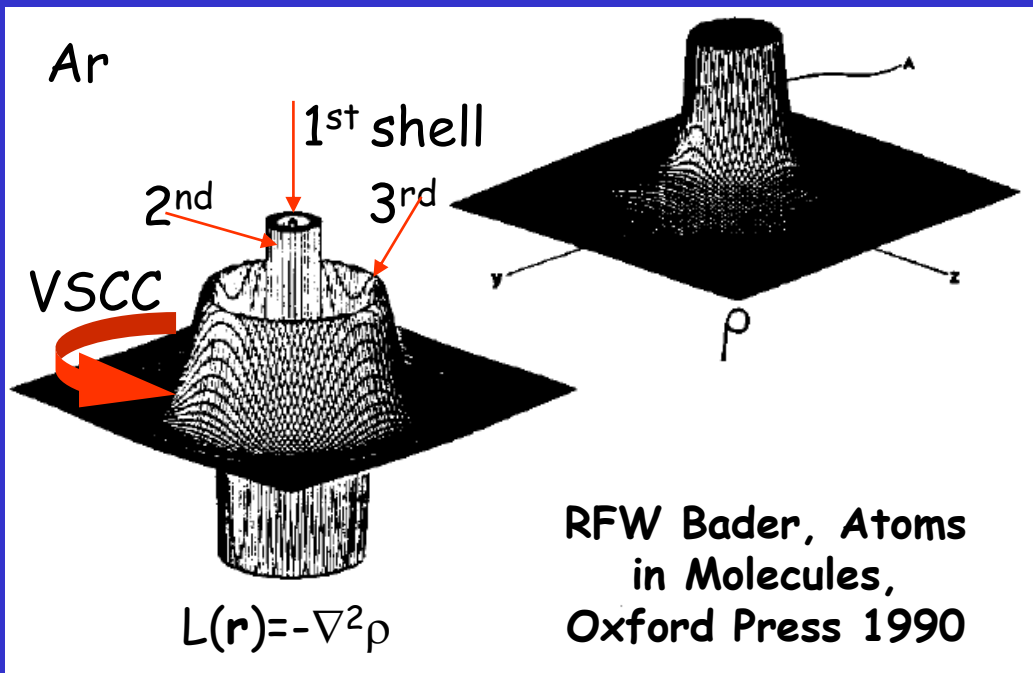


Identified with the region of incipient
 covalent bond formation using a NBO analysis

Formulated for X-H...F-Y systems. 79 cases with $d_{H...F}$ ranging from 0.8 to 2.5 Å.

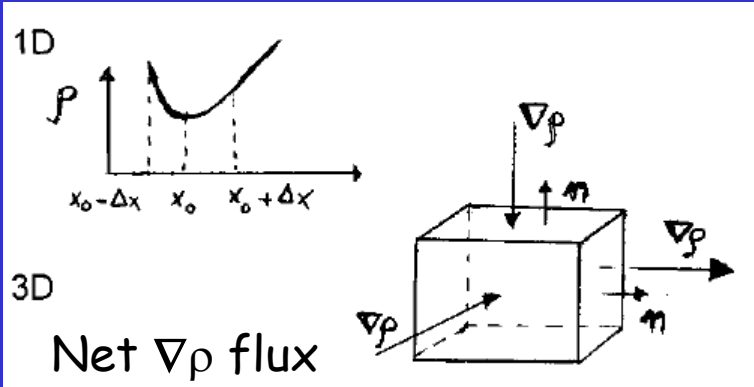
The Laplacian of the electron density, $\nabla^2\rho$

$$\nabla \cdot \nabla \rho = \nabla^2 \rho = \sum_i \lambda_i = \sum (\partial^2 \rho / \partial x_{ii}^2), i=1-3$$



a positive (negative) second derivative at x indicates that the ED is on average lower (higher) in x than it is in a symmetrical neighborhood of x .

The ED is depleted (concentrated) at x .



CC regions : a net $\nabla \rho$ flux enters the region

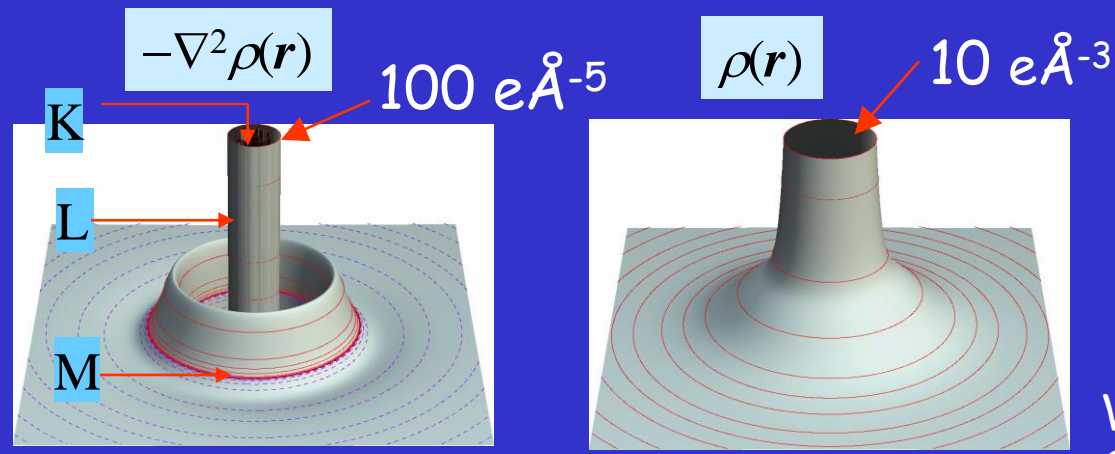
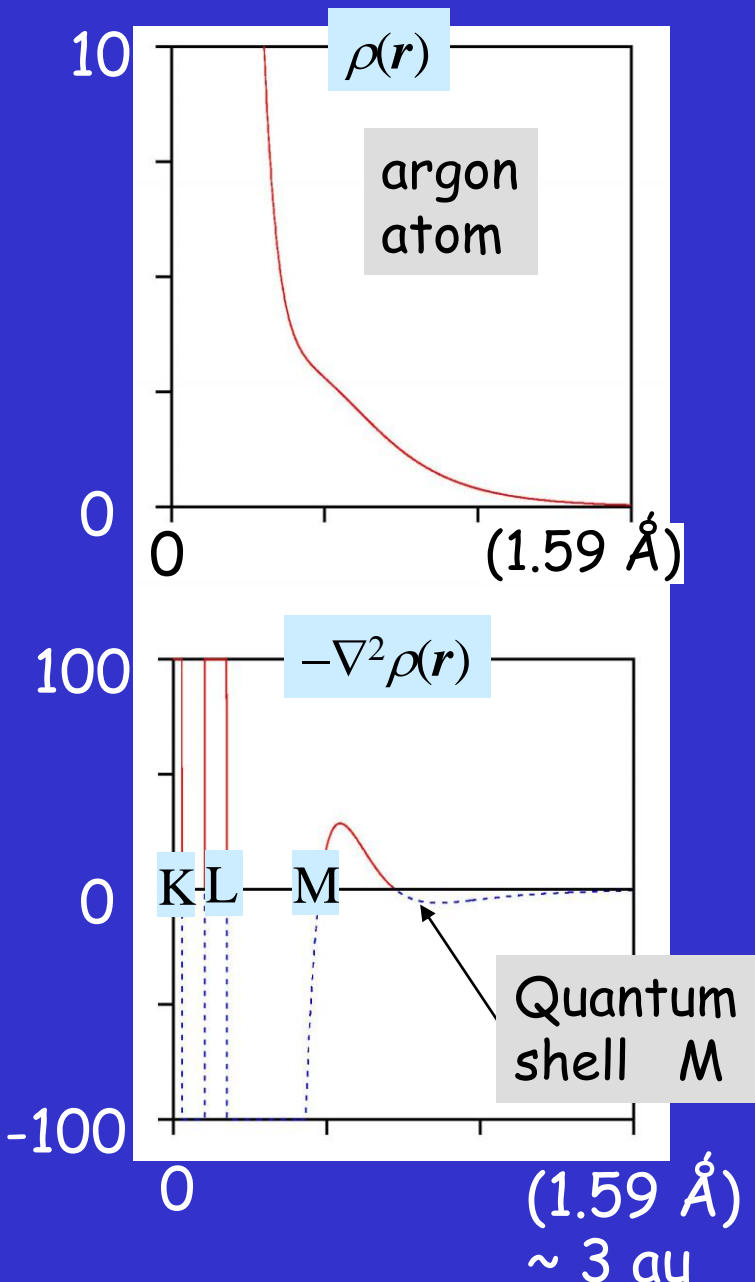
CD regions : a net $\nabla \rho$ flux leaves the region

- $\nabla^2 \rho > 0$ electron density is depleted at \mathbf{r}
- $\nabla^2 \rho < 0$ electron density is concentrated at \mathbf{r}

Through the Divergence theorem

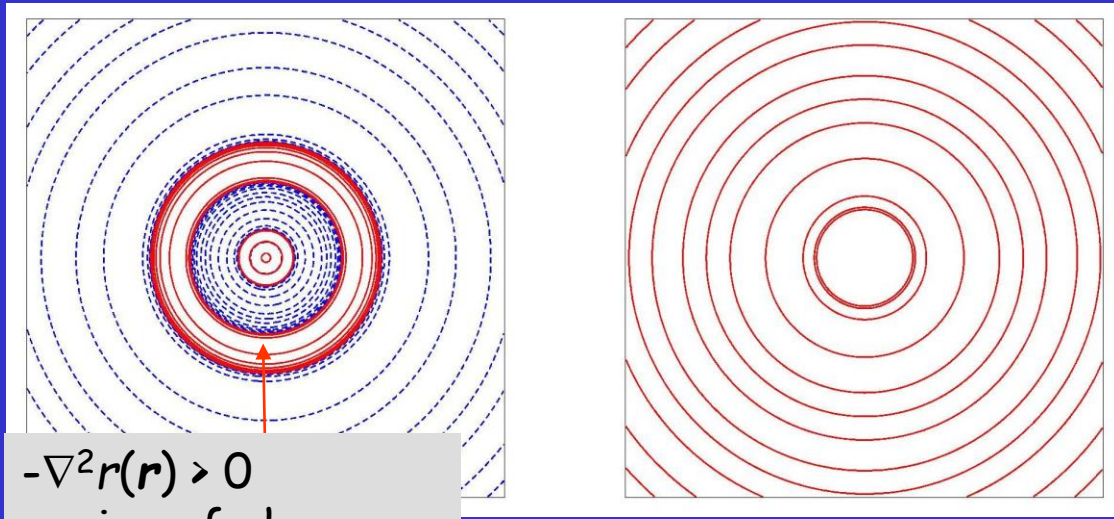
$$\int_V \nabla^2 \rho(\mathbf{r}) d\tau = \int_V \nabla \cdot \nabla \rho(\mathbf{r}) d\tau = \oint_{S(\Omega)} \nabla \rho \cdot \mathbf{n}(\mathbf{r}_s) dS$$

The Laplacian as a Magnification Glass for the Shell Structure of Atoms



relief maps
contour maps

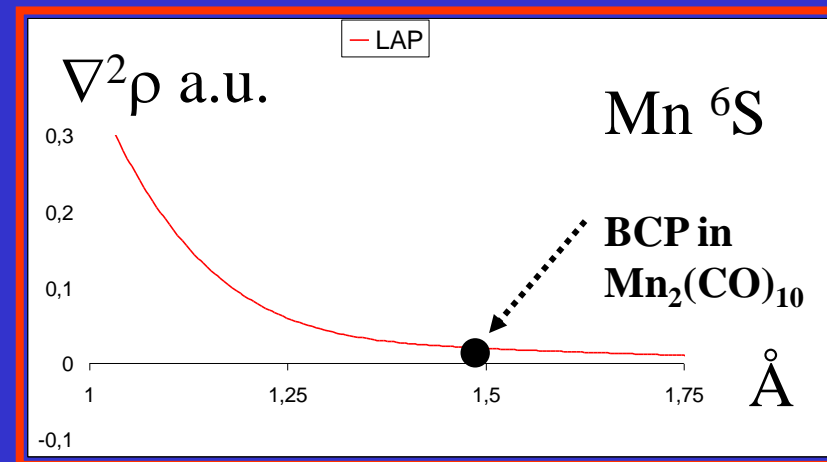
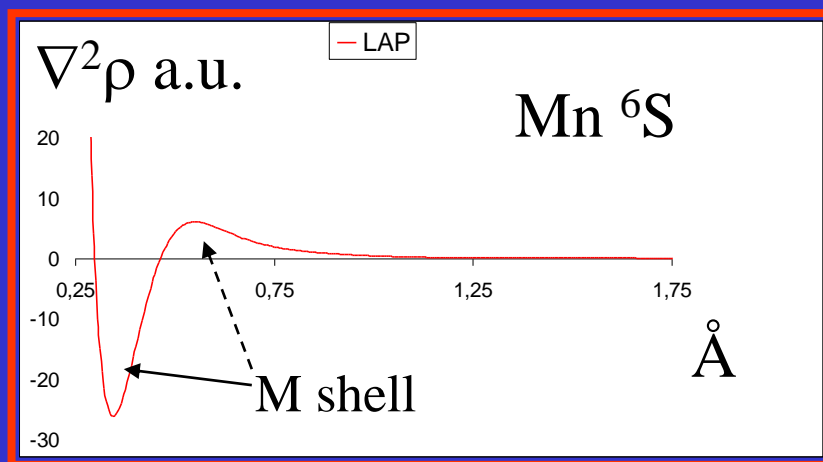
Wolfgang Scherer,
private communication



Level of approximation:
B3LYP/6-311++G(2d,2p)

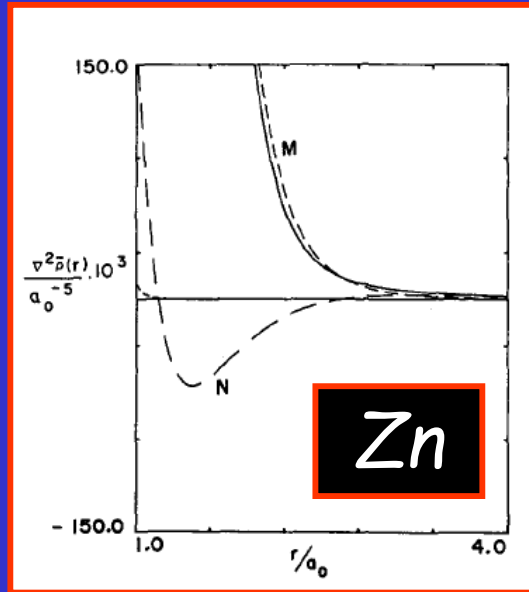
The 1:1 correspondence of the $\nabla^2\rho$ distribution with the shell structure of isolated atoms is lost for all the d-block elements

Sagar et al., J. Chem. Phys. 88, 4367 (1988); Shi et al. J. Chem. Phys. 88, 4375 (1988)



Shell M (3s,3p,3d) : $0.298 \text{ \AA} \leq r \leq 0.463 \text{ \AA}$ VSCC
 $0.463 \text{ \AA} \leq r$ to ∞ VSCD

From Sc to Ge, the N shell becomes indistinguishable from the M shell and the corresponding regions of CC and CD are missing

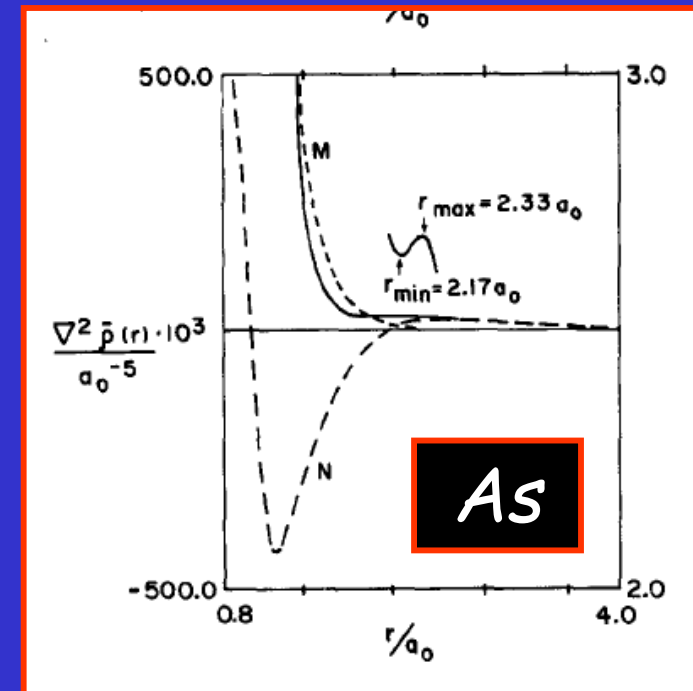


From Sc to Ge, the N shell becomes indistinguishable from the M shell

Zn: M-shell and N-shell contributions

M-shell CD overweights N-shell CC

M and N shells separate again from As up to Kr, but the sign of the Laplacian at the outermost minimum is found to be positive, rather than negative as for the other minima.



Similar trends were observed for the successive rows, with five being the number of maximum distinguishable shells

Warning for bonding classification schemes in terms of the sign of the $\nabla^2 \rho$

The shell structure of atoms and the Laplacian of the charge density

Zheng Shi and Russell J. Boyd

Citation: *J. Chem. Phys.* **88**, 4375 (1988); doi: 10.1063/1.454711

VSCC maxima of $-\nabla^2\rho$ (au)

Te

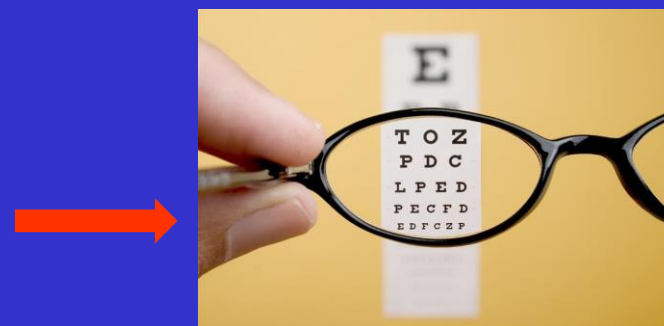


Shell-L Shell-M Shell-N

TABLE I. Radii of minima in the Laplacian of the charge density of the spherical atoms Li–Xe.*

Atom	r_2	r_3	Atom	r_2	r_3	r_4	Atom	r_2	r_3	r_4	r_5
Li 2S	2.494		K 2S	0.226	0.981	4.938	Rb 2S	0.106	0.381	1.376	5.516
	0.002			1.115	2.219	$-3.1E-5$		49.977	435.2	0.152	$-3.5E-5$
	1.594			0.213	0.898	3.773		0.103	0.367	1.278	4.369
Be 1S	0.027		Ca 1S	1544	3.818	$-1.2E-4$	Sr 1S	58.191	541.4	0.275	$-2.0E-4$
	1.188			0.201	0.834			0.100	0.354	1.204	
B 2P	0.141		Sc 2D	2067	5.804		Y 2D	67.246	653.7	0.517	
	0.942			0.190	0.779			0.098	0.342	1.140	
C 3P	0.506		Ti 3F	2712	8.478		Zr 3F	77.430	788.6	0.879	
	0.776			0.181	0.731			0.095	0.331	1.082	
N 4S	1.447		V 4F	3507	12.05		Nb 4F	88.851	943.2	1.438	
	0.658			0.172	0.691			0.092	0.320	1.031	
O 3P	3.480		Cr 5D	4433	15.84		Mo 5D	101.420	1116	2.277	
	0.569			0.165	0.652			0.090	0.310	0.984	
F 2P	7.592		Mn 6S	5614	22.71		Tc 6S	115.450	1320	3.450	
	0.500			0.158	0.618			0.088	0.301	0.940	
Ne 1S	15.29		Fe 5D	6993	30.39		Ru 5D	131.010	1551	4.976	
	0.442	3.436		0.151	0.587			0.086	0.292	0.901	
Na 2S	29.99	$1.5E-4$	Co 4F	8648	39.84		Rh 4F	148.210	1807	7.074	
	0.396	2.549		0.145	0.559			0.084	0.284	0.865	
Mg 1S	55.61	0.002	Ni 3F	10.554	51.67		Pd 3F	167.080	2092	9.772	
	0.359	2.081		0.140	0.535			0.082	0.276	0.830	
Al 2P	96.15	0.009	Cu 2S	12.705	63.72		Ag 2D	187.700	2413	13.22	
	0.327	1.760		0.134	0.510			0.080	0.269	0.802	
Si 3P	157.4	0.038	Zn 1S	15.398	83.76		Cd 1S	210.880	2691	17.66	
	0.301	1.522		0.130	0.487			0.078	0.261	0.770	
P 4S	247.4	0.115	Ga 2P	18.494	109.0		In 2P	236.010	3186	23.23	
	0.278	1.341		0.125	0.466			0.076	0.254	0.740	
S 3P	375.3	0.273	Ge 3P	22.126	140.2		Sn 3P	263.580	3662	30.14	
	0.258	1.198		0.121	0.446	2.175		0.075	0.248	0.713	
Cl 2P	553.3	0.592	As 4S	26.303	179.7	-0.026	Sb 4S	293.890	4186	38.66	
	0.241	1.080		0.117	0.427	1.833		0.073	0.242	0.688	
Ar 1S	794.7	1.196	Se 3P	31.124	226.9	-0.025	Te 3P	327.020	4779	48.91	
				0.113	0.410	1.652		0.072	0.236	0.665	2.228
			Br 2P	36.615	288.3	-0.010	I 2P	363.180	5446	61.10	-0.037
				0.110	0.394	1.503		0.070	0.230	0.643	2.000
			Kr 1S	42.961	361.4	-0.052	Xe 1S	402.520	6184	76.09	-0.037

*Each radius, r_i , is followed by the negative value of the Laplacian of the charge density at a radial distance r_i . All values are in atomic units.

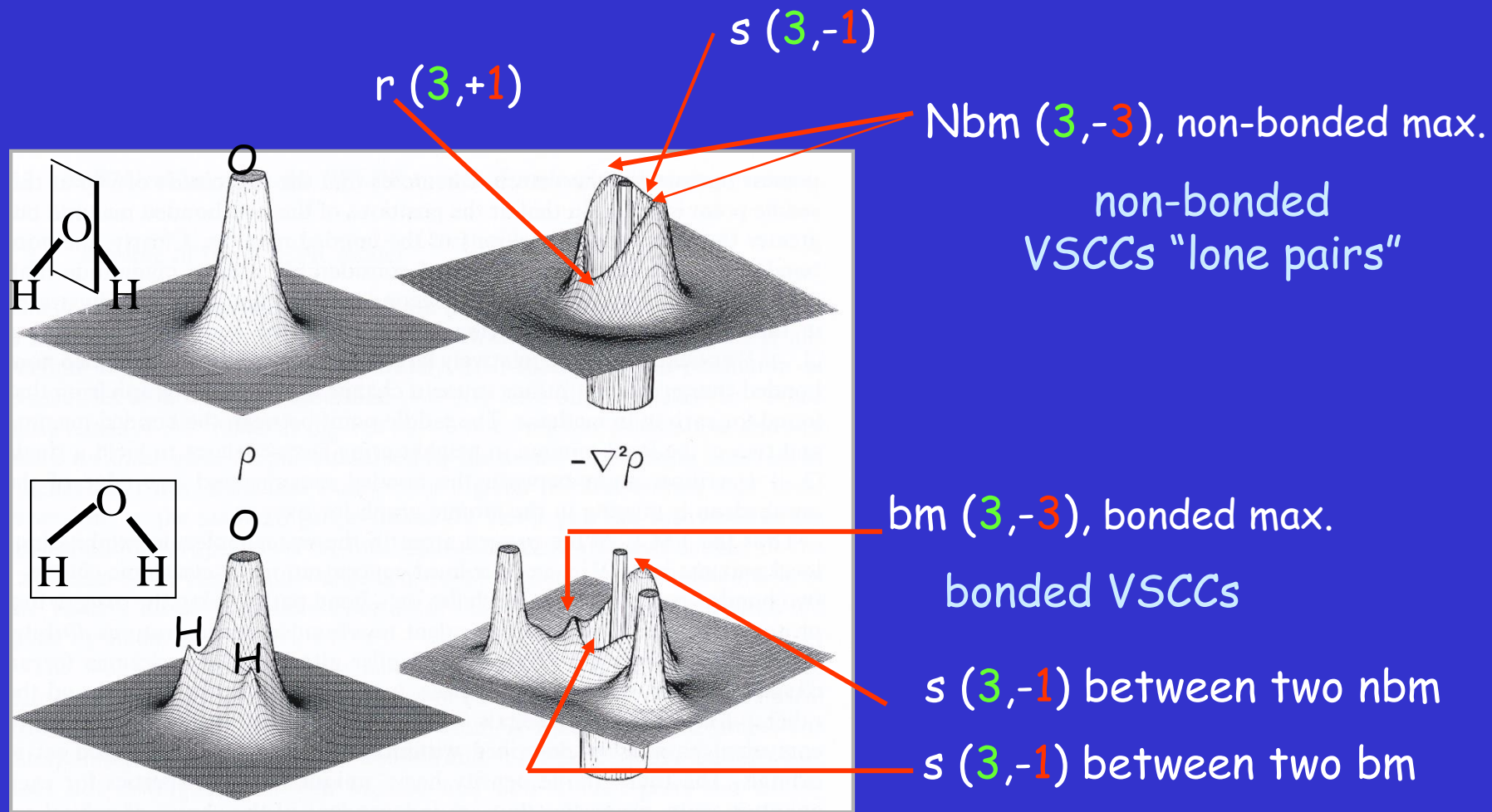


Shell-N and -O are not resolved, only 3 rather than 4 maxima for shells with $n=2-5$

R, au	0.073	0.242	0.688
Te 3P	327 020	4779	48.91

$-\nabla^2\rho$ (au) Shell-L Shell-M Shell-N

$\nabla^2\rho$ and the Lewis Electron Pair Model



R. F. W. Bader et al. *J. Am. Chem. Soc.* **1984**, 106, 1594.

$$\nabla\rho = 0 \longleftarrow CPs \longrightarrow \nabla(\nabla^2\rho) = 0$$

Charge Density Analysis of Actinide Compounds from the Quantum Theory of Atoms in Molecules and Crystals

Alessandro Cossard, Jacques K. Desmarais, Silvia Casassa, Carlo Gatti, and Alessandro Erba*

Cite This: *J. Phys. Chem. Lett.* 2021, 12, 1862–1868

Read Online

Need to be very careful !!

The VSCC for $n=7$ is not visible both for the isolated U atom $\nabla^2\rho$ profile and for the UF_6^- compound as the negative $\nabla^2\rho$ due to $n=7$ concentration region is overcompensated by positive $\nabla^2\rho$ contributions due to the depletion regions of the innermost shells

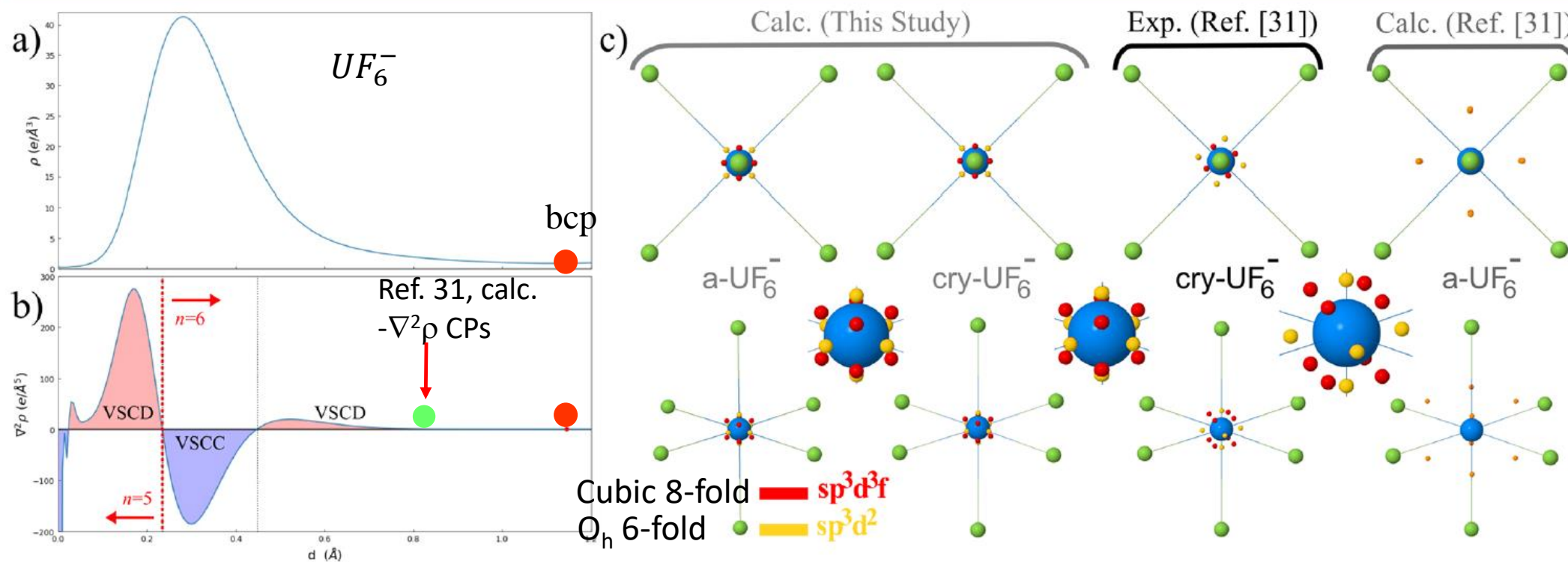


Figure 3. Topology of the Laplacian $\nabla^2\rho(\mathbf{r})$ of the electron density of UF_6^- : (a) electron density profile along the U–F_e bond (the red circle denotes the location of the bond critical point); (b) Laplacian profile along the U–F_e bond (the dashed red vertical line separates the $n = 5$ from the $n = 6$ valence radial region); (c) spatial distribution of the VSCC critical points (3, +3) of the Laplacian around the U atom in present calculations, in the experiments, and in previous calculations. A zoomed-in view in the vicinity of the U atom is also provided for the first three data sets (*i.e.*, for present calculations and previous experiments).

Bond classification



P. Macchi

Macchi, P., Proserpio, D. M., Sironi, A. , J. Am. Chem. Soc. 120 (1998) 13429

Macchi, P.; Sironi, A.: Coordination Chem. Rev. 238-239 (2003) 383.

The classification^d based on the atomic valence shell and on both the local (*bcp*) and integral properties

	ρ_b	$\nabla^2 \rho_b$	G_b/ρ_b	H_b/ρ_b	$\delta(A,B)$	$\oint_{AB} \rho(\mathbf{r}_s) d\mathbf{r}_s$
<i>Bonds between light atoms</i>						
Open-shell (covalent bonds); e.g. C–C, C–H, B–B	Large	$\ll 0$	< 1	$\ll 0$	\sim Formal bond order	Large
Intermediate interactions (polar bonds, donor-acceptor bonds; e.g. C–O, H ₃ B–CO	Large	any value	≥ 1	$\ll 0$	$<$ Formal bond order	Large
Closed-shell (ionic bonds, HBs, van der Waals interactions; e.g. LiF, H...O, Ne...Ne	Small	> 0	≥ 1	> 0	~ 0	Small
<i>Bonds between heavy atoms</i>						
Open-shell (e.g. Co–Co)	Small	~ 0	< 1	< 0	Formal bond order (unless bond delocalisation occurs)	Medium/large
Donor acceptor (e.g. Co–As)	Small	> 0	~ 1	< 0	$<$ Formal bond order	Medium/large

General and detailed discussion on several bond classification schemes

Gatti, C. , *Chemical bonding in crystals: new directions*, (2005) Z. Kristallogr. 220, 399-457

Chemical bond nature vs BCP properties in solids

$\rho_b, \nabla^2\rho_b, \lambda_{1-3}$ of closed shell interactions are generally one or two order of magnitude smaller than for shared interactions

$|\lambda_{1,2}|/\lambda_3 \approx 1$ shared interactions

$|\lambda_{1,2}|/\lambda_3 \approx 0.1$ closed-shell int.

Shared interactions

SYSTEM	BOND	R_e (Å)	ρ_b	$\nabla^2\rho_b$	λ_1	λ_2	λ_3	$ \lambda_{12} /\lambda_3$
UREA	C-O	1.261	0.38	-0.3	-1.0	-1.0	1.8	0.6
	C-N	1.345	0.35	-1.2	-0.9	-0.8	0.5	1.6
	N-H	1.009	0.34	-2.0	-1.5	-1.4	0.9	1.6
DIAMOND	C-C	1.545	0.26	-0.9	-0.5	-0.5	0.2	2.5

Not shared closed-shell interactions

SYSTEM	BOND	R_e (Å)	ρ_b	$\nabla^2\rho_b$	λ_1	λ_2	λ_3	$ \lambda_{12} /\lambda_3$
			*10	*10	*10	*10	*10	

Dative interactions

LCOB ^a	Co-N	1.966	0.92	5.4	-0.7	-0.6	6.7	0.1
	Li-O	2.030	0.21	2.0	-0.4	-0.4	2.8	0.2

Hydrogen bonds

UREA	NH...O	2.05	0.19	0.8	-0.3	-0.2	1.3	0.2
		8						
IceVIII	OH...O	2.08	0.18	0.6	-0.2	-0.2	1.0	0.2
		0						
LCOB ^a	CH...O	2.52	0.06	0.4	-0.1	-0.1	0.5	0.1
		8						

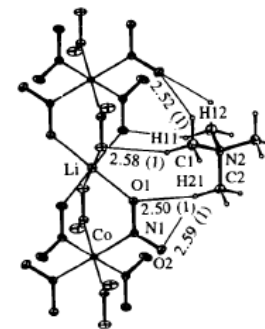
(a) Lithium Bis (tetramethylammonium)Hexanitrocobaltate (III)

Ionic (or not shared) interactions

Li oxide	Li-O	1.980	0.29	2.2	-0.5	-0.5	3.1	0.2
K oxide	K-O	2.789	0.18	0.8	-0.1	-0.1	1.0	0.1
Li-H	Li-H	2.042	0.13	0.7	-0.1	-0.1	1.0	0.1
		8						
Li-H	H-H	4.083	0.09	0.1	-0.1	-0.0	0.2	0.2

Metals

SYSTEM	BOND	R_e (Å)	ρ_b	$\nabla^2\rho_b$	λ_1	λ_2	λ_3	$ \lambda_{12} /\lambda_3$
			*100	*100	*100	*100	*100	
Li, bcc		3.040	0.81	0.6	-0.1	-0.1	0.8	0.1



Acta Cryst. (1996). **B52**, 471–478

Theoretical and Experimental (113 K) Electron-Density Study of Lithium Bis(tetramethylammonium) Hexanitrocobaltate(III)

Some general warning about chemical bonding characterization

- ❑ Use of too precise rules to characterize a specific bonding interaction may be dangerous and should be always done *cum grano salis*, especially if these rules are given in terms of typical intervals for the values of properties at BCP, like ρ_b , $\nabla^2\rho_b$, G_b , V_b , and H_b .
- ❑ Regardless of the nature of bonding (ionic, covalent, metallic, charge-shift, etc.), the numerical values of any bond property for a given A–B pair are very much related to the principal quantum number of the A and B valence shell electrons and to their difference from A to B
- ❑ By keeping in mind this fact, bond properties, especially for ‘heavy atoms,’ that is, from the first-transition element row on, are often more properly understood if compared with those predicted by the IAM model. Or even better, and, whenever possible, with those predicted by the fragment model – the sum of electron densities of not-interacting fragments, that is, of a model system where the bond under study is not yet formed

See

B. Silvi*, R.J. Gillespie*, C. Gatti*, **Electron Density analysis**, J. Reedijk and K. Poeppelmeier, Eds, in *Comprehensive Inorganic Chemistry II* vol. 9, Elsevier 2013

Inorganic Chemistry

Article
pubs.acs.org/IC

Experimental and Theoretical Charge Densities of a Zinc-Containing Coordination Polymer, $\text{Zn}(\text{HCOO})_2(\text{H}_2\text{O})_2$

Mads R. V. Jørgensen,[†] Simone Cenedese,[‡] Henrik F. Clausen,[†] Jacob Overgaard,^{*†} Yu-Sheng Chen,[§] Carlo Gatti,[‡] and Bo B. Iversen^{*†}

General discussion on several bond classification schemes: Gatti, C. , Chemical bonding in crystals: new directions, (2005) Z. Kristallogr. 220, 399-457, special issue on *Computational Crystallography*, edited by A.R. Oganov

Chemical bonding in crystals: new directions 409

Table 4. Classification of atomic interactions.

The dichotomous classification^a based on the sign of $\nabla^2 \varrho_b$

Property	Shared shell, $\nabla^2 \varrho_b < 0$ Covalent and polar bonds	Closed-shell, $\nabla^2 \varrho_b > 0$ Ionic, H-bonds and vdW molecules
λ_1 VSCC ^b	$\lambda_{1,2}$ dominant; $ \lambda_{1,2} / \lambda_3 > 1$ The VSCCs of the two atoms form one continuous region of charge concentration	λ_3 dominant; $ \lambda_{1,2} / \lambda_3 \ll 1$ $\nabla^2 \varrho > 0$ over the entire interaction region. The spatial display of $\nabla^2 \varrho$ is mostly atomic-like
ϱ_b Energy lowering	Large By accumulating ϱ in the interatomic region	Small Regions of dominant $V(r)$ are separately localized within the boundaries of interacting atoms
Energy components	$2G_b < V_b $; $G_b/\varrho_b < 1$; $G_b \ll G_{b1}$; $H_b < 0$	$2G_b > V_b $; $G_b/\varrho_b > 1$, $G_b \gg G_{b1}$; H_b any value

Bond polarity is increasing \dashrightarrow \dashleftarrow Bond covalency is increasing

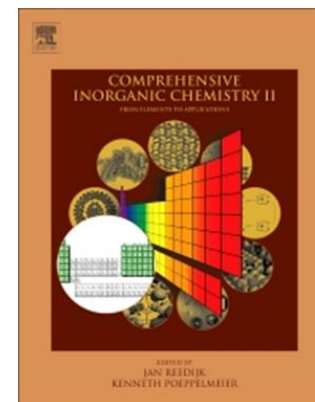
The classification^c based on the adimensional $|V_b|/G_b < 1$ ratio

Shared shell (SS)	Transit region, incipient covalent bond formation	Closed-shell (CS)
$ V_b /G_b > 2$	$1 < V_b /G_b < 2$	$ V_b /G_b < 1$
$H_b < 0$; $\nabla^2 \varrho_b < 0$ Bond degree (BD) = H_b/ϱ_b = Covalence degree (CD) BD large and negative	$H_b < 0$; $\nabla^2 \varrho_b > 0$ BD \equiv CD BD negative and smaller in magnitude than for SS interactions BD Approaching zero at the boundary with CS region	$H_b > 0$; $\nabla^2 \varrho_b > 0$ BD \equiv Softness degree (SD) SD positive and large The larger is SD the weaker and closed-shell in nature is the bond

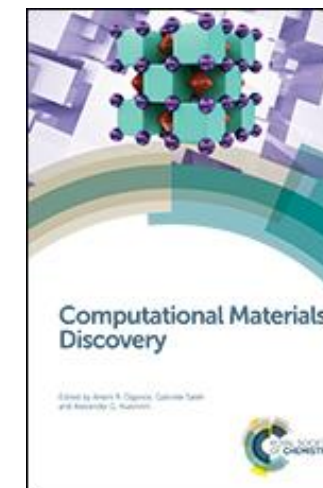
The classification^d based on the atomic valence shell and on both the local (*bcp*) and integral properties

	ϱ_b	$\nabla^2 \varrho_b$	G_b/ϱ_b	H_b/ϱ_b	$\delta(A,B)$	$\int_{AB} \varrho(\mathbf{r}_s) d\mathbf{r}_s$
<i>Bonds between light atoms</i> Open-shell (covalent bonds); e.g. C–C, C–H, B–B	Large	$\ll 0$	< 1	$\ll 0$	\sim Formal bond order	Large
Intermediate interactions (polar bonds, donor-acceptor bonds; e.g. C–O, H ₃ B–CO)	Large	any value	≥ 1	$\ll 0$	$<$ Formal bond order	Large
Closed-shell (ionic bonds, HBS, van der Waals interactions; e.g. LiF, H...O, Ne...Ne)	Small	> 0	≥ 1	> 0	~ 0	Small
<i>Bonds between heavy atoms</i> Open-shell (e.g. Co–Co)	Small	~ 0	< 1	< 0	Formal bond order (unless bond delocalisation occurs)	Medium/large
Donor acceptor (e.g. Co–As)	Small	> 0	~ 1	< 0	$<$ Formal bond order	Medium/large

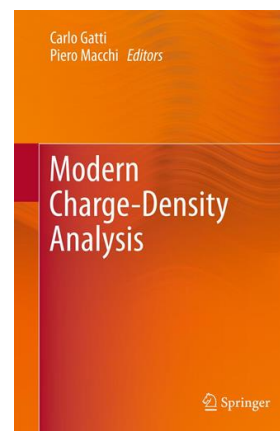
a: according to Ref. [90].
b: VSCC is the Valence Shell Charge Concentration, that is the valence region of the isolated atom where the Laplacian is negative [13]
c: according to Ref. [93]
d: according to Ref. [109]; the lower part of this Table is an adaptation of Table 5 and Table 4 of Ref. [109] and Ref. [97], respectively. Ref. [109] defines as heavy atoms the atoms having more than three atomic shells, i.e. from K atom onwards.



B. Silvi*, R.J. Gillespie*, C. Gatti*, **Electron Density analysis**, J. Reedijk and K. Poeppelmeier, Eds, in *Comprehensive Inorganic Chemistry II* vol. 9, Elsevier 2013



G. Saleh, D. Ceresoli, G. Macetti and C. Gatti*, **Chapter 5: Chemical Bonding Investigations for Materials**, in *Computational Materials Discovery*, A.R. Oganov, G. Saleh, A.G. Kvashnin Eds., RSC 2019



C. Gatti and P. Macchi, Eds, Springer 2012

Crystal field effects on the topological properties of the electron density in molecular crystals: The case of urea

C. Gatti

Centro CNR per lo Studio delle Relazioni tra Struttura e Reattività Chimica, via Golgi 19, I-20133 Milano, Italy

V. R. Saunders

DRAL Daresbury Laboratory, Daresbury, Warrington, Cheshire, WA4 4AD, United Kingdom

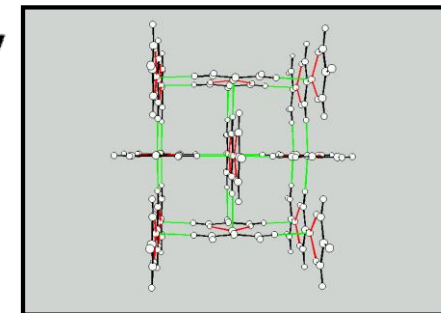
C. Roetti

Gruppo di Chimica Teorica, Università di Torino, via Giuria 5, I-10125 Torino, Italy

JCP 101 , 10686-10696 (1994)



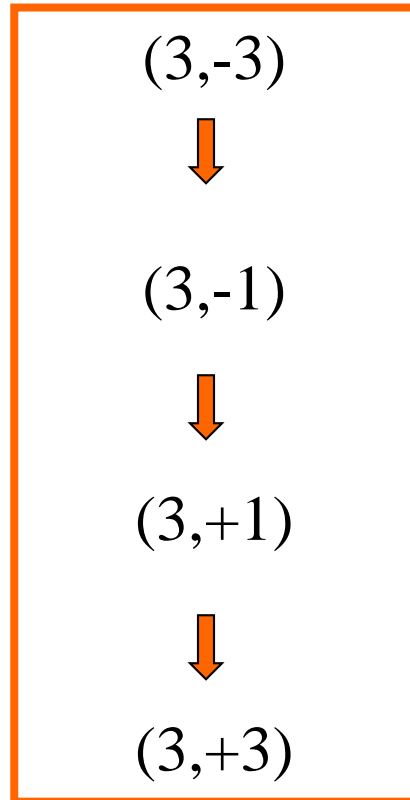
C. Roetti



➔ Crystal graph - retrieving intermolecular interactions in the crystal

- ✓ How important are packing effects on intramolecular bonds?
- ✓ Does the packing have different impact on the different atoms/chemical groups present in the molecule?
- ✓ How large is the enhancement of the molecular dipole on crystallization?
- ✓ How can each oxygen atom in the urea crystal be involved in four OH...O hydrogen bonds (HBs)?

Fully-automated and chain-like CP searches



← Sequence of the chainlike search strategy for locating CPs

At each search stage, an EF step specific for the kind of CP searched for is adopted.

Fully-automated and chain-like CP searches

1. Search of $(3, -3)$ associated to **nuclear maxima**, starting from the nuclear position of each of the unique atoms of the unit cell
2. Search of all $(3, -1)$ unique **bcps** associated to the unique bonded atom pairs within the cluster. Search started from internuclear axis midpoint



3. **Non-nuclear $(3, -3)$ attractors**, if any, are recovered at this stage by determining the nature of the termini of the atomic lines (**bond paths**) associated to the unique $(3, -1)$ CPs found
4. Search of unique $(3, +1)$ **rcps** by considering all unique nuclear triplets having at least 2 of their 3 atoms bonded to each other and **CM** (Center of Mass) not too differently distant from each of the 3 nuclei. CP search started from **CM** (mass =1 assigned to each nucleus)
5. Search of unique $(3, +3)$ **cage** CPs between all pairs of ring CPs

Brute force approach: Search on a grid

A grid-search for CPs in a given portion of the cell

⇒ x_{\min} x_{\max} x_{inc}

⇒ y_{\min} y_{\max} y_{inc}

⇒ z_{\min} z_{\max} z_{inc}

all in fractionary units

Constraint	Constraint type
1	$X \leq ay$
2	$X \leq (a+y)/2$
3	$Y \leq ax$
4	$Y \leq \min [a - x, (a + x)/2]$
5	$Y \leq \min (x, a - x)$
6	$Y \leq \min (2x, a - x)$
7	$Y \leq a - x$
8	$z \leq ay$
9	$z \leq a + y$
10	$z \leq \min (y, a - x)$

- Warning: the grid search is very costly if the whole asymmetric unit is explored.
- The CP search algorithm can be chosen (EF or NR). NR is strongly recommended here, because the starting point of the CP search is moved slightly and smoothly during the search on a grid. On top of this, the general interest is in locating all CPs in the asymmetric unit, rather than one peculiar type of CP
- Space group constraints among x, y, z fractional coordinates may be exploited

Brute force approach: Search on a grid

Why?

$$n - b + r - c = 0$$

For a closed domain
Morse Relation

n	(3,-3) nuclei or NNA
b	(3,-1) bcps
r	(3,+1) rcps
c	(3,+3) ccps

Grid search in the
asymmetric unit may be
the only way to fulfill
Morse's relationship

Fulfillment of the relationship implies a compatible CP set, not necessarily the complete set of CPs within the cell !

Fulfillment of Morse relationship in urea crystal

w	m		
c	2	(3,-3)	C
c	2	(3,-3)	O
e	4	(3,-3)	N
e	4	(3,-3)	H'
e	4	(3,-3)	H''

w, Wyckoff positions
m, multiplicity

c	2	(3,+1)	ring
e	4	(3,+1)	ring
e	4	(3,+1)	ring
f	8	(3,+1)	ring
f	8	(3,+1)	ring

c	2	(3,-1)	C-O
e	4	(3,-1)	C-N
e	4	(3,-1)	N-H'
e	4	(3,-1)	N-H''
e	4	(3,-1)	O...H'
e	4	(3,-1)	O...H''
d	4	(3,-1)	N...N, 4.3 Å
f	8	(3,-1)	N...N, 3.4 Å

e	4	(3,+3)	cage
a	2	(3,+3)	cage
b	2	(3,+3)	cage

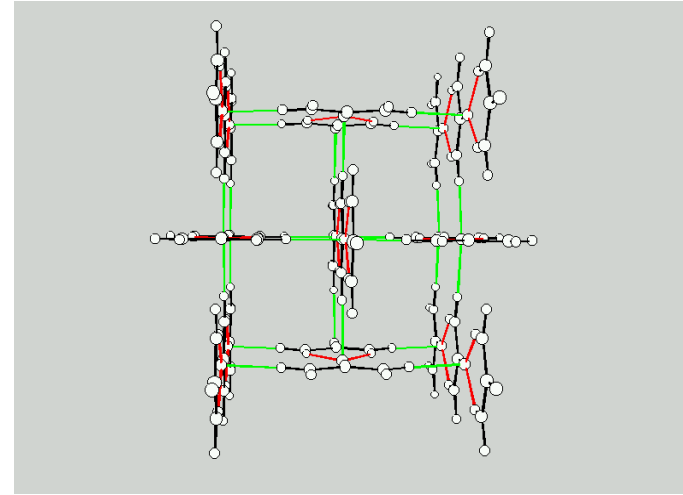
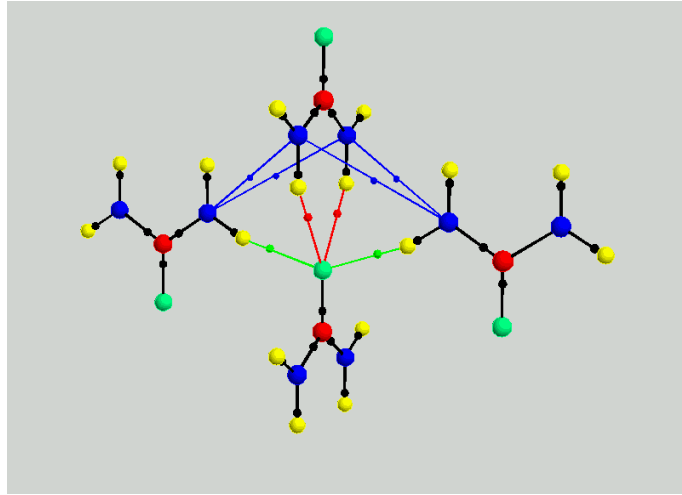
$$n - b + r - c = 0$$

$$16 - 26 + 18 - 8 = 0$$

Gatti et al. JCP, 101,10686 (1994)

$$16 - 34 + 26 - 8 = 0$$

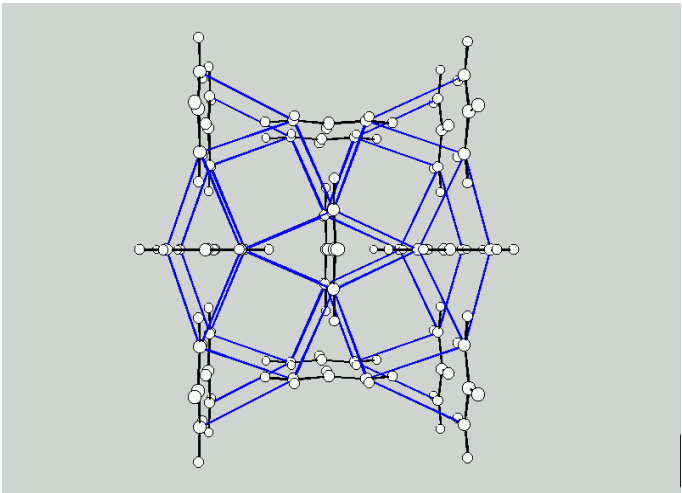
The complete bond network in urea crystal



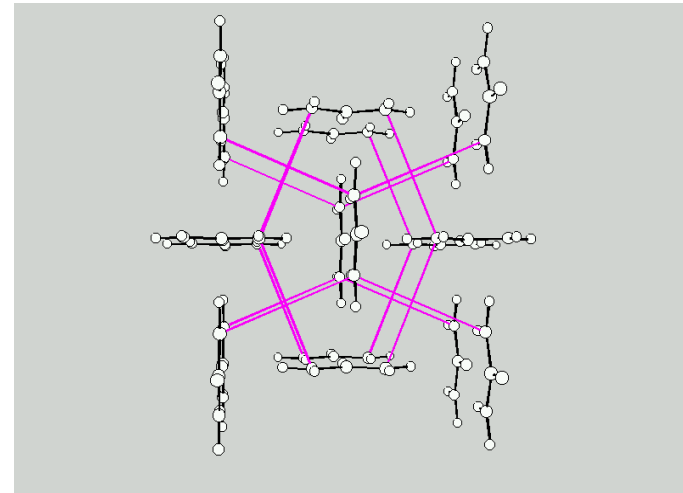
N-H...O

1.99 Å

2.06 Å



N...N, 3.4 Å



N...N, 4.3 Å

Crystal field effects on the topological properties of the electron density in molecular crystals: The case of urea

C. Gatti

Centro CNR per lo Studio delle Relazioni tra Struttura e Reattività Chimica, via Golgi 19, I-20133 Milano, Italy

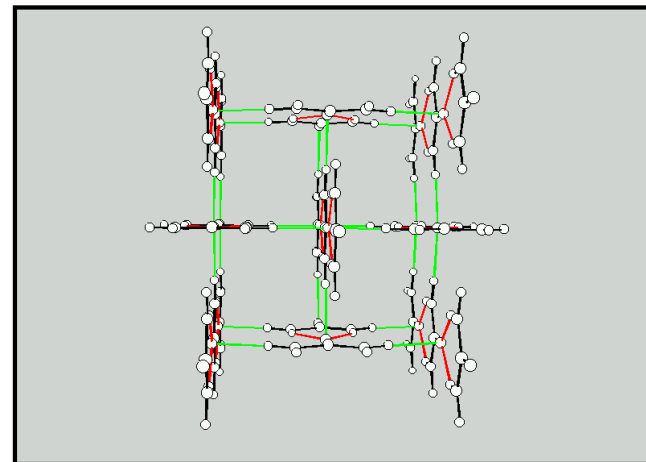
V. R. Saunders

DRAL Daresbury Laboratory, Daresbury, Warrington, Cheshire, WA4 4AD, United Kingdom

C. Roetti

Gruppo di Chimica Teorica, Università di Torino, via Giuria 5, I-10125 Torino, Italy

JCP 101 , 10686-10696 (1994)



How important are packing effects on intramolecular bonds?



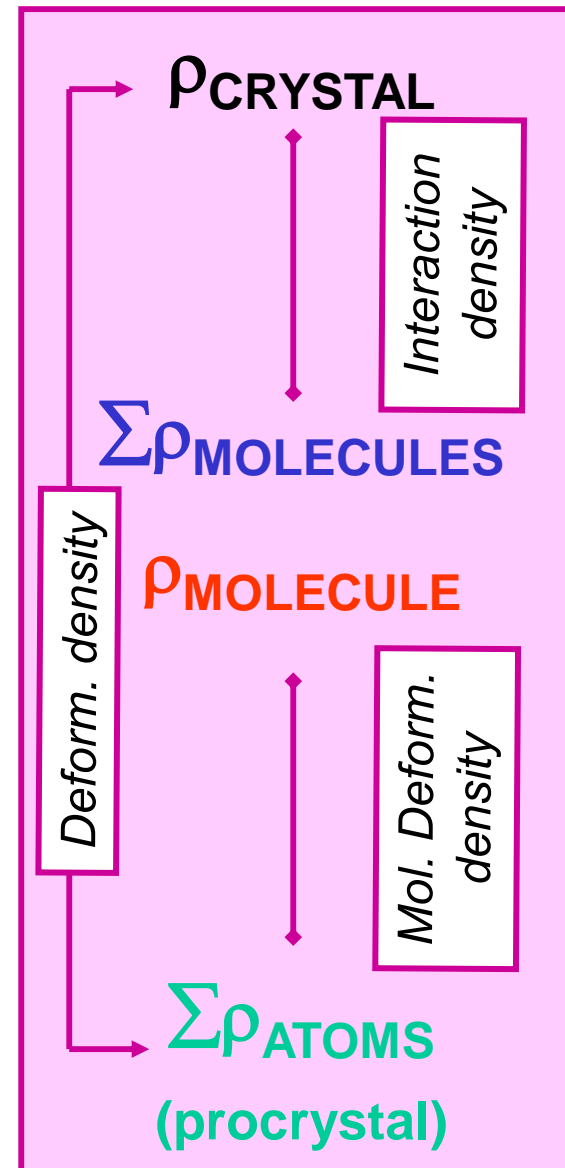
Does the packing have different impact on the different atoms/chemical groups present in the molecule?

- ✓ How large is the enhancement of the molecular dipole on crystallization?
- ✓ How can each oxygen atom in the urea crystal be involved in four OH...O hydrogen bonds (HBs)?
- ✓ How does the global molecular volume contraction observed in the solid result from the individual atomic volume change on crystallization?

Deformation and interaction density and changes in bcp properties of urea

X-Y	ρ	$\nabla^2 \rho$	λ_3	ε
C-O	0.374	-0.550	1.409	0.038
	0.384	-0.666	1.239	0.125
	0.384	-0.666	1.229	0.125
	0.299	0.118	0.974	0.038
C-N	0.342	-0.952	0.721	0.143
	0.334	-0.825	0.817	0.097
	0.334	-0.825	0.817	0.097
	0.262	-0.099	0.627	0.044
N-H	0.347	-2.003	0.874	0.052
	0.346	-1.735	0.945	0.070
	0.346	-1.735	0.945	0.070
	0.234	-0.271	1.240	0.006
O...H'N	0.023	0.081	0.143	0.024
d _{O...H} = 1.992	0.021	0.092	0.147	0.003
	0.030	0.088	0.164	0.059
O...H''N	0.019	0.080	0.130	0.034
d _{O...H} = 2.058	0.019	0.086	0.136	0.006
	0.026	0.083	0.145	0.045

all in au
 $\varepsilon = (\lambda_1 / \lambda_2) - 1$



The dichotomous classification based on the sign of $\nabla^2\rho$

Property	Shared shell, $\nabla^2\rho_b < 0$ Covalent and polar bonds	Closed-shell, $\nabla^2\rho_b > 0$ Ionic, H- bonds and vdW molecules
λ_I	$\lambda_{1,2}$ dominant ; $ \lambda_{1,2} / \lambda_3 > 1$	λ_3 dominant; $ \lambda_{1,2} / \lambda_3 \ll 1$
VSCC	The VSCCs of the two atoms form one continuous region of CC	$\nabla^2\rho > 0$ over the entire interaction region. The spatial display of $\nabla^2\rho$ is mostly atomic-like
ρ_b	Large	Small
Energy Lowering	By accumulating ρ in the interatomic region	Regions of dominant $V(r)$ are separately localized within the boundaries of interacting atoms
Energy components	$2G_b < V_b $; $G_b/\rho_b < 1$; $G_{b } \ll G_{b\perp}$; $H_b < 0$	$2G_b > V_b $; $G_b/\rho_b > 1$, $G_{b } \gg G_{b\perp}$; H_b any value

Electron sharing is decreasing
(and polarity increasing)



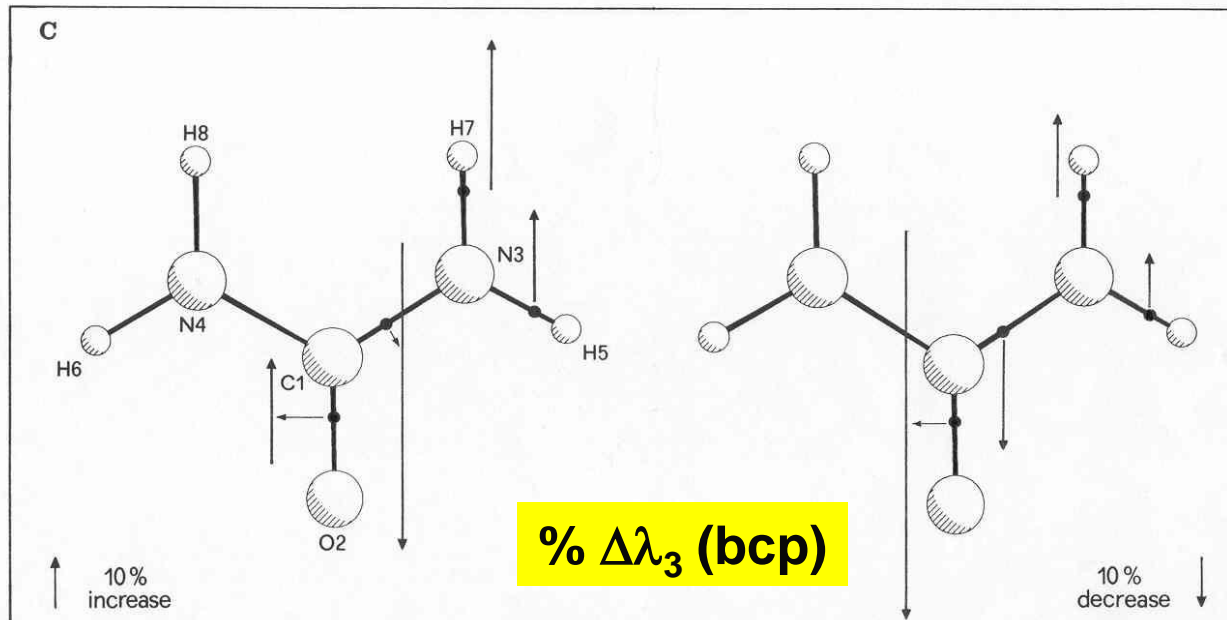
Electron sharing (covalency) is
increasing (and polarity decreasing)

Interaction density and changes in BCP properties of urea

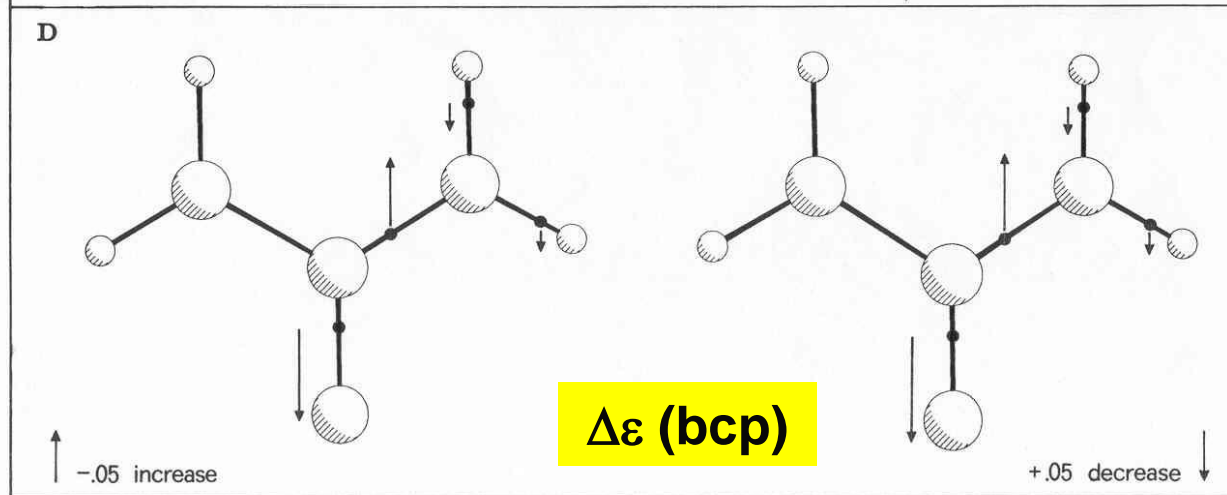
CG molecule

OG molecule

Bulk - molecule
10% increase/decrease
↑
↓



+0.05 increase/decrease
↑
↓



C=O, N-H become more ionic; C-N more covalent

Interaction density and changes in BCP properties of urea. The dimer model

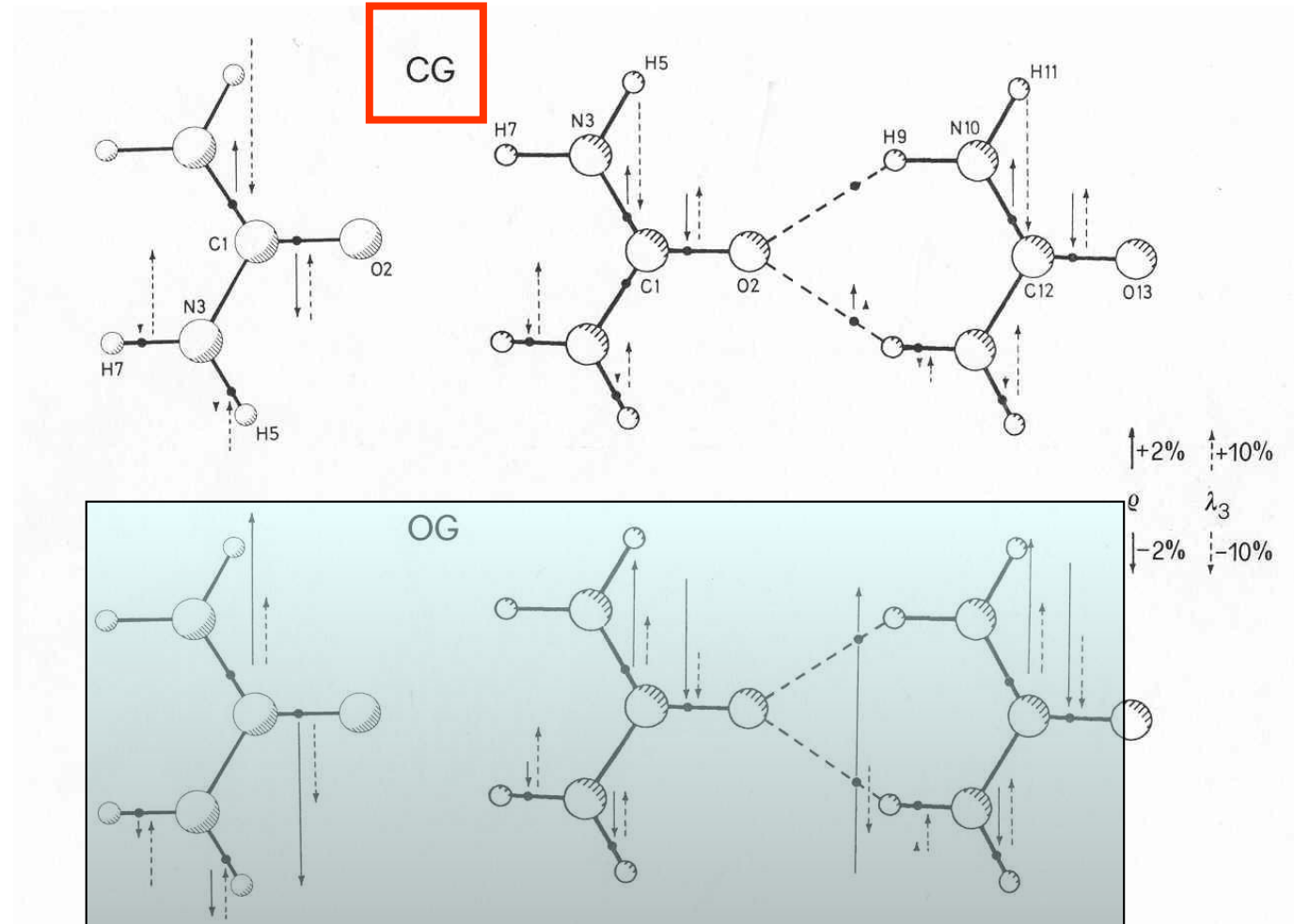
Bulk - molecule

Bulk - dimer

$\% \Delta \lambda_3$ (bcp)



$\% \Delta \rho$ (bcp)



Crystal field effects on the topological properties of the electron density in molecular crystals: The case of urea

C. Gatti

Centro CNR per lo Studio delle Relazioni tra Struttura e Reattività Chimica, via Golgi 19, I-20133 Milano, Italy

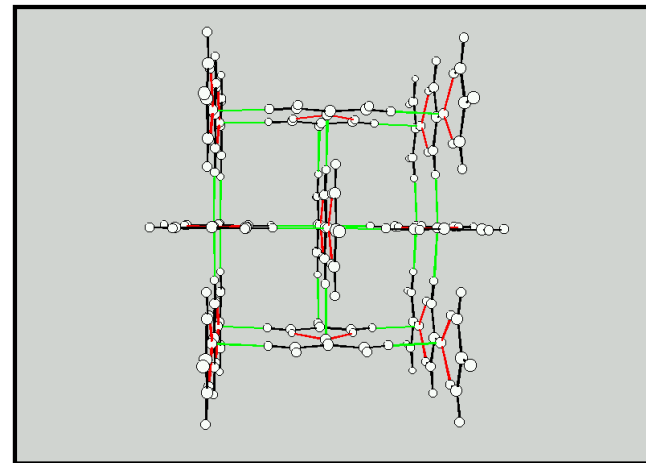
V. R. Saunders

DRAL Daresbury Laboratory, Daresbury, Warrington, Cheshire, WA4 4AD, United Kingdom

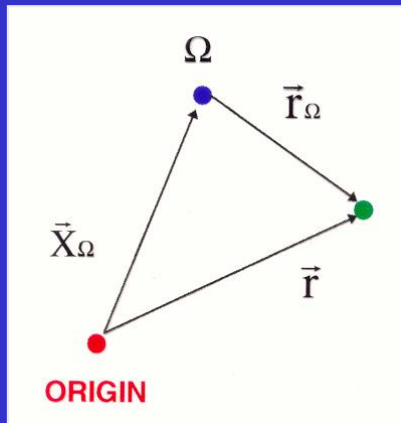
C. Roetti

Gruppo di Chimica Teorica, Università di Torino, via Giuria 5, I-10125 Torino, Italy

JCP 101 , 10686-10696 (1994)



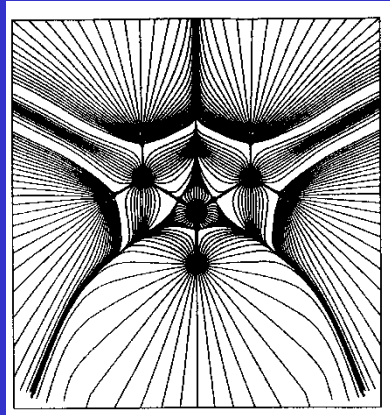
- ✓ How important are packing effects on intramolecular bonds?
- ✓ Does the packing have different impact on the different atoms/chemical groups present in the molecule?
- ➔ How large is the enhancement of the molecular dipole on crystallization?
- ✓ How can each oxygen atom in the urea crystal be involved in four OH...O hydrogen bonds (HBs)?
- ✓ How does the global molecular volume contraction observed in the solid result from the individual atomic volume change on crystallization?



Evaluation of molecular dipole from the basin charge and first moment Bader, Larouche, Gatti et al. JCP 87, 1142 (1987)

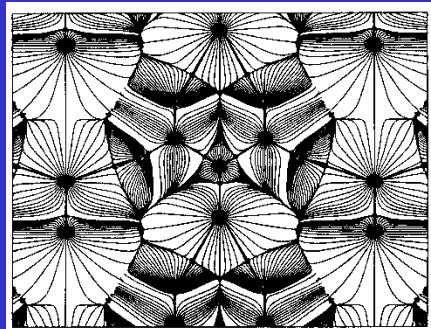
$$\mu = \mu_{el} + \mu_{nuc} = \sum_{\Omega} [-\int_{\Omega} \mathbf{r} \rho(\mathbf{r}) d\tau + \mathbf{X}_{\Omega} Z_{\Omega}]$$

$$\mathbf{r} = \mathbf{r}_{\Omega} + \mathbf{X}_{\Omega} \quad ; \quad q_{\Omega} = Z_{\Omega} - \int_{\Omega} d\mathbf{r} \rho(\mathbf{r}) = Z_{\Omega} - N_{\Omega}$$



$$\mu = \sum_{\Omega} [-\int_{\Omega} \mathbf{r}_{\Omega} \rho(\mathbf{r}) d\tau + \mathbf{X}_{\Omega} (Z_{\Omega} - \int_{\Omega} \rho(\mathbf{r}) d\tau)]$$

$$\mu = \sum_{\Omega} [\mathbf{M}_{\Omega} + \mathbf{X}_{\Omega} q_{\Omega}] = \mu_{AP} + \mu_{CT}$$

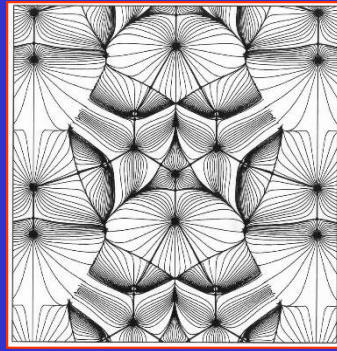
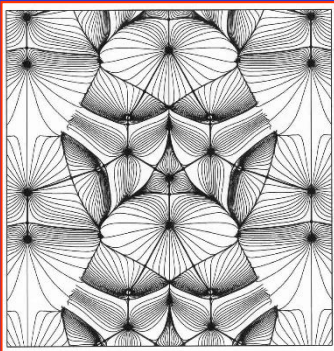
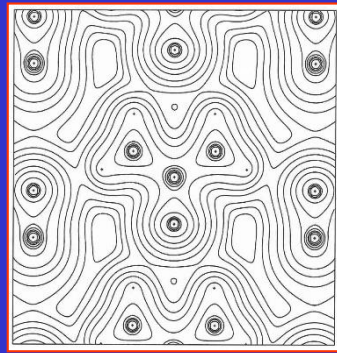
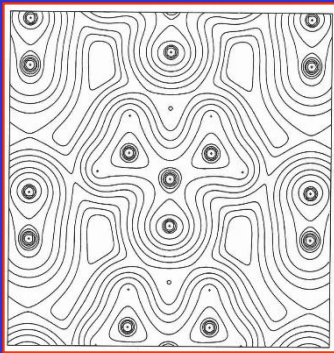


Both sums are origin independent (if $\sum q_{\Omega} = 0$)

For μ_{AP} also each term in the Σ is origin independent

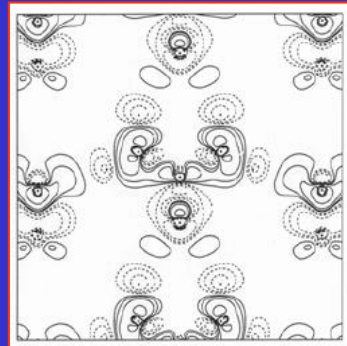
Enhancement of molecular dipole moment of urea in the bulk

- The non-interacting molecules and the crystal periodic RHF densities look very much alike despite the 37% $|\mu|$ enhancement in the crystal



Non interacting molecules

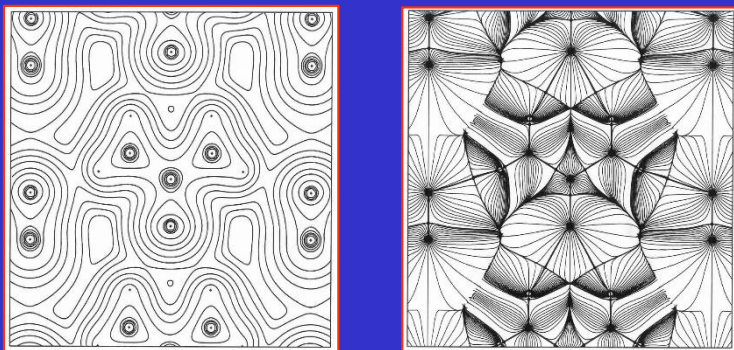
Crystal



Inter. density , Highest contour level $\pm 2 \cdot 10^{-3}$ au

- $|\mu|$ values are very sensitive to the atomic boundaries location and to the atomic ED distribution changes

Contribution	OG Mol.	CG Mol	Crystal
$\mu_A, (\Delta \mu_A \%)$	0.71	0.54	0.45 (-16.7)
$\mu_{CT}, (\Delta \mu_{CT} \%)$	-2.52	-2.56	-3.22 (+25.8)
$\mu, (\Delta \mu \%)$	-1.81	-2.01	-2.77 (+37.1)



Crystal

Clearly the result of a more polarized molecule in the bulk

All the heavy atoms gain electrons at the expense of the H's in the bulk

Following HB formation there is a net flux of 0.067 e^- from the amino-group hydrogen donor to the carbonyl acceptor.

Ω	Mol (CG)	Crystal	
	N (Ω)	N(Ω)	$\Delta N(\Omega)$
C	3.512	3.545	+0.032
O	9.383	9.476	+0.092
N	8.481	8.568	+0.087
H'	0.508	0.454	-0.053
H''	0.565	0.465	-0.100
CO	12.895	13.021	+0.126
NH ₂	9.554	9.487	-0.067

Gatti et al, JCP 101, 10686 (1994)

Crystal field effects on the topological properties of the electron density in molecular crystals: The case of urea

C. Gatti

Centro CNR per lo Studio delle Relazioni tra Struttura e Reattività Chimica, via Golgi 19, I-20133 Milano, Italy

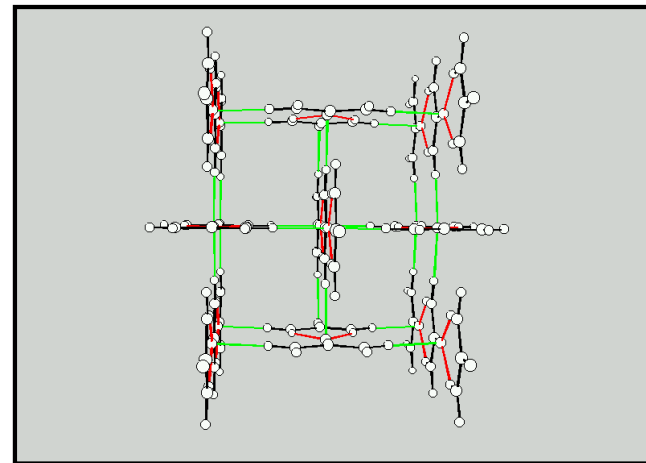
V. R. Saunders

DRAL Daresbury Laboratory, Daresbury, Warrington, Cheshire, WA4 4AD, United Kingdom

C. Roetti

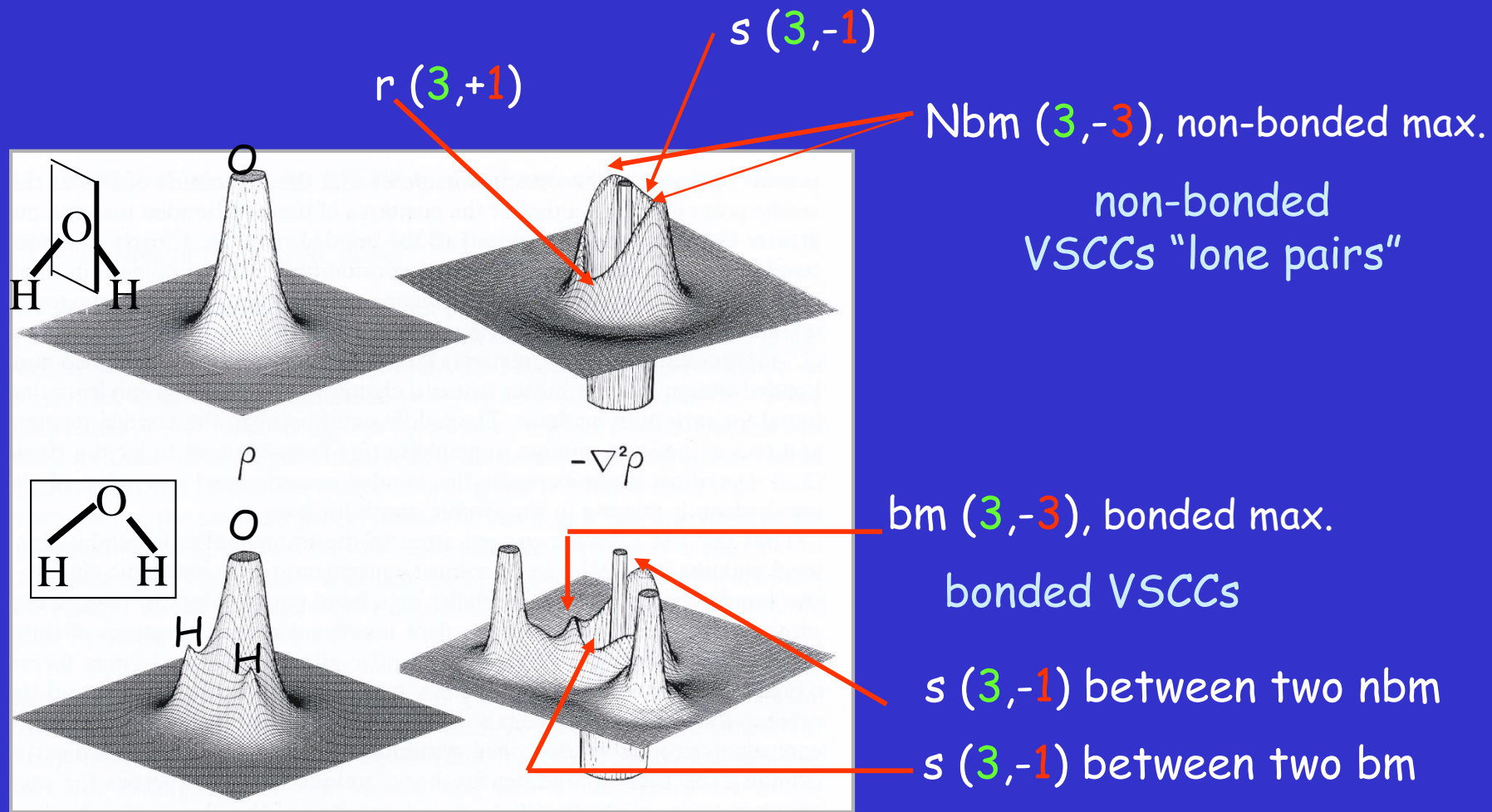
Gruppo di Chimica Teorica, Università di Torino, via Giuria 5, I-10125 Torino, Italy

JCP 101 , 10686-10696 (1994)



- ✓ How important are packing effects on intramolecular bonds?
- ✓ Does the packing have different impact on the different atoms/chemical groups present in the molecule?
- ✓ How large is the enhancement of the molecular dipole on crystallization?
- ➔ How can each oxygen atom in the urea crystal be involved in four OH...O hydrogen bonds (HBs)?
- ✓ How does the global molecular volume contraction observed in the solid result from the individual atomic volume change on crystallization?

$\nabla^2\rho$ and the Lewis Electron Pair Model

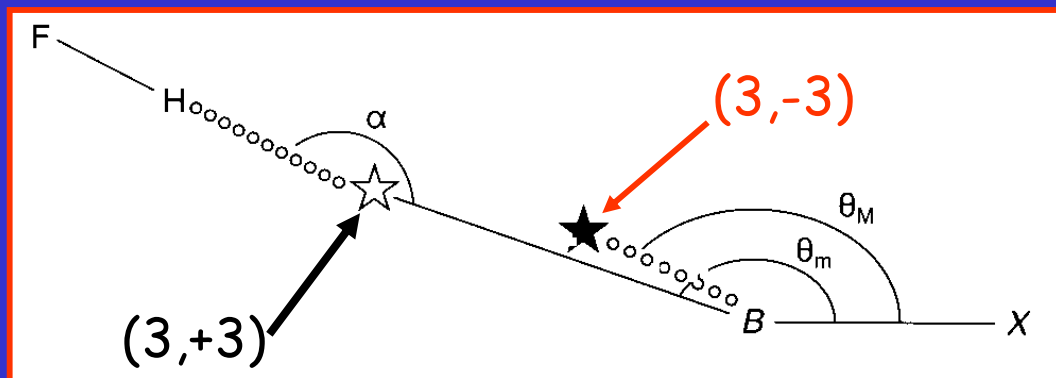


R. F. W. Bader et al. *J. Am. Chem. Soc.* **1984**, 106, 1594.

$$\nabla\rho = 0 \longleftarrow CPs \longrightarrow \nabla(\nabla^2\rho) = 0$$

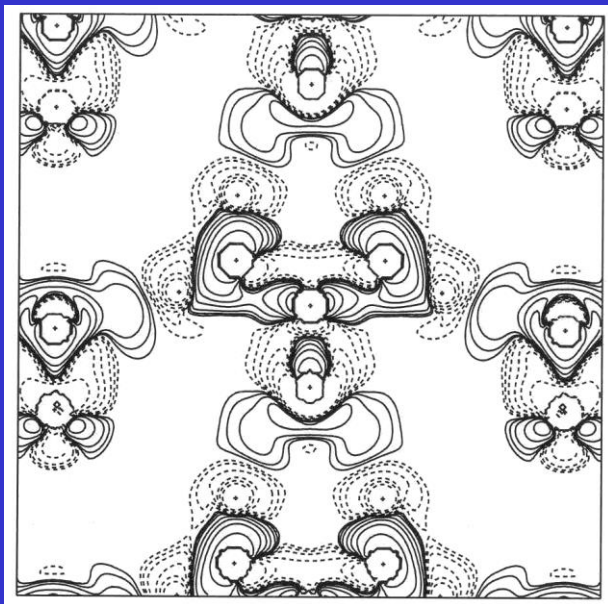
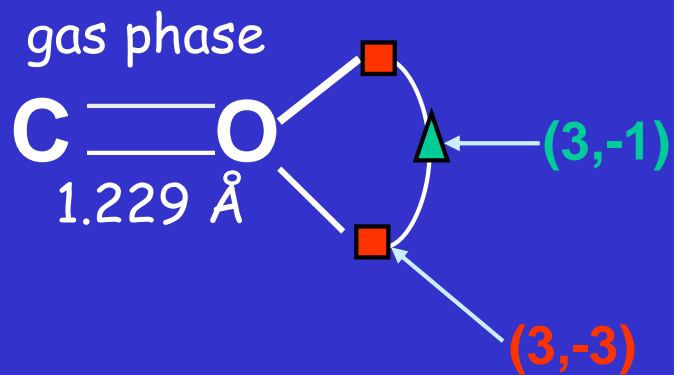
The Laplacian distribution and the H-bonds

- HBs may be seen in terms of a generalized Lewis acid and base interaction

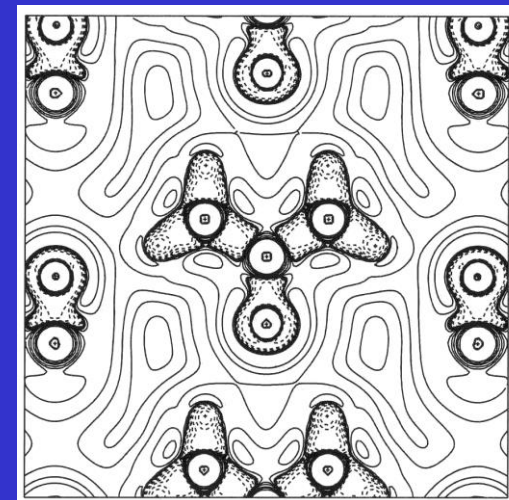
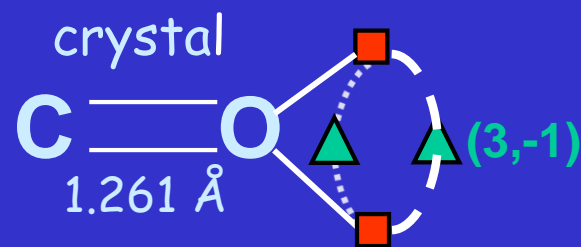
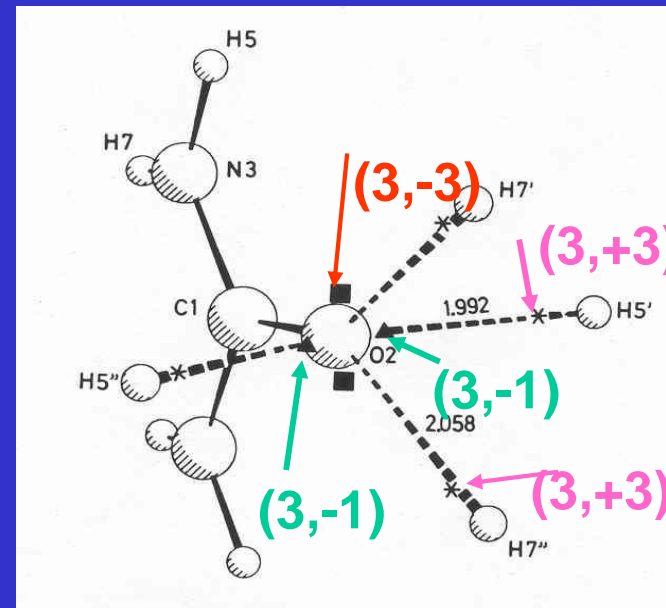


- Generally the approach of the acidic hydrogen to the base will be such as to align the $(3,+3)$ minimum in the VSCC of the H with the most suitable $(3,-3)$ Base maximum

3D-Hydrogen Bonding network in urea: the $-\nabla^2\rho$ description



$$-(\nabla^2\rho_{\text{crystal}} - \nabla^2\rho_{\text{molecule}})$$



$$\nabla^2\rho_{\text{crystal}}$$

Gatti et al., JCP 101,
10686 (1994)

Crystal field effects on the topological properties of the electron density in molecular crystals: The case of urea

C. Gatti

Centro CNR per lo Studio delle Relazioni tra Struttura e Reattività Chimica, via Golgi 19, I-20133 Milano, Italy

V. R. Saunders

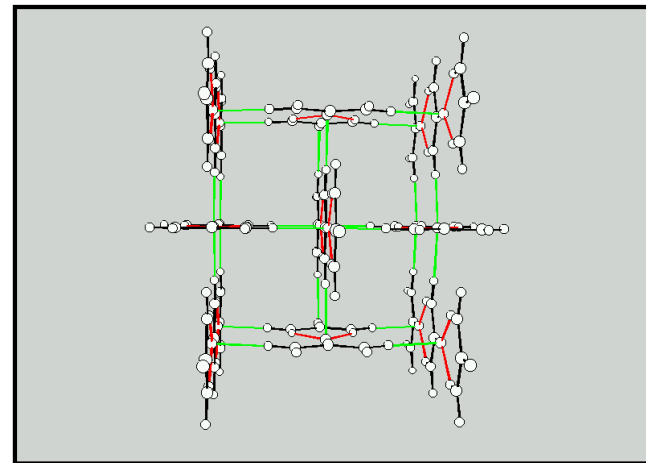
DRAL Daresbury Laboratory, Daresbury, Warrington, Cheshire, WA4 4AD, United Kingdom

C. Roetti

Gruppo di Chimica Teorica, Università di Torino, via Giuria 5, I-10125 Torino, Italy

JCP 101 , 10686-10696 (1994)

- ✓ How important are packing effects on intramolecular bonds?
- ✓ Does the packing have different impact on the different atoms/chemical groups present in the molecule?
- ✓ How large is the enhancement of the molecular dipole on crystallization?
- ✓ How can each oxygen atom in the urea crystal be involved in four OH...O hydrogen bonds (HBs)?
- ➔ How does the global molecular volume contraction observed in the solid result from the individual atomic volume change on crystallization?



Atomic volumes

$$V(\Omega) = \int_{\Omega} d\tau$$

$$\sum_{\Omega \text{ of all cell}} V(\Omega) = V_{\text{cell}}$$

Generally infinite in the molecular case; always finite in the crystalline case

Normally the atomic volume is however defined as the region of space enclosed by the intersection of the atomic zero-flux surface and a particular envelope of ρ

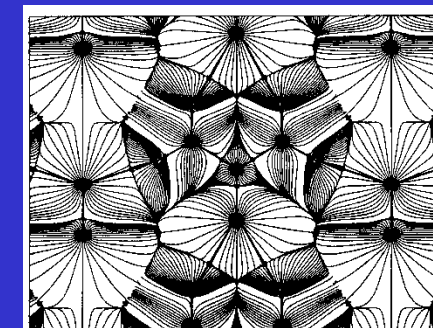
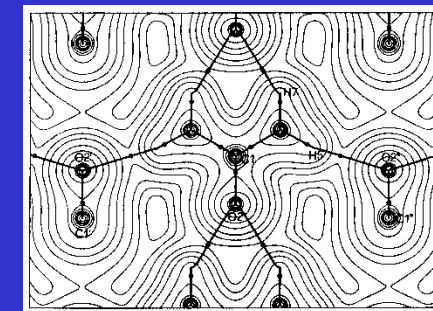
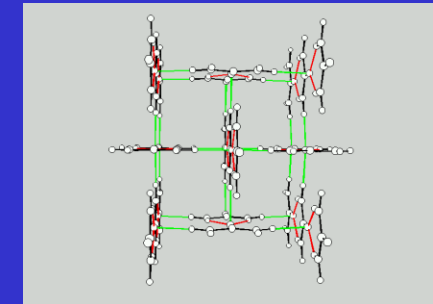
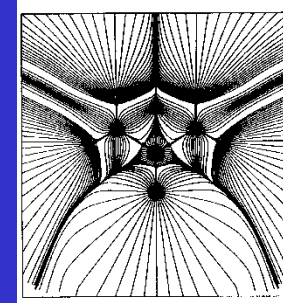
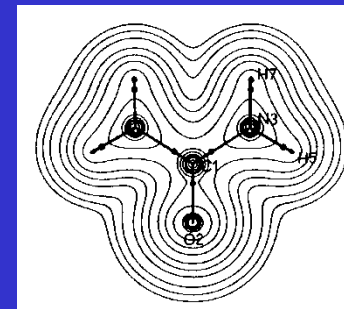
$$V_{0.001}(\Omega) \equiv V1 = \int_{\Omega^*} d\tau ; \quad \Omega^*: \forall \mathbf{r} \in \Omega \text{ where } \rho \geq 0.001 \text{ au}$$

$V_{0.001}$ yields molecular sizes in agreement with those determined from the analysis of the kinetic theory data for gas-phase molecules (van der Waals volumes)

$$V_{0.002}(\Omega) \equiv V2 = \int_{\Omega^{**}} d\tau ; \quad \Omega^{**}: \forall \mathbf{r} \in \Omega \text{ where } \rho \geq 0.002 \text{ au}$$

$V_{0.002}$ yields molecular sizes compatible with the closer packing found in the solid state

Ω	Molecule (CG)		Crystal		
	V1	V2	V1	V2	V_{tot}
C	19.9	18.5	21.0	19.1	21.2
O	132.2	111.1	115.6	104.6	124.3
N	117.9	101.4	120.2	107.5	135.0
H'	24.6	18.8	16.8	15.3	17.7
H''	27.4	20.8	18.2	16.3	18.7
CO	152.1	129.6	136.6	123.7	145.5
NH ₂	170.0	140.9	155.2	139.1	171.4
Molec	492.2	411.5	447.0	401.8	488.2



As a reaction of molecules to the intermolecular exch. forces:

✓ V1 -10% ; V2 -2% ; $V_{\text{tot, cry}} \approx V1$, gas phase

✓ V2 is $\approx 90\%$ and 83% of V1 in the bulk and gas phase: the molecular density dies off more rapidly in the bulk

✓ the reported trends do not apply to single Ω , but they do to the functional groups CO and NH₂

✓ Contraction of mol. volume in crystal arises primarily from contraction of the Ω 's directly involved in H-bonds

O : $\Delta V_2 = -6\%$, $\Delta V_1 = -13\%$; H'(H'') : $\Delta V_2 = -19(-28)\%$

- ❑ Few studies have appeared on $s(\mathbf{r})$ thus far despite its role in Spin DFT Functional theory and it being the basic observable for describing and understanding magnetic phenomena
- ❑ A systematic full topological analysis of this function is lacking, in seemingly contrast to the blossoming in the last 20 years of many studies on the topological features of other scalar fields of chemical interest.
- ❑ Filling this gap, we may unveil that kind of information hidden in the $s(\mathbf{r})$ distribution which only its topology can disclose.

 $s(\mathbf{r})$ Critical points (CPs)

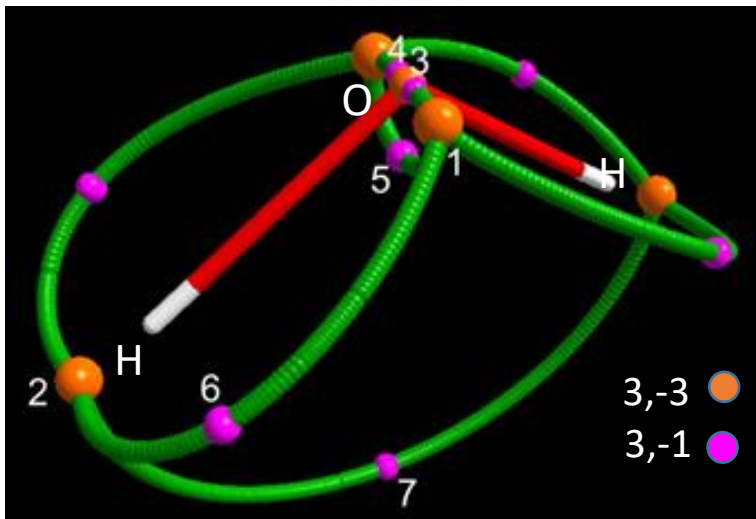
$$\nabla S(\mathbf{r}_{CP}) = \nabla(\rho_{\alpha}(\mathbf{r}_{CP}) - \rho_{\beta}(\mathbf{r}_{CP})) = 0 \rightarrow \nabla\rho_{\alpha}(\mathbf{r}_{CP}) \equiv \nabla\rho_{\beta}(\mathbf{r}_{CP})$$

This condition is opposite to that for $\rho(\mathbf{r})$ at CP : $\nabla\rho_{\alpha}(\mathbf{r}_{CP}) \equiv -\nabla\rho_{\beta}(\mathbf{r}_{CP})$. This latter, in the case of a non-spin-polarized system is also more stringent as both derivatives need to be equal to zero.

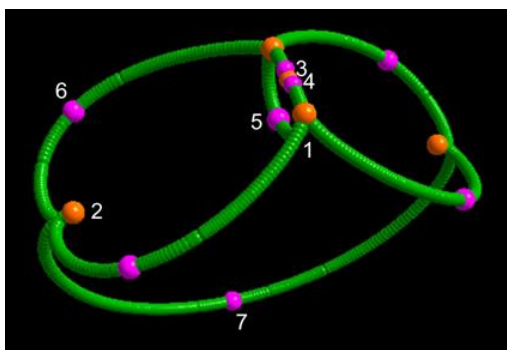


$s(\mathbf{r})$ CPs will clearly differ in number and location relative to those of $\rho(\mathbf{r})$

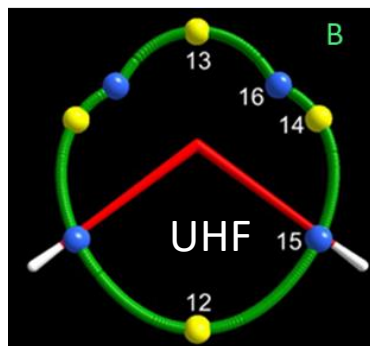
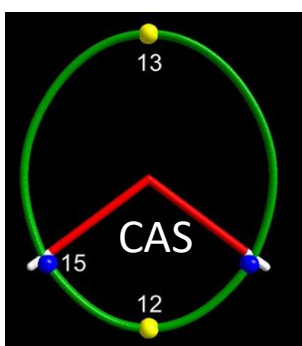
H₂O in the ³B₁ state



s spin graph (α - α maxima joining paths) and molecular graph (CAS)



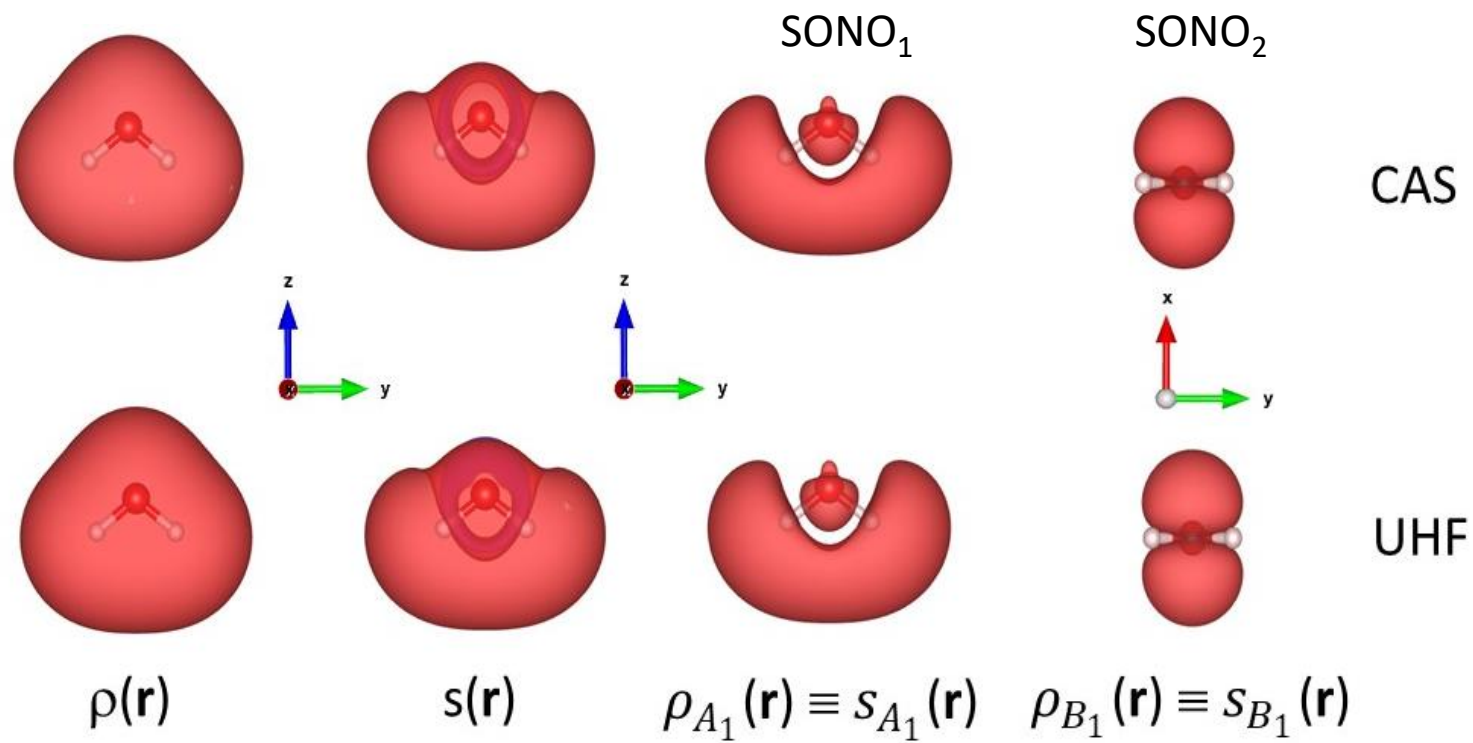
s spin graph of only s_{mag} (CAS)



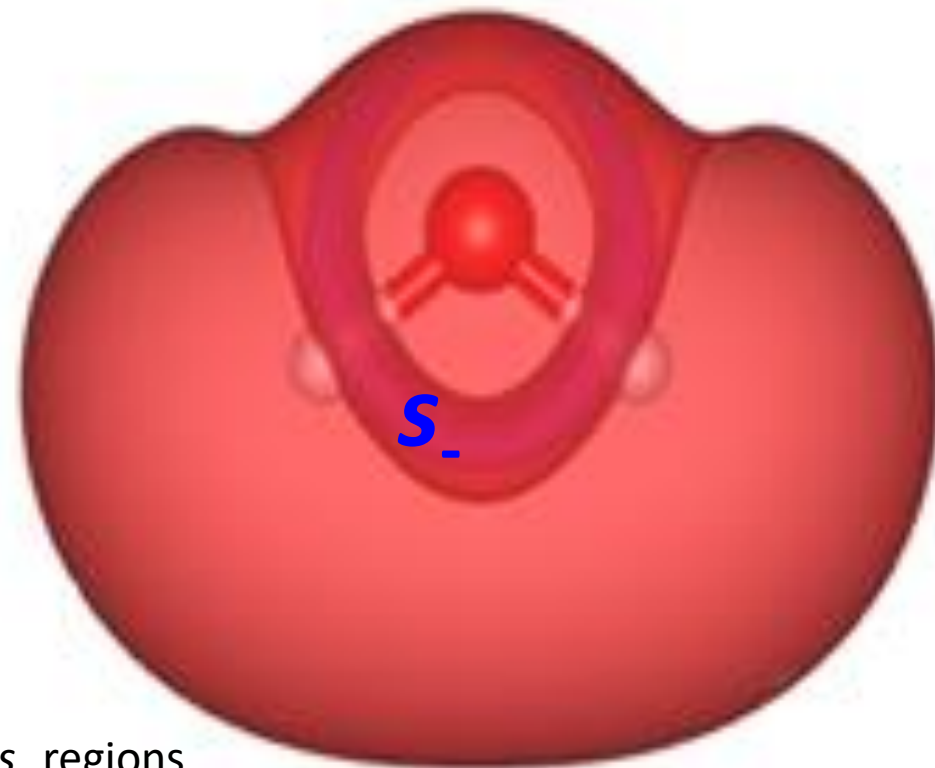
s spin graph (β - β maxima joining paths)

3,-3 ●
3,-1 ● $-s(r)$

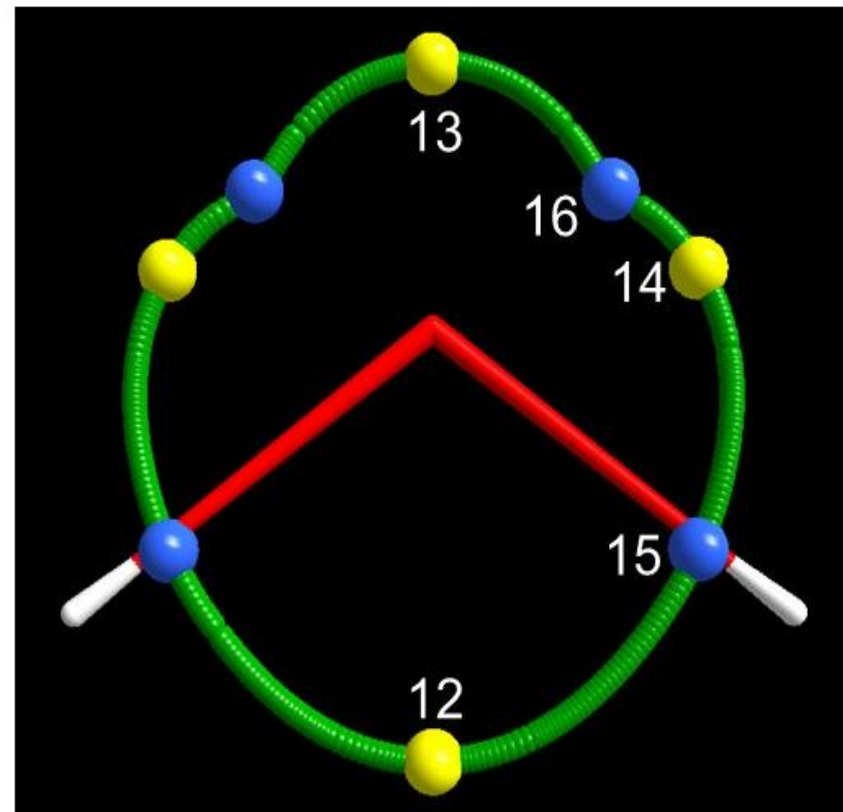
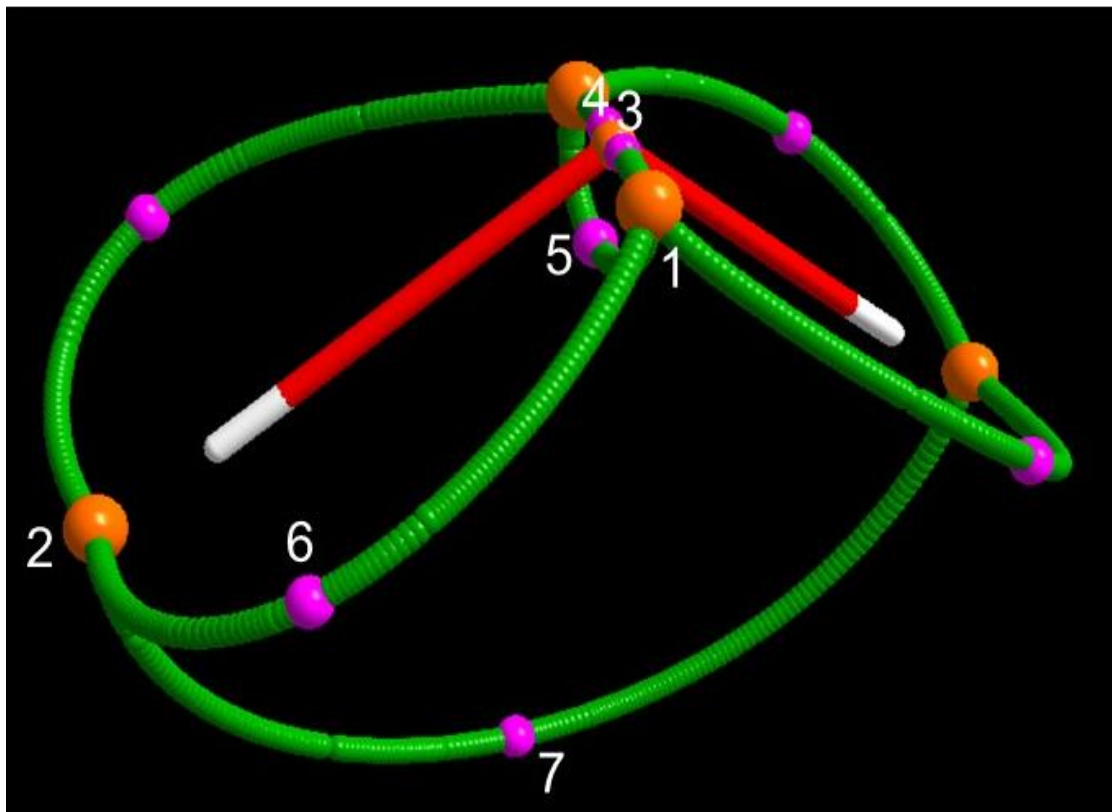
- ❑ s topology is richer and less trivial than that of $\rho(r)$, **25 CPs vs 5, 15 vs 3** unique CPs (CAS level).
- ❑ $s(r)$, differently from $\rho(r)$ and likewise ESP or $\nabla^2\rho(r)$ exhibits either positive (s_+) or negative (s_-) local values. The only constraint on s is that $\int_{R^3} s(r) = n_\alpha$ (number of the excess α -electrons)
- ❑ The possibility of negative values for a scalar has an impact on the total number and kind of its CPs. The scalar is topologically analysed by separating regions where it is >0 from those where it is <0 and by treating each of them as a distinct system.
- ❑ s_+ topology is (almost) stable with the method, while s_- is largely method dependent (or absent by nature, ROHF)
- ❑ Each $s(r)$ may be decomposed into a *magnetic* (due to the fully unpaired α -electron density, SONOs) and a *relaxation* part (due to the remaining α - and β -electrons density). The magnetic part is “stable” and resembles s_+ while the relaxation part is rather method dependent
- ❑ $n_{-3} - n_{-1} + n_{+1} - n_{+3} = n_+ - n_-$ (n_+ and n_- number of asymptotic minima and maxima) If the s_- regions are **fully embedded** in s_+ regions, n_- will be equal to 0 and the CPs of the whole $s(r)$ fulfils $n_{-3} - n_{-1} + n_{+1} - n_{+3} = 1$ as $\rho(r)$ (Poincaré-Hopf relationship)
- ❑ The collection of α - α maxima (or β - β maxima) joining paths is a *molecular spin graph*. A spin-polarised system has as many α - α and β - β *molecular spin graphs* as is the number of its s_+ and s_- separate regions. α - α (β - β) maxima joining paths link maximally α - (β -)polarized centers



s_+
 s_-

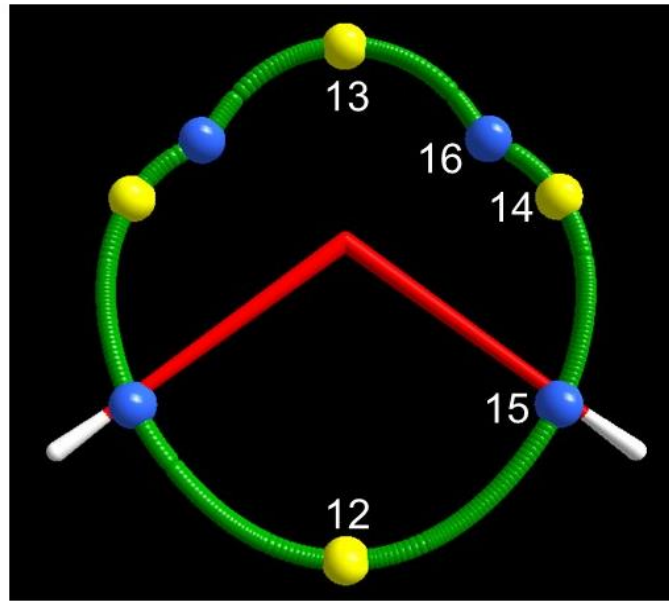
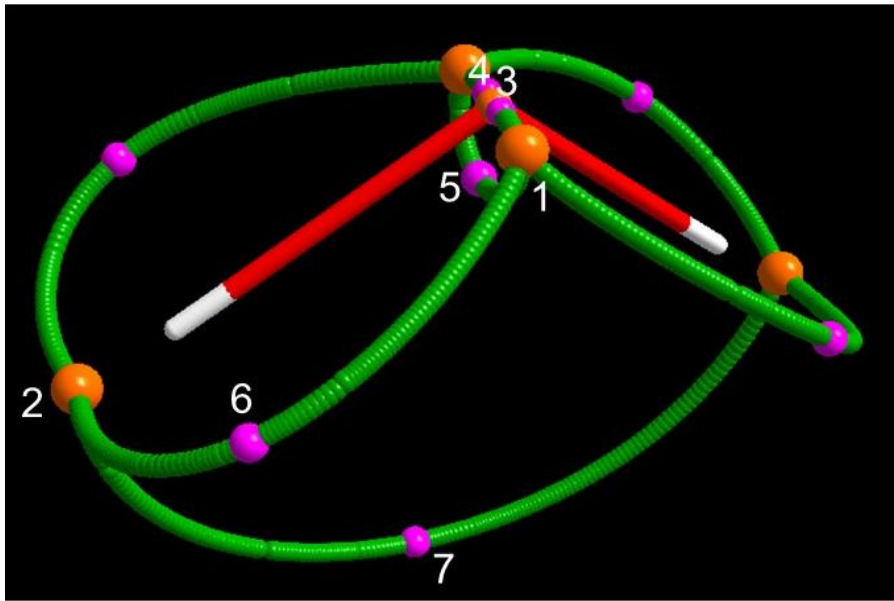


For 3B_1 H₂O the s_- regions are **fully embedded** in s_+ regions



Two kinds of structures are associated with a spin-polarized molecule:

- ❑ *Molecular graph* structure (defined through $\nabla\rho$ and the collection of bond paths)
- +
- ❑ *Spin graph* magnetic structure (defined through ∇s and composed in general by at least two independent spin graphs, related to spin-density maxima and minima)



- ❑ The spin structure of the 3B_1 H_2O molecule is more complex than its total electron structure, but both concur to a complete description of the molecule. It is like observing the same molecule by wearing two different pairs of lenses.
- ❑ One of these pairs is working in summation of the α - and β -densities, while the other in subtraction of the same densities.

The spin density structure does not have a direct connection between O and H nuclei as in the molecular graph. Yet, it exhibits a direct link between the maxima located nearby the H nuclei. The two O-H linkages of the conventional structure of H_2O are replaced in the spin graph by 4 much longer linkages between maxima associated with the unpaired electrons of the O atom, lying quite far apart from the nucleus and the maxima close to the H nuclei. In addition, there are 3 more gradient paths, all contained within the O atomic basin

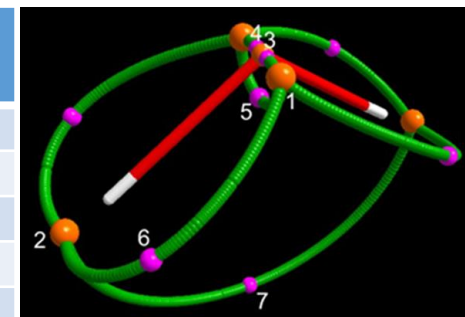
□ The four kind of CPS may be further classified in 18 different types depending on relative concentration/depletion of the α and β densities at CP

	CP(r,s)	$-\nabla^2s$	Type	$-\nabla^2\rho_\alpha$	$-\nabla^2\rho_\beta$	Constraint
3	(3, -3), max	> 0	1	> 0	> 0	$-\nabla^2\rho_\alpha > -\nabla^2\rho_\beta$
		> 0	2	> 0	< 0	None
		> 0	3	< 0	< 0	$ \nabla^2\rho_\alpha < \nabla^2\rho_\beta $
6	(3, -1), 1st order SP	> 0	1	> 0	> 0	$-\nabla^2\rho_\alpha > -\nabla^2\rho_\beta$
		> 0	2	> 0	< 0	None
		> 0	3	< 0	< 0	$ \nabla^2\rho_\alpha < \nabla^2\rho_\beta $
		< 0	4	> 0	> 0	$-\nabla^2\rho_\alpha < -\nabla^2\rho_\beta$
		< 0	5	< 0	> 0	None
		< 0	6	< 0	< 0	$ \nabla^2\rho_\alpha > \nabla^2\rho_\beta $
6	(3, +1), 2nd order SP	Same as for (3, -1)				
3	(3, +3), min	< 0	1	> 0	> 0	$-\nabla^2\rho_\alpha < -\nabla^2\rho_\beta$
		< 0	2	< 0	> 0	None
		< 0	3	< 0	< 0	$ \nabla^2\rho_\alpha > \nabla^2\rho_\beta $

18 in total

Electron Spin density (3,-3) and (3,-1) CPs in the H₂O ³B₁ state

N	M	WFN	Type	s	s _{mag}	ρ	∇ρ _α ≡ ∇ρ _β	∇ ² s	∇ ² ρ _α	∇ ² ρ _β	SPI(r _c)
1	2	ROHF	3	0.603	0.603	1.938	8.715	-26.978	81.209	108.186	1.269
	2	UHF	3	0.613	0.607	1.816	7.714	-25.944	71.334	97.278	1.346
	2	CAS	3	0.617	0.615	1.820	7.681	-25.670	71.105	96.775	1.351
2	2	ROHF	1	0.018	0.018	0.263	0.341	-0.697	-5.517	-4.821	0.765
	2	UHF	2	0.015	0.016	0.090	0.123	-0.119	-0.091	0.028	0.923
	2	CAS	3	0.012	0.014	0.072	0.096	-0.082	0.003	0.086	0.936
3	1	ROHF	1	0.683	0.683	295.534	557.768	-5.6 × 10 ³	-1.2 × 10 ⁶	-1.2 × 10 ⁶	0.670
	1	UHF	1	0.840	0.706	295.432	587.366	-6.7 × 10 ³	-1.2 × 10 ⁶	-1.2 × 10 ⁶	0.670
	1	CAS	1	1.262	0.725	295.814	408.328	-10.1 × 10 ³	-1.2 × 10 ⁶	-1.2 × 10 ⁶	0.672
4	2	ROHF	1	0.367	0.367	82.250	648.694	-45.534	-4.85 × 10 ³	-4.80 × 10 ³	0.673
	2	UHF	1	0.415	0.380	64.569	503.389	-47.064	-1.91 × 10 ³	-1.86 × 10 ³	0.675
	2	CAS	1	0.474	0.417	41.885	323.092	-45.172	-66.122	-20.950	0.682
5	1	ROHF	6	0.094	0.094	1.265	1.691	2.051	8.785	6.734	0.773
	1	UHF	6	0.130	0.100	1.308	1.921	1.206	11.013	9.807	0.813
	1	CAS	6	0.147	0.102	1.327	2.032	0.850	11.728	10.877	0.833
6	4	ROHF	6	0.006	0.006	0.085	0.098	0.023	0.099	0.077	0.744
	4	UHF	6	0.005	0.006	0.048	0.057	0.013	0.086	0.073	0.819
	4	CAS	6	0.004	0.005	0.039	0.047	0.010	0.076	0.066	0.826
7	1	ROHF	3	0.003	0.003	0.006	0.003	-0.002	0.003	0.006	2.455
	1	UHF	3	0.003	0.004	0.006	0.003	-0.003	0.003	0.005	2.575
	1	CAS	3	0.003	0.003	0.006	0.003	-0.003	0.002	0.005	2.581



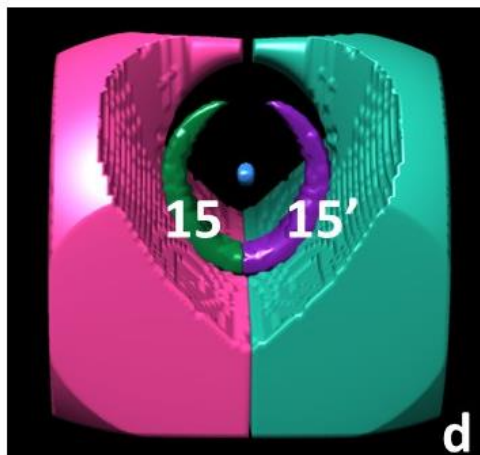
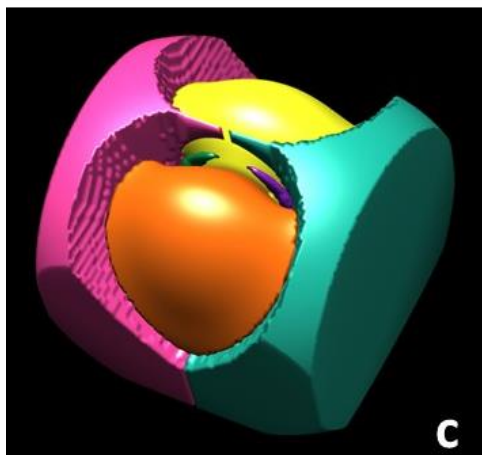
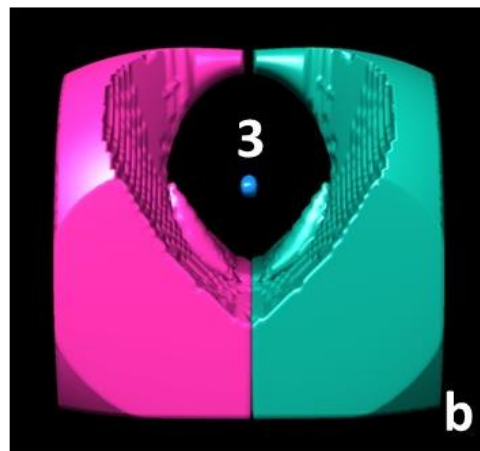
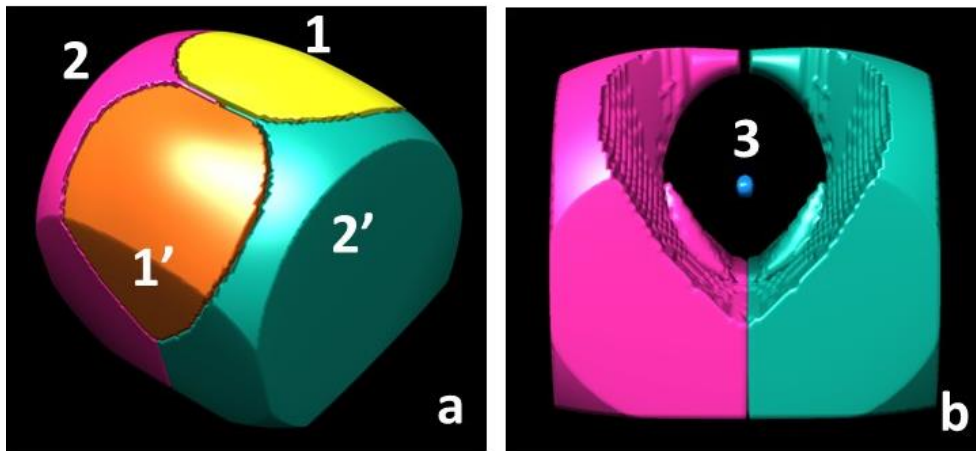
$$\text{SPI}(\mathbf{r}) = \frac{\rho_{\alpha}(\mathbf{r})/\rho_{\beta}(\mathbf{r})}{N_{\alpha}/N_{\beta}}$$

Spin Polarization Index

SPI ≡ 1 if local polarization is = to the average

> 1 higher; < 1 lower

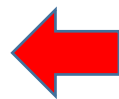
No polarization
1/ (N_α/N_β)
(0.667 for H₂O ³B₁ state)



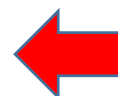
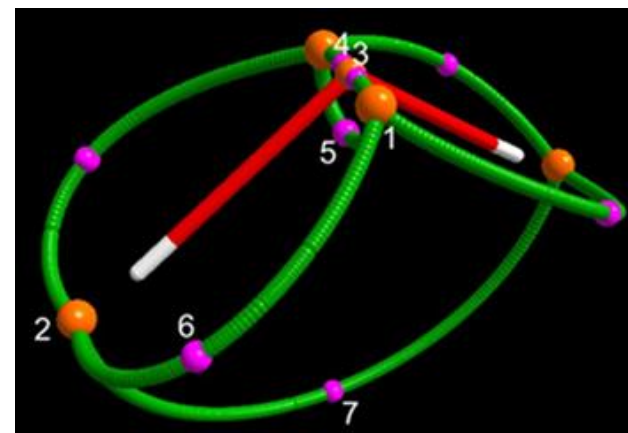
3B_1 H₂O CAS spin-density basins

Basins labelled by their enclosed (3, -3) spin maximum or, for basin 15, by its enclosed (3, +3) spin minimum

Each basin retains the same colour in all panels



Basins bounded by local Zero-Flux Surfaces (ZFS) of ∇s
 May contain points with either $s(\mathbf{r}) > 0$ and $s(\mathbf{r}) < 0$
 The ∇s ZFS basins are not “quantum” object, so other basins are worth of being considered



Basins bounded by $s = 0$ isosurfaces (s_+ and s_- basins)
 They contains only positive (s_+) or only negative (s_-) s points.
 This disjoint, exhaustive and alternative R^3 space partition, separates molecular regions in terms of their α - or β -density dominance. The sum of population of s_- basins yields a quantitative measure of the spin counter-polarization effect, enabling to judge the quality of the wf model ($\Sigma = 0$ for ROHF)

Panels **b** (**d**) differ from panels **a** (**c**) for the removal of basins 1 and 1'. The small, embedded basin 3 around the O nucleus is disclosed

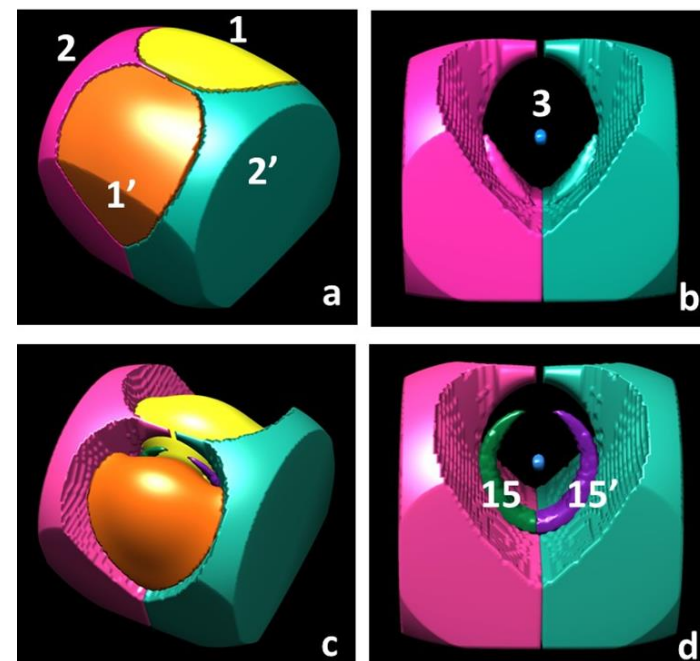
Ω	M	WFN	N_Ω	SP_Ω	$SP_{mag,\Omega}$	SPI_Ω	$V1_\Omega$	$V2_\Omega$	\bar{s}_Ω
$\nabla\rho$ ZFS boundaries									
O	1	ROHF	8.867	1.409	=	0.919	180.6	127.4	0.008
	1	UHF	8.856	1.417	1.409	0.921	179.2	126.8	0.008
	1	CAS	8.743	1.406	1.387	0.922	173.3	122.5	0.008
H	2	ROHF	0.565	0.294	=	2.113	71.8	39.8	0.004
	2	UHF	0.571	0.290	0.295	2.046	72.2	40.3	0.004
	2	CAS	0.628	0.296	0.306	1.856	76.9	42.6	0.004
∇s ZFS boundaries									
Ω_1	2	ROHF	3.469	0.587	=	0.938	53.9	42.0	0.011
	2	UHF	3.740	0.597	0.591	0.920	52.1	40.9	0.011
	2	CAS	3.620	0.604	0.595	0.934	52.4	40.9	0.012
Ω_2	2	ROHF	0.901	0.409	=	1.773	108.3	61.4	0.004
	2	UHF	0.907	0.402	0.407	1.727	109.8	62.7	0.004
	2	CAS	0.913	0.394	0.403	1.676	111.2	63.0	0.004
Ω_3	1	ROHF	1.231	0.006	=	0.673	0.04	0.04	0.174
	1	UHF	0.699	0.003	0.002	0.672	0.01	0.01	0.196
	1	CAS	0.935	0.005	0.002	0.674	0.02	0.02	0.231
$s = 0$ isovalue surface boundaries									
Ω_1	2	UHF	3.574	0.598	0.587	0.935	50.9	39.7	0.012
	2	CAS	3.509	0.606	0.589	0.945	51.6	40.2	0.012
Ω_2	2	UHF	0.836	0.403	0.409	1.906	109.4	62.3	0.004
	2	CAS	0.821	0.395	0.407	1.901	110.6	62.3	0.004
Ω_3	1	UHF	0.640	0.002	0.002	0.671	0.01	0.01	0.210
	1	CAS	0.916	0.005	0.004	0.674	0.02	0.02	0.237
Ω_{15}	2	UHF	0.173	-0.002	0.002	0.653	1.02	1.02	-0.002
	2	CAS	0.212	-0.003	0.003	0.650	1.45	1.45	-0.002
Ω_{16}	2	UHF	0.097	-0.000	0.001	0.660	0.68	0.68	-0.001

$$SPI_\Omega = \frac{N_{\alpha,\Omega} / N_{\beta,\Omega}}{N_\alpha / N_\beta}$$

Basin SPI :Same meaning as the local SPI, but referred to the whole basin

$$\bar{s}_\Omega = SP_\Omega / V1_\Omega$$

\bar{s}_Ω is an absolute measure of the basin average α -electron excess.



Ω	M	WFN	N_{Ω}	SP_{Ω}	$SP_{mag,\Omega}$	SPI_{Ω}	$V1_{\Omega}$	$V2_{\Omega}$	\bar{s}_{Ω}
$\nabla\rho$ ZFS boundaries									
O	1	ROHF	8.867	1.409	=	0.919	180.6	127.4	0.008
	1	UHF	8.856	1.417	1.409	0.921	179.2	126.8	0.008
	1	CAS	8.743	1.406	1.387	0.922	173.3	122.5	0.008
H	2	ROHF	0.565	0.294	=	2.113	71.8	39.8	0.004
	2	UHF	0.571	0.290	0.295	2.046	72.2	40.3	0.004
	2	CAS	0.628	0.296	0.306	1.856	76.9	42.6	0.004
∇s ZFS boundaries									
Ω_1	2	ROHF	3.469	0.587	=	0.938	53.9	42.0	0.011
	2	UHF	3.740	0.597	0.591	0.920	52.1	40.9	0.011
	2	CAS	3.620	0.604	0.595	0.934	52.4	40.9	0.012
Ω_2	2	ROHF	0.901	0.409	=	1.773	108.3	61.4	0.004
	2	UHF	0.907	0.402	0.407	1.727	109.8	62.7	0.004
	2	CAS	0.913	0.394	0.403	1.676	111.2	63.0	0.004
Ω_3	1	ROHF	1.231	0.006	=	0.673	0.04	0.04	0.174
	1	UHF	0.699	0.003	0.002	0.672	0.01	0.01	0.196
	1	CAS	0.935	0.005	0.002	0.674	0.02	0.02	0.231
$s = 0$ isovalue surface boundaries									
Ω_1	2	UHF	3.574	0.598	0.587	0.935	50.9	39.7	0.012
	2	CAS	3.509	0.606	0.589	0.945	51.6	40.2	0.012
Ω_2	2	UHF	0.836	0.403	0.409	1.906	109.4	62.3	0.004
	2	CAS	0.821	0.395	0.407	1.901	110.6	62.3	0.004
Ω_3	1	UHF	0.640	0.002	0.002	0.671	0.01	0.01	0.210
	1	CAS	0.916	0.005	0.004	0.674	0.02	0.02	0.237
Ω_{15}	2	UHF	0.173	-0.002	0.002	0.653	1.02	1.02	-0.002
	2	CAS	0.212	-0.003	0.003	0.650	1.45	1.45	-0.002
Ω_{16}	2	UHF	0.097	-0.000	0.001	0.660	0.68	0.68	-0.001

- ❑ The electron and (α - β) spin population of all s_{\cdot} basins sum up to 0.424 and $-0.006 e^{-}$ at the CAS level and to 0.540 and $-0.004 e^{-}$ at the UHF level.
- ❑ About 6% of the valence electrons in the molecule are included in these basins.
- ❑ The spin populations of these basins are dominated by the relaxation component, $SP_{mag,\Omega}$ being, by nature, positive.
- ❑ The spin polarization index SPI_{Ω} needs to be smaller than $2/3$, but it is just below this value (about 0.65), marginally different from the $\rho_{\alpha} = \rho_{\beta}$ reference value ($2/3$)
- ❑ N_{Ω} and SP_{Ω} values, sizes and other properties of the s_{\cdot} basins collectively highlight the relevance of going beyond ROHF restriction

Preliminary Conclusions

- ❑ Novel notions, such as *spin graphs*, *spin basins* and *spin valence*, and novel descriptors, such as the local/integral *Spin Polarization Indices (SPI)* or the *basin average spin density*
- ❑ Two kinds of structures associated with a spin-polarized molecule (the usual one and the magnetic structure consisting of at least two spin graphs)
- ❑ Local and nonlocal $s(\mathbf{r})$ descriptors help to explain real-space magnetic structure and to single out those features that are largely model dependent
- ❑ Spin-density topology discloses a wealth of chemically and physically meaningful information. Most of the introduced spin-density descriptors do not require the explicit knowledge of the system's wavefunction, being therefore amenable to experimental investigation of the $s(\mathbf{r})$ observable
- ❑ Pioneering studies based on combined X-ray and neutron structure factors are already available; in the next future, it is foreseeable that a combination of accurate neutron detectors and more intense sources will disclose more and more reliable and precise experimental spin-density distributions in crystalline materials
- ❑ The topological toolbox helps to gain insights into yet unexplored aspects of complex magnetic structures



ISTITUTO DI SCIENZE E TECNOLOGIE CHIMICHE GIULIO NATTA

The Electrostatic Potential Source Function (EPSF)
reconstruction: a valuable tool to study High-Performance
Liquid Chromatography (HPLC) enantioseparations involving
 σ - and π -holes as recognition sites

Carlo Gatti (c.gatti@scitec.cnr.it)

Milano, Golgi



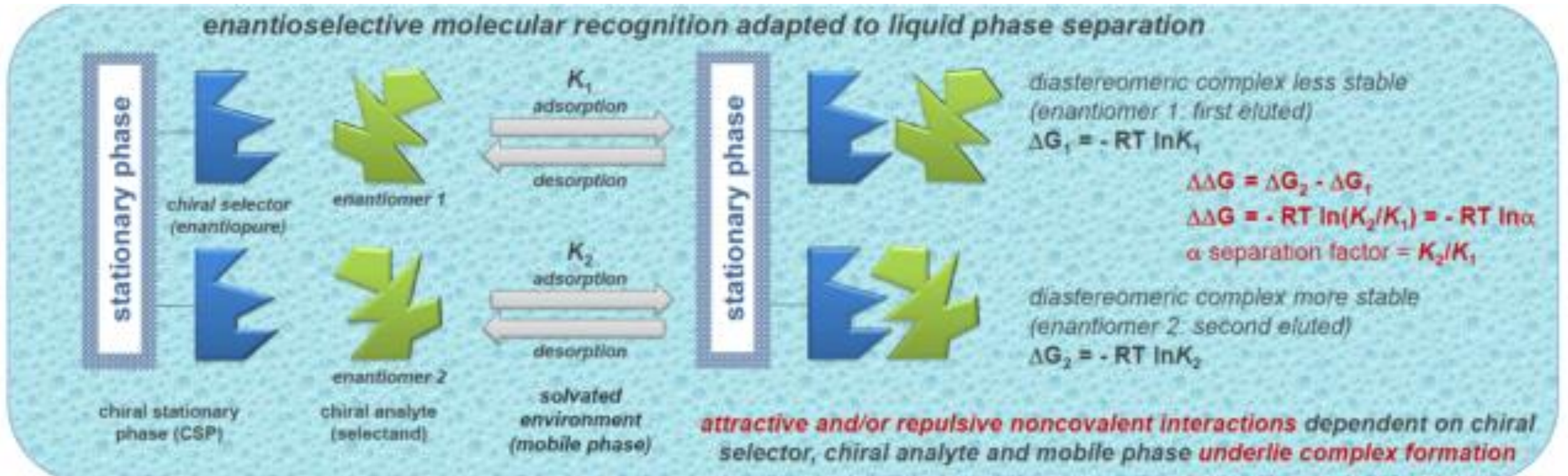
«SCITEC Days»
presentiamoci

COMPUTATIONAL
MODELING

29 Aprile 2021

HPLC enantioselective molecular recognition

- Stereospecific recognition of chiral molecules is an important issue in various aspects of life sciences and chemistry including analytical separation sciences

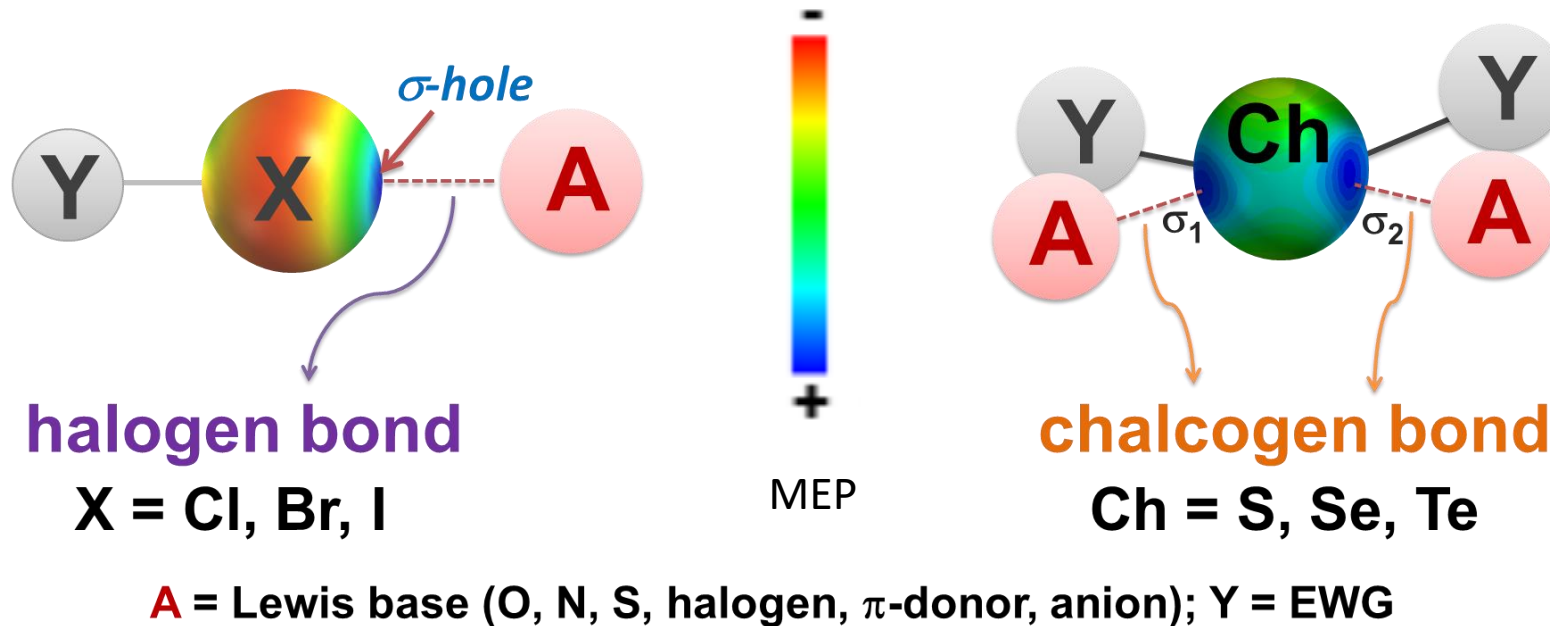


- The basis of analytical enantioseparations is the formation of transient diastereomeric complexes driven by **hydrogen bonds or ionic, ion-dipole, dipole-dipole, van der Waals as well as π - π interactions**



Halogen and chalcogen bonds

- XB can drive enantioseparations in HPLC environment. XB is profiled as a chemo-, regio-, site- and stereoselective interaction which is active in HPLC environment *besides* other known interactions based on the complementarity between selector and selectand
- Chalcogen bonds (ChB) were also found to act as stereoselective secondary interactions for HPLC enantioseparations



ChB: σ -hole based NCI between a Lewis base and an electrophilic element of group VI, which behaves as a Lewis acid

Journal of Chromatography A, 1467 (2016) 228–238

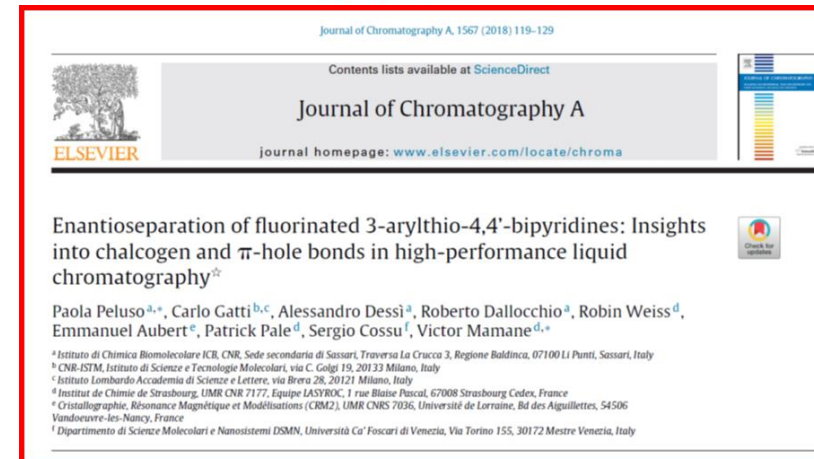


Contents lists available at ScienceDirect
 Journal of Chromatography A
 journal homepage: www.elsevier.com/locate/chroma

Insights into halogen bond-driven enantioseparations
 Paola Peluso^{a,*}, Victor Mamane^{b,a}, Emmanuel Aubert^c, Alessandro Dessì^a, Roberto Dallocchio^a, Antonio Dore^d, Patrick Pale^b, Sergio Cossu^e

^a Istituto di Chimica Biomolecolare ICB, CNR, UOS di Sassari, Traversa La Crucca 3, Regione Baidinca, I-07100 Li Punti, Sassari, Italy
^b Institut de Chimie de Strasbourg, UMR 7177, Equipe IASVROC, 1 rue Blaise Pascal, BP 206 88, 67088 Strasbourg Cedex, France
^c Cristallographie, Résonance Magnétique et Modélisations (CRM2), UMR CNRS 7036, Université de Lorraine, BP 70239, Bd des Aiguillettes, 54506 Vandœuvre-lès-Nancy, France
^d ICPA, CNR, UOS di Sassari, Traversa La Crucca 3, Regione Baidinca, I-07100 Li Punti, Sassari, Italy
^e Dipartimento di Scienze Molecolari e Nanosistemi, Università Ca' Foscari di Venezia, Via Torino 155, I-30172 Mestre Venezia, Italy

Journal of Chromatography A, 1567 (2018) 119–129



Journal of Chromatography A, 1567 (2018) 119–129
 Contents lists available at ScienceDirect
 Journal of Chromatography A
 journal homepage: www.elsevier.com/locate/chroma

Enantioseparation of fluorinated 3-arylthio-4,4'-bipyridines: Insights into chalcogen and π -hole bonds in high-performance liquid chromatography[†]

Paola Peluso^{a,*}, Carlo Gatti^{b,c}, Alessandro Dessì^a, Roberto Dallocchio^a, Robin Weiss^d, Emmanuel Aubert^e, Patrick Pale^d, Sergio Cossu^f, Victor Mamane^{d,a}

^a Istituto di Chimica Biomolecolare ICB, CNR, Sede secondaria di Sassari, Traversa La Crucca 3, Regione Baidinca, 07100 Li Punti, Sassari, Italy
^b CNR-ISTM, Istituto di Scienze e Tecnologie Molecolari, via C. Golgi 19, 20133 Milano, Italy
^c Istituto Lombardo Accademia di Scienze e Lettere, via Brera 28, 20121 Milano, Italy
^d Institut de Chimie de Strasbourg, UMR CNR 7177, Equipe IASVROC, 1 rue Blaise Pascal, 67088 Strasbourg Cedex, France
^e Cristallographie, Résonance Magnétique et Modélisations (CRM2), UMR CNRS 7036, Université de Lorraine, Bd des Aiguillettes, 54506 Vandœuvre-lès-Nancy, France
^f Dipartimento di Scienze Molecolari e Nanosistemi DSMN, Università Ca' Foscari di Venezia, Via Torino 155, 30172 Mestre Venezia, Italy

Selectand and selector examples

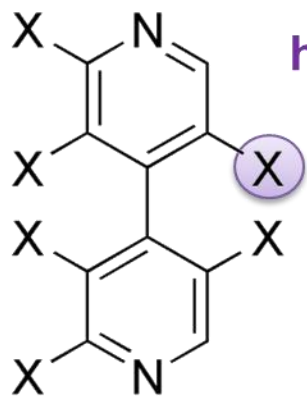
selectand

selector

chiral analytes

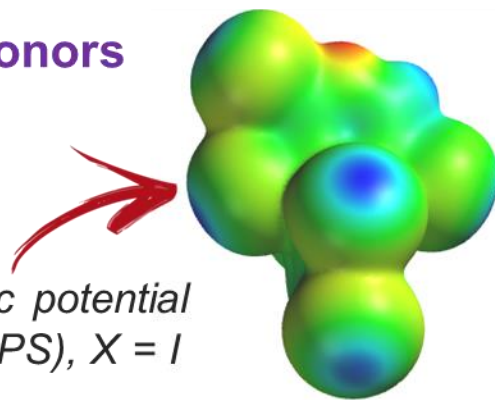
(EP legend: -  +)

chiral stationary phase

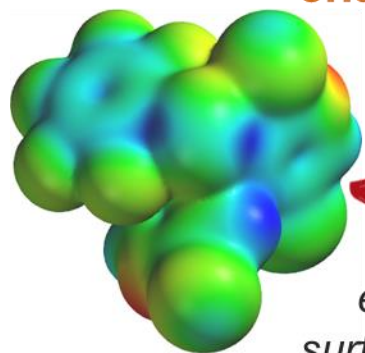


halogen bond donors

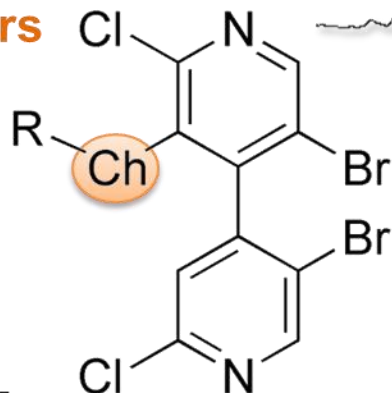
electrostatic potential surface (EPS), $X = I$



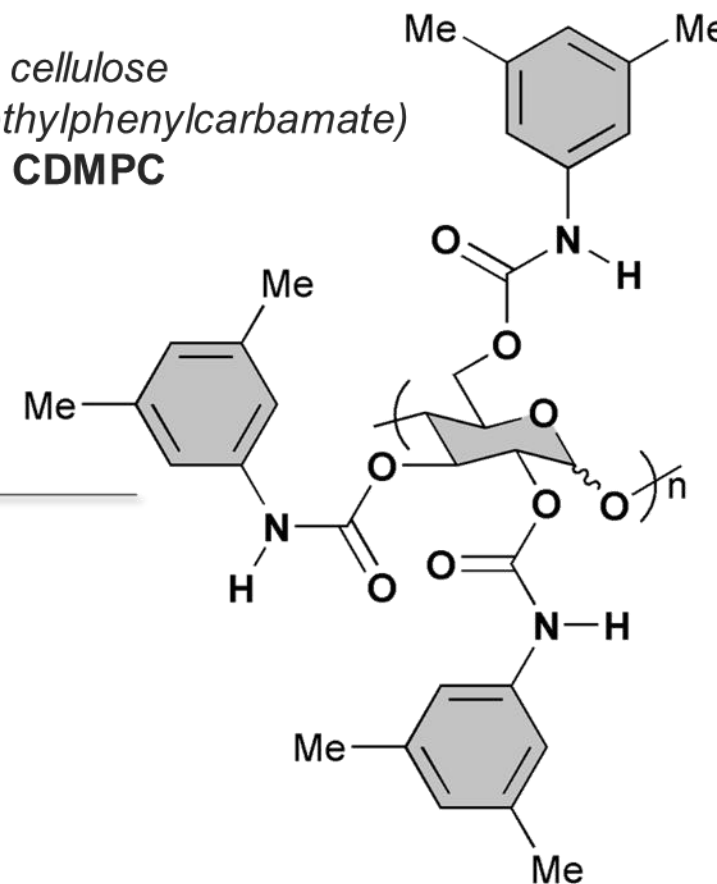
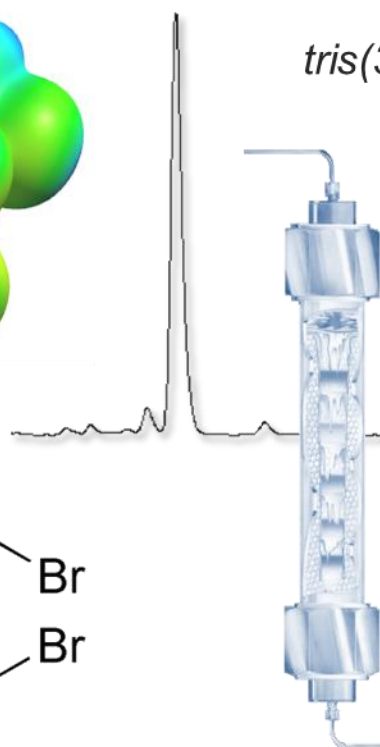
chalcogen bond donors



electrostatic potential surface (EPS), $R = \text{SeC}_6\text{F}_5$



cellulose
tris(3,5-dimethylphenylcarbamate)
CDMPC



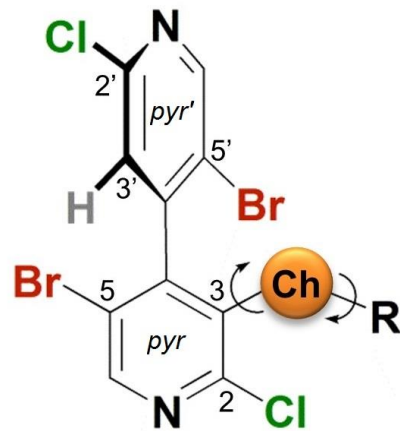
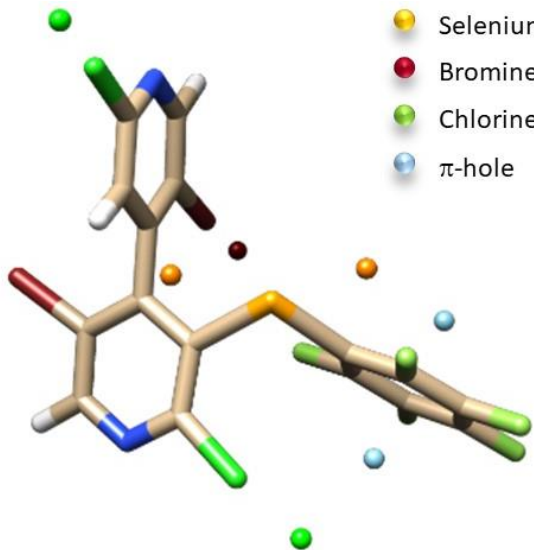
X- or Ch- substituted atropisomeric 4,4'-bipyridines as σ -donors

Cellulose-based polymers as XB acceptors



σ - and π -hole magnitude variability

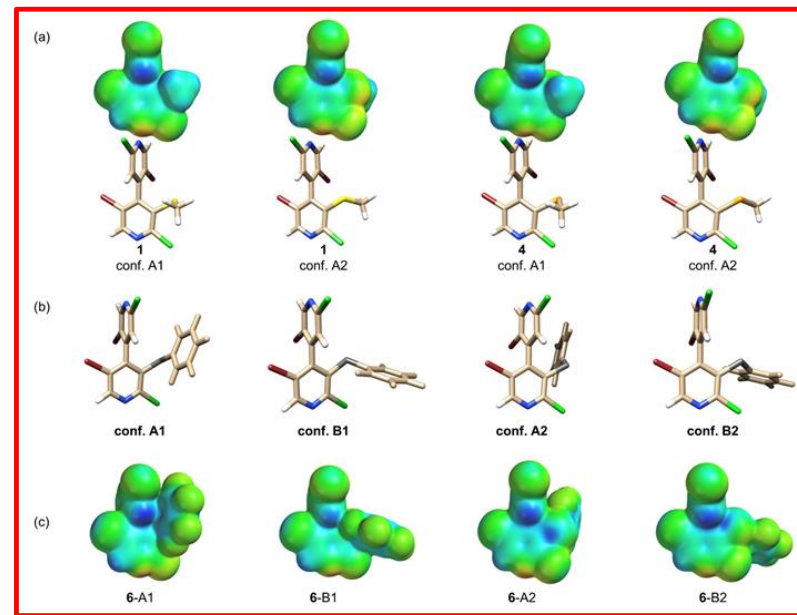
- Selenium σ -hole
- Bromine σ -hole
- Chlorine σ -hole
- π -hole



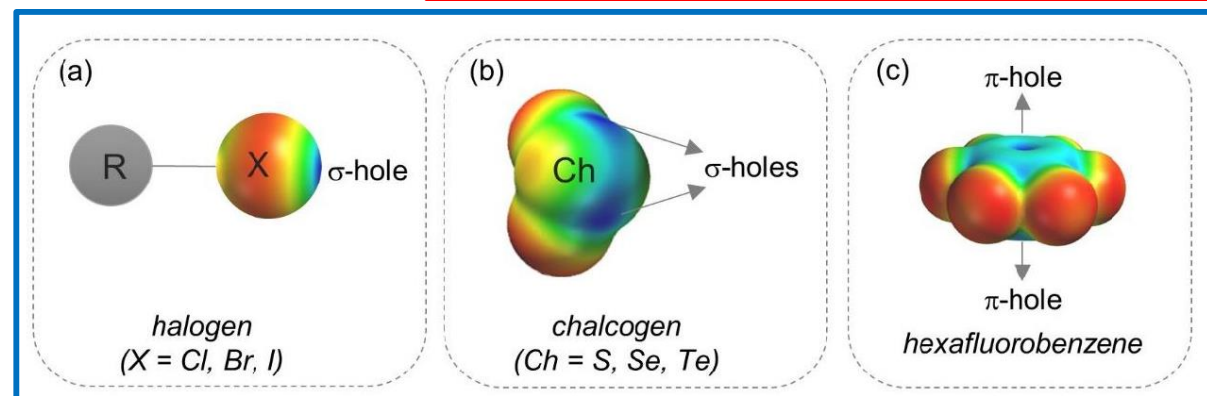
Substitution pattern

- 1: Ch = S, R = Me
- 2: Ch = S, R = Ph
- 3: Ch = S, R = C₆F₅
- 4: Ch = Se, R = Me
- 5: Ch = Se, R = Ph
- 6: Ch = Se, R = C₆F₅

$V(r)$ Extrema on the 0.002 au ED isosurface



Hole	$V_{\min} \leftrightarrow V_{\max}$, au	ΔV , au
σ -hole C _{pyr} -Ch	0.027 \leftrightarrow 0.059	0.032
σ -hole C _R -Ch	0.017 \leftrightarrow 0.061	0.044
π -holes	-0.015 \leftrightarrow 0.054	0.069



□ How can we interpret these dramatic changes in the σ/π hole V values?

□ Can we find a tool enabling us to design changes in the σ - and π -hole regions aimed at affecting their potential involvement in noncovalent interactions in a desired way?



The Source Function (SF) Electrostatic potential (SFEP)

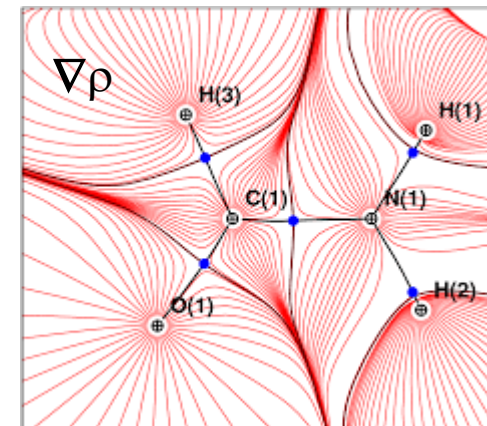
- σ - and π -hole regions are important in molecular recognition processes (e.g. in HPLC enantiomeric separation)
- Hole regions may be revealed through V . However $V(r)$ is a function of the whole molecular electron/nuclear distribution

QUESTION : Which group/moiety is/are responsible of ΔV due to chemical/conformational changes?

$$V(\mathbf{r}) = V_{elec}(\mathbf{r}) + V_{nuc}(\mathbf{r}) = \left[- \int \frac{\rho(\mathbf{r}')}{|\mathbf{r} - \mathbf{r}'|} d\mathbf{r}' + \sum_A \frac{Z_A}{|\mathbf{r} - \mathbf{R}_A|} \right] = \sum_{\Omega} \left[- \int_{\Omega} \frac{\rho(\mathbf{r}')}{|\mathbf{r} - \mathbf{r}'|} d\mathbf{r}' + \frac{Z_{\Omega}}{|\mathbf{r} - \mathbf{R}_{\Omega}|} \right] =$$

Ω , Bader's atomic or atomic group basin

$$= \sum_{\Omega} [V_{elec}(\mathbf{r}, \Omega) + V_{nuc}(\mathbf{r}, \Omega)] = \sum_{\Omega} V(\mathbf{r}, \Omega) \rightarrow V(\mathbf{r}, \Omega) \equiv SF(\mathbf{r}, \Omega) \text{ to } V(\mathbf{r})$$



$\nabla \rho \cdot \mathbf{n} = 0 \quad \forall \mathbf{r}_s \in S$ where S are the bounding surfaces of quantum atoms Ω

$$\rho(\mathbf{r}) = \int_{all\ space} LS(\mathbf{r}, \mathbf{r}') \cdot d\mathbf{r}' = \sum_{\Omega} \int_{\Omega} LS(\mathbf{r}, \mathbf{r}') \cdot d\mathbf{r}' \equiv \sum_{\Omega} SF(\mathbf{r}, \Omega)$$

$$LS(\mathbf{r}, \mathbf{r}') = - \frac{(1/4\pi)}{|\mathbf{r} - \mathbf{r}'|} \nabla^2 \rho(\mathbf{r}') \quad \text{For } V, \nabla^2 V(\mathbf{r}) = \rho(\mathbf{r}), \text{ Poisson equation}$$

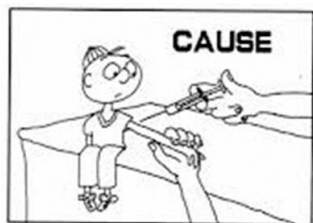
Source Function approach to chemistry, Bader RFW and Gatti C, *Chem. Phys. Lett.* 287, 233 (1998)

ANSWER : Rigorous V decomposition in group/moiety contributions enables to get insights on group/atomic contributions to $V(r)$ and enables efficient molecular design

$\nabla^2 \rho$



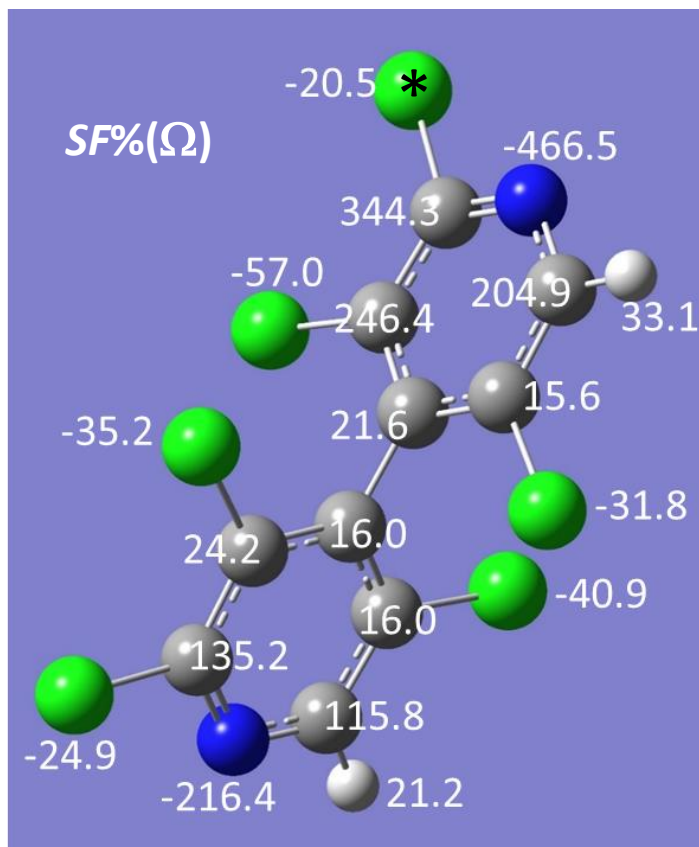
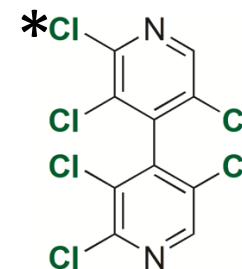
ρ



A useful tool or just a nightmare?

SF% decomposition of EP σ -hole close to Cl*

$$V(\mathbf{r}) = V_{elec}(\mathbf{r}) + V_{nuc}(\mathbf{r}) = \left[- \int \frac{\rho(\mathbf{r}')}{|\mathbf{r} - \mathbf{r}'|} d\mathbf{r}' + \sum_A \frac{Z_A}{|\mathbf{r} - \mathbf{R}_A|} \right] = \sum_{\Omega} \left[- \int_{\Omega} \frac{\rho(\mathbf{r}')}{|\mathbf{r} - \mathbf{r}'|} d\mathbf{r}' + \frac{Z_{\Omega}}{|\mathbf{r} - \mathbf{R}_{\Omega}|} \right]$$



Two problems:

- 1) V_{elec} and V_{nuc} have different sign and on the 0.002 au ρ isosurface their sum, i.e. V , is very small and typically 4 order of magnitude smaller in magnitude than either V_{elec} or V_{nuc}
- 2) The individual Ω give SF% contributions that are either positive or negative and of the same order of magnitude as the value of V itself

Apparently a nightmare....



The suite of developed SW codes and the solution

GAUSSIAN-XX

.wfn file

MULTIWFN

module enabling quantitative analyses of molecular surfaces

$V(\mathbf{r})$ σ -hole maxima on the 0.002 au ED isosurface

VEXTLOC

associate EP extrema to Ω 's. Select those of interest for the SF EP analysis

$V(\mathbf{r})$ values + $\{\mathbf{r}\}$ rps
SF analysis of $V(\mathbf{r})$

ANASFR_EP_ED

Check accuracy of SF reconstructions
Extract and combine $SF_V(\mathbf{r},\Omega)$ and $SF_\rho(\mathbf{r},\Omega)$ values in SF group contributions

$V(\mathbf{r},\Omega) \equiv SF_V(\mathbf{r},\Omega)$ and $SF_\rho(\mathbf{r},\Omega)$ values

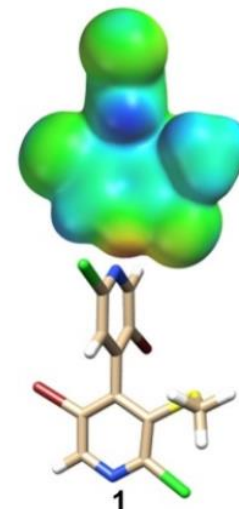
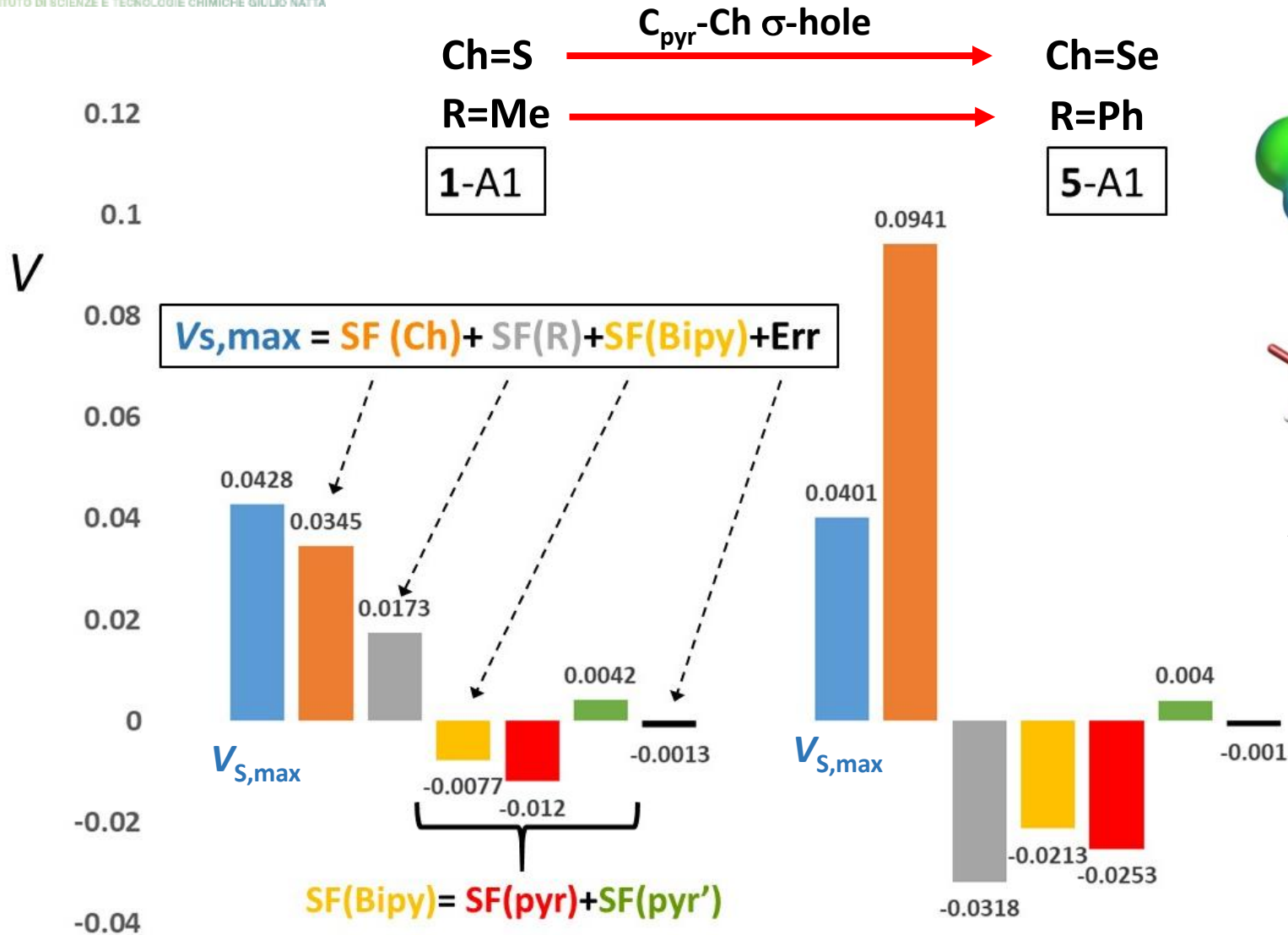
SF_ESI code

$V(\mathbf{r})$ and $\rho(\mathbf{r})$ SF reconstructions

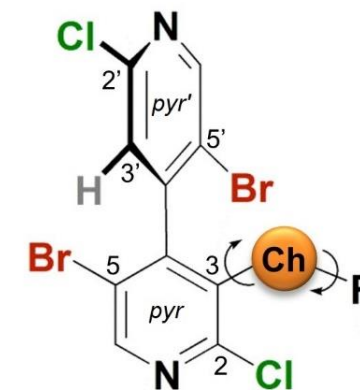
- ❑ **Multiwfn** T. Lu, F. Chen, J.Comp. Chem. 33, (2012) 580-592
- ❑ **Quantitative Analysis of Molecular Surfaces** based on improved Marching Tetrahedra algorithm, T. Lu, F. Chen, J. Mol. Graph. Model., 38 (2012) 314
- ❑ **Other codes**, except Gaussian-XX, **are home made** (C. Gatti)



Example I



A1 conformer



 *molecules* 25, 4409 (2020)



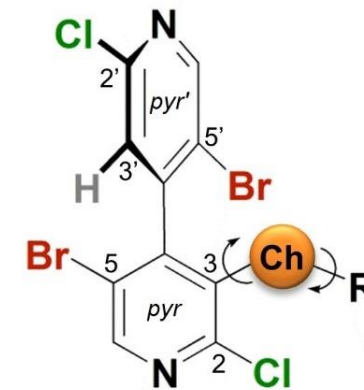
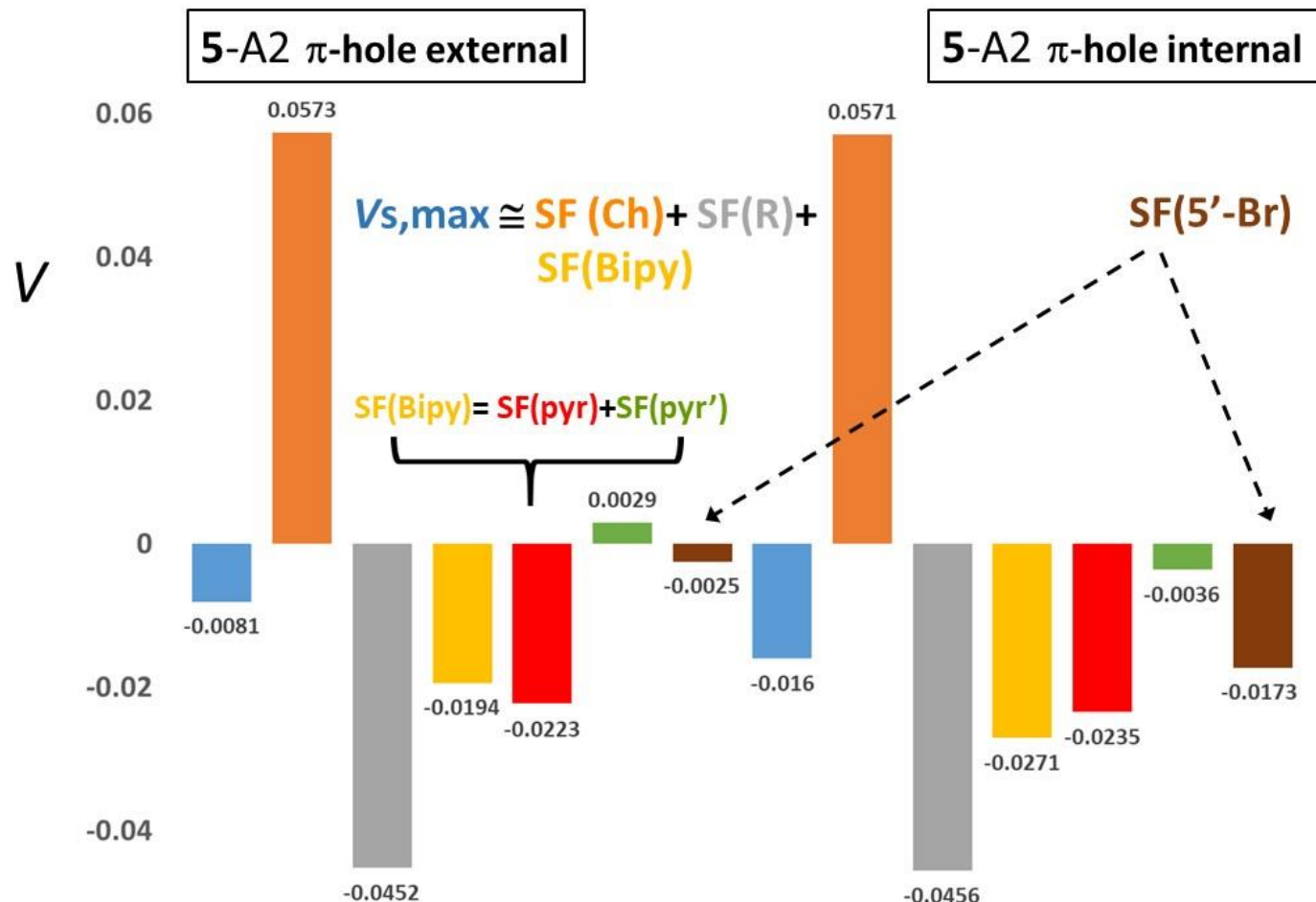
Article

Factors Impacting σ - and π -Hole Regions as Revealed by the Electrostatic Potential and Its Source Function Reconstruction: The Case of 4,4'-Bipyridine Derivatives

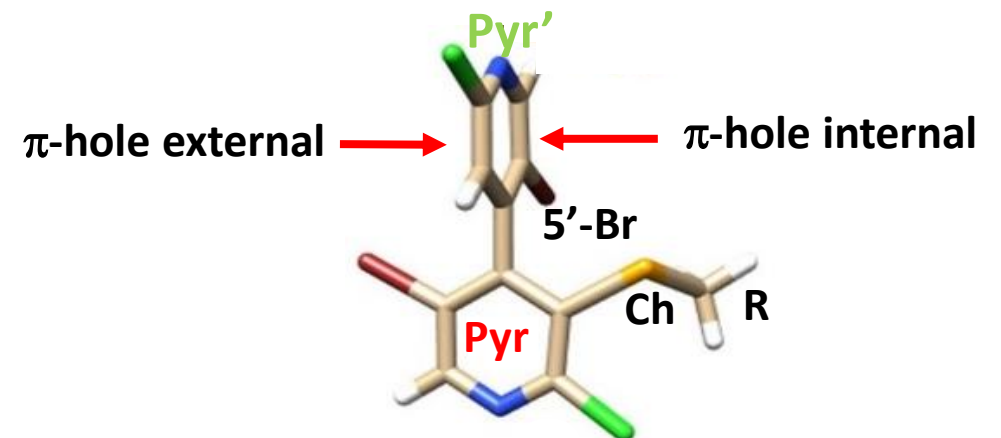
Similar $V_{s,\text{max}}$ (1-A1 \rightarrow 5-A1) C_{pyr} -Se σ -hole values, yet the roles of the Ch, R and Bipy moieties are strikingly different



Example II



- Substitution pattern*
- 1: Ch = S, R = Me
 - 2: Ch = S, R = Ph
 - 3: Ch = S, R = C₆F₅
 - 4: Ch = Se, R = Me
 - 5: Ch = Se, R = Ph
 - 6: Ch = Se, R = C₆F₅



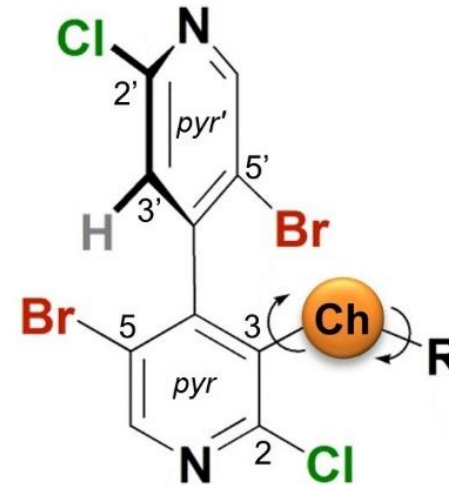
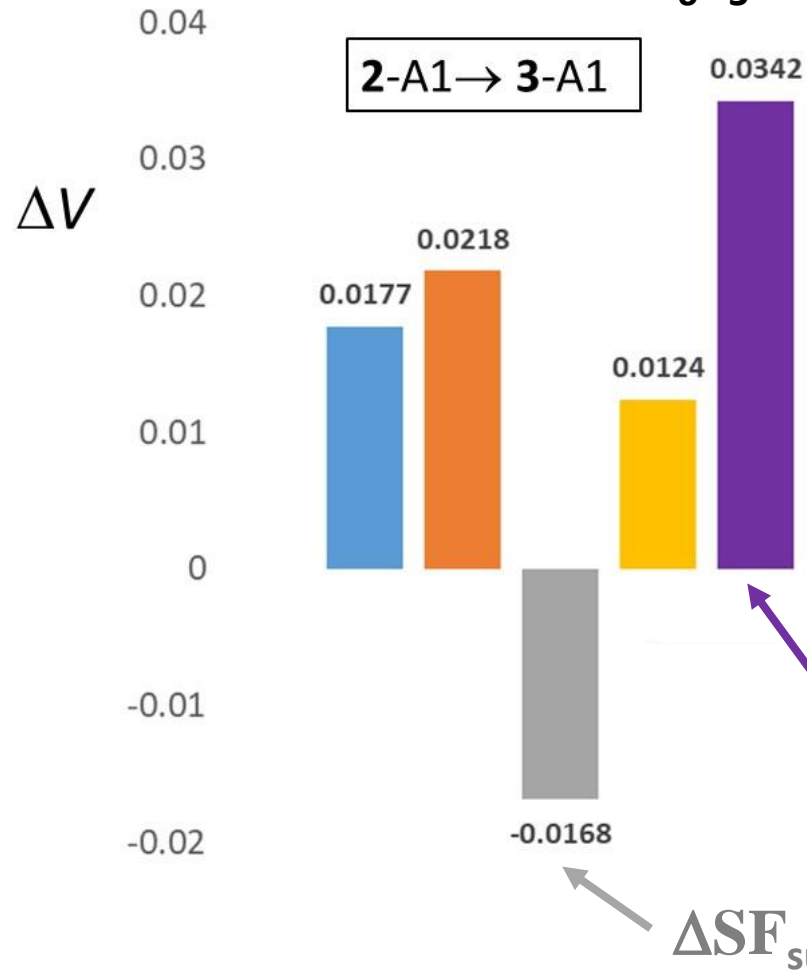
SF (Ch) and SF(R) are almost equal for the two holes, while SF(Bipy) is the responsible for the internal π -hole $V_{s,max}$ of 5-A2 being twice as negative because of the different sign SF contribution from its pyr', hosting the 5'-Br atom. This atom points its p-cloud towards the phenyl ring internal p-hole making this hole negative rather than positive



Example III

C_R-S σ-hole

R=Ph → R=C₆F₅



Substitution pattern

- 1: Ch = S, R = Me
- 2: Ch = S, R = Ph
- 3: Ch = S, R = C₆F₅
- 4: Ch = Se, R = Me
- 5: Ch = Se, R = Ph
- 6: Ch = Se, R = C₆F₅

$$\Delta V_{s,max} = \Delta SF(\text{Ch}) + \Delta SF(\text{R}) + \Delta SF(\text{Bipy})$$

$$\Delta V_{S,max} (2-A1 \rightarrow 3-A1) \cong \Delta SF_{\text{substitution}} + \Delta SF_{\text{rearrangement}}$$

$$\Delta SF_{\text{rearrangement}} (2-A1 \rightarrow 3-A1) = \Delta SF(\text{Ch}) + \Delta SF(\text{Bipy})$$



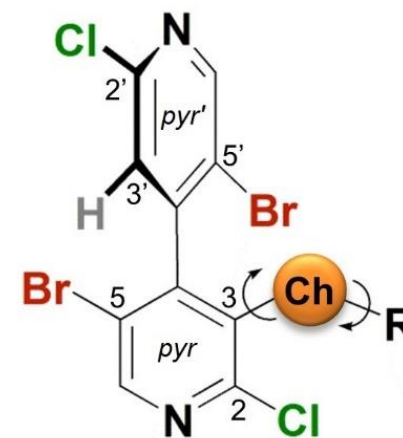
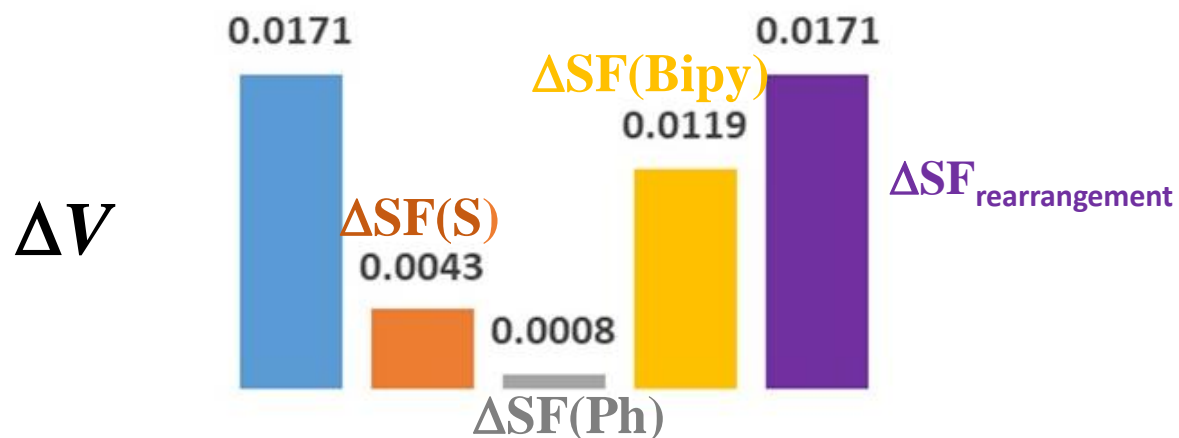
Example IV

C_R-S σ-hole

$$\Delta V_{S,\max} \cong \Delta SF_{\text{substitution}} + \Delta SF_{\text{rearrangement}}$$

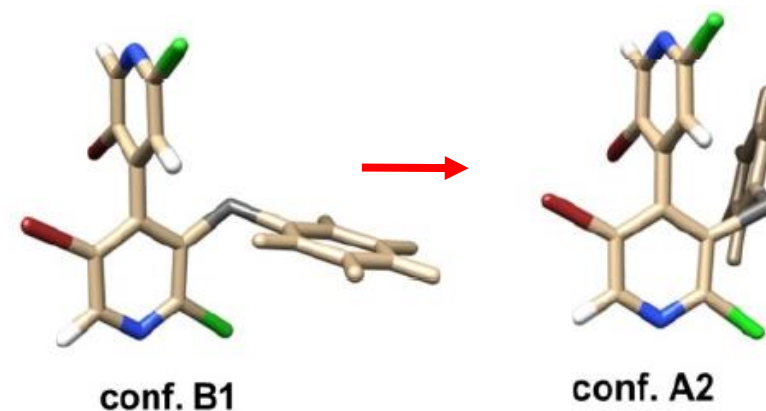


$$\Delta V_{s,\max}(2\text{-B1} \rightarrow 2\text{-A2}) \equiv \Delta SF_{\text{rearrangement}}$$



Substitution pattern

- 1: Ch = S, R = Me
- 2: Ch = S, R = Ph
- 3: Ch = S, R = C₆F₅
- 4: Ch = Se, R = Me
- 5: Ch = Se, R = Ph
- 6: Ch = Se, R = C₆F₅

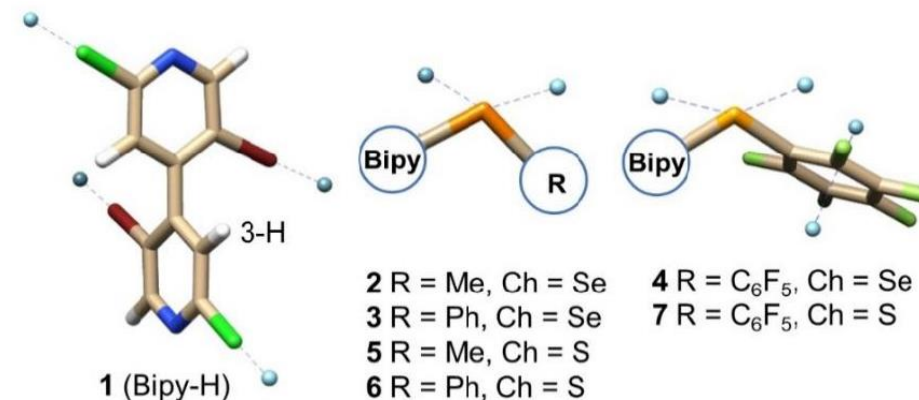
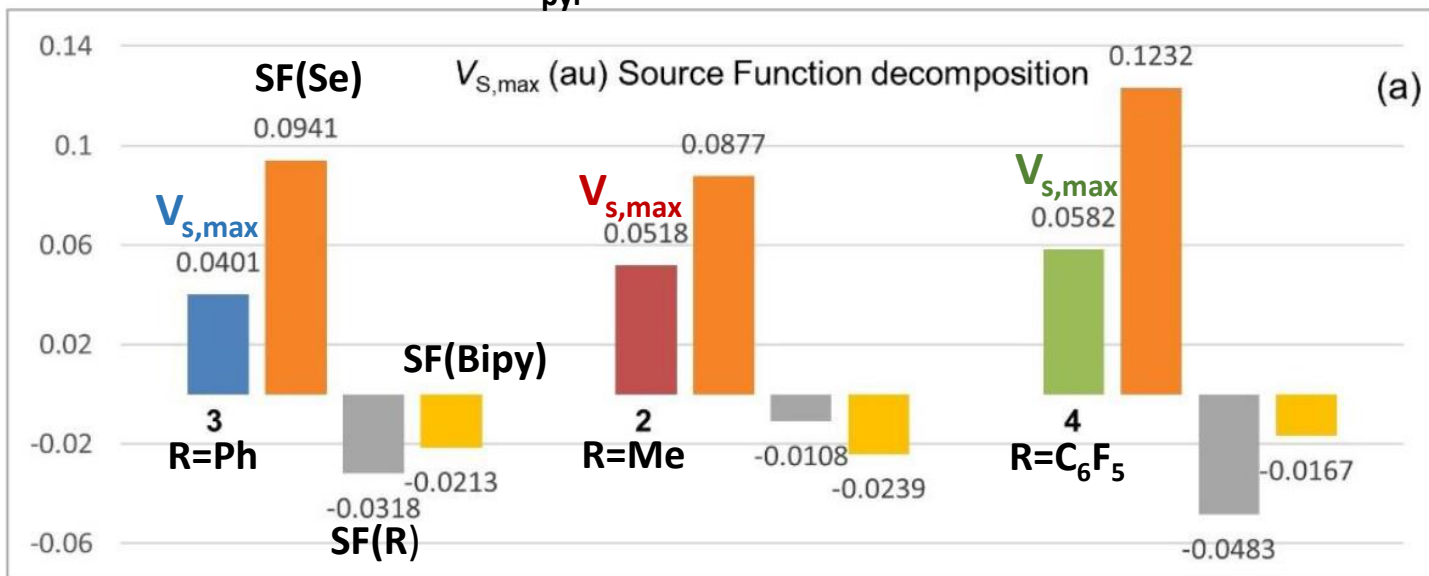


The molecular transformations of examples III and IV yield quite similar $V_{S,\max}$ variations, yet the roles of the Ch, R and Bipy moieties in producing such similar changes strikingly differ. It is shown that **a change of molecular conformation only may be as effective as a chemical substitution in its impact on the $V_{S,\max}$ value.**

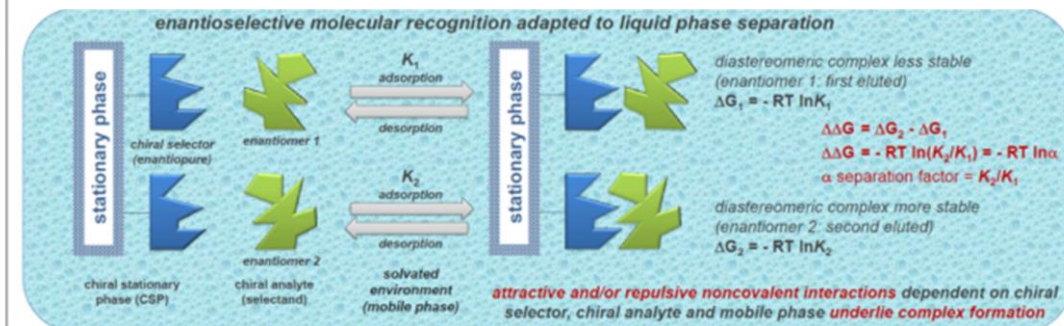
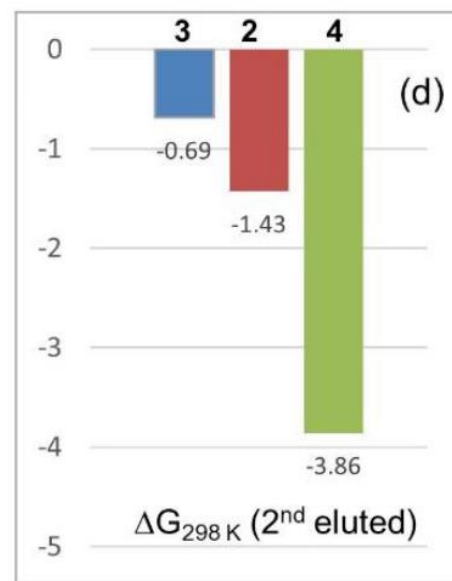
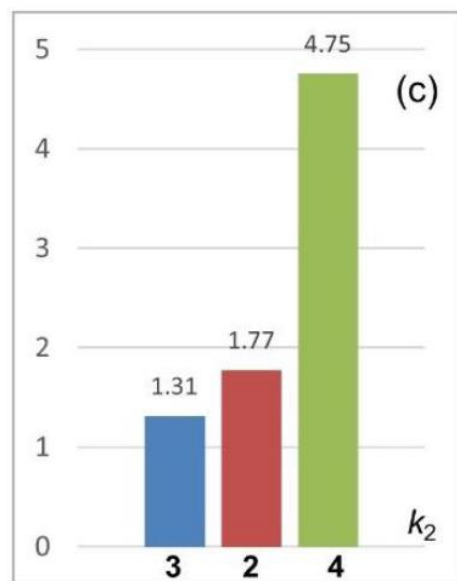
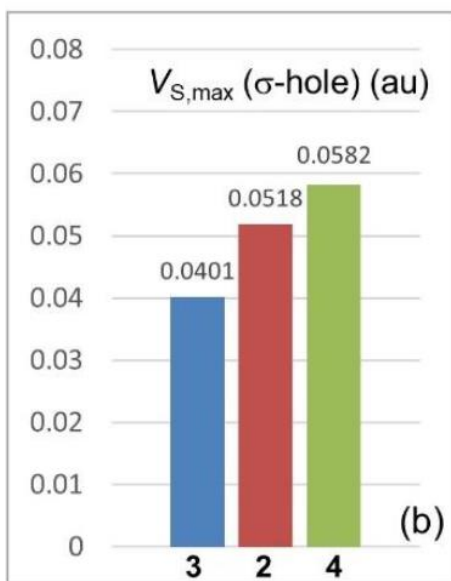


Example V

C_{pyr} -Se σ -hole



$$V_{s,max} \text{ (au)} = SF(Ch) + SF(Bipy) + SF(R)$$



Thanks to

all (mentioned + photos!) coauthors

DNRF for funding through



...to all of you for
your attention

Table 1 Crucial properties of phase-change alloys

Required property of PC material	Specification
High-speed phase transition	Induced by nanosecond laser or voltage pulse
Long thermal stability of amorphous state	At least several decades at room temperature
Large optical change between the two states (for rewriteable optical storage)	Considerable difference in refractive index or absorption coefficient
Large resistance change between the states (for non-volatile electronic storage)	Natural consequence of the transformation from amorphous to crystalline state
Large cycle number of reversible transitions	More than 100,000 cycles with stable composition
High chemical stability	High water-resistivity

- ❑ Can be rapidly and reversibly switched between the amorphous (AS) and the crystalline state (CS). **Yet** this transition is accompanied by a **pronounced change** of **optical** and **electronic** properties
- ❑ Though their transformation occurs through very fast melt, quench and anneal cycles, the 2 states are extremely long lived at ambient T: they do represent 2 stable and competing structural/bonding alternatives
- ❑ Their portfolio of properties is very appealing for **memory applications** and **photonics**
- ❑ PCMs have been successfully employed in : a) rewriteable optical data storage (DVD, Blue Ray, HD Digital Versatile Disks) b) fast, yet nonvolatile electronic memories (**PCM, PCME, PRAM, PCRAM, OUM**). Their pronounced optical contrast is also utilized in nanophotonic applications and has been discussed as a means to realize ultrafast optical switches

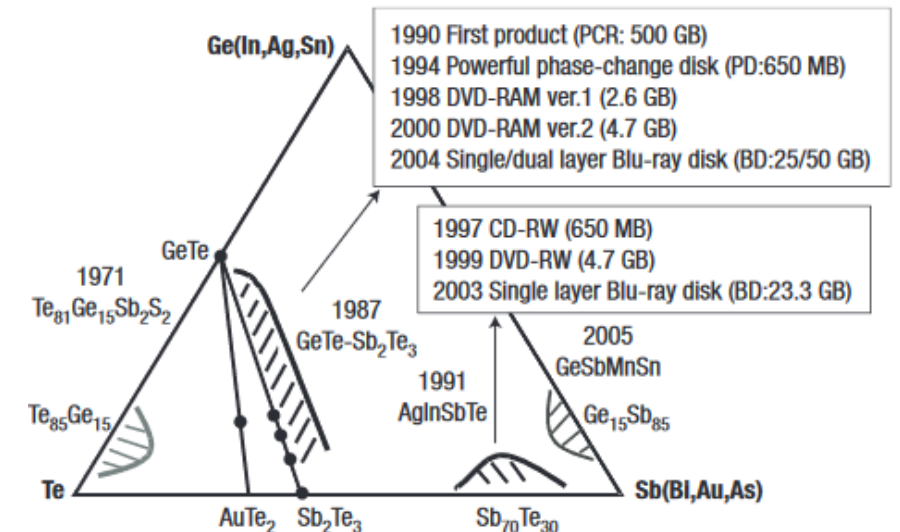


Figure 2 Ternary phase diagram depicting different phase-change alloys, their year of discovery as a phase-change alloy and their use in different optical storage products.

Upon transition to CS....

Special *fingerprints* of PCM crystalline phases

- ❑ Unusually high coordination number (Zintl-Klemm 8-*N* rule no longer fulfilled)
- ❑ Electronic polarizability rises sharply  Extraordinary large optical dielectric constant
- ❑ Chemical bond polarizability increases  unusually high Born effective charges
- ❑ Almost metal-like conductivity
- ❑ Vibrational properties are largely affected, with unusual phonon softening
Huge mode-specific Grüneisen parameter for transverse optical phonons
- ❑ Unusual bond breaking mechanism in laser-assisted atom probe tomography

Zhu, M., Cojocaru-Mirédin, O., Mio, A. M., Keutgen, J., Küpers, M., Yu, Y., Cho, J. Y., Dronskowski, R., Wuttig, M., *Adv. Mater.* 2018, 30, 1706735.

These findings imply that the *bonding* mechanism in crystalline PCMs differs substantially from conventional bonding mechanisms such as metallic, ionic, and covalent bonding....

Really a novel bonding mechanism besides those already established?

Metavalent bonding?

Upon transition to CS....

GS Static view of bonding (1e and 2e distributions)

Special *fingerprints* of PCM crystalline phases

or

Property view of bonding as a specific reaction to an external stimulus?

❑ Unusually high coordination number (Zintl-Klemm 8-*N* rule no longer fulfilled)

Geometry

❑ Electronic polarizability rises sharply → Extraordinary large optical dielectric constant

❑ Chemical bond polarizability increases → unusually high Born effective charges

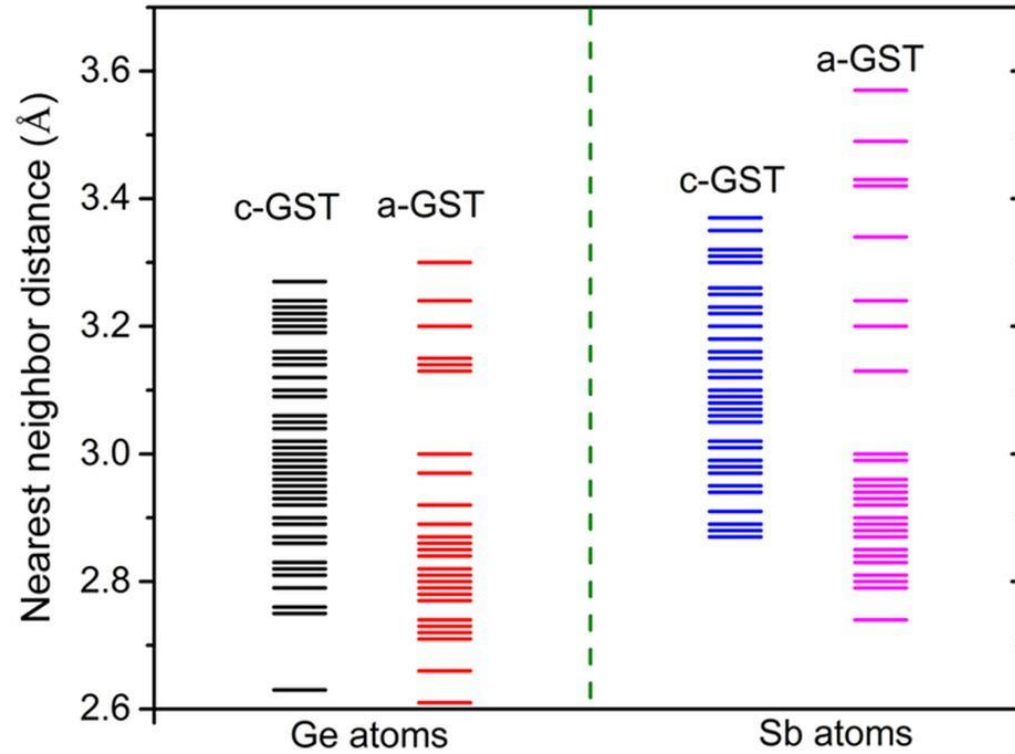
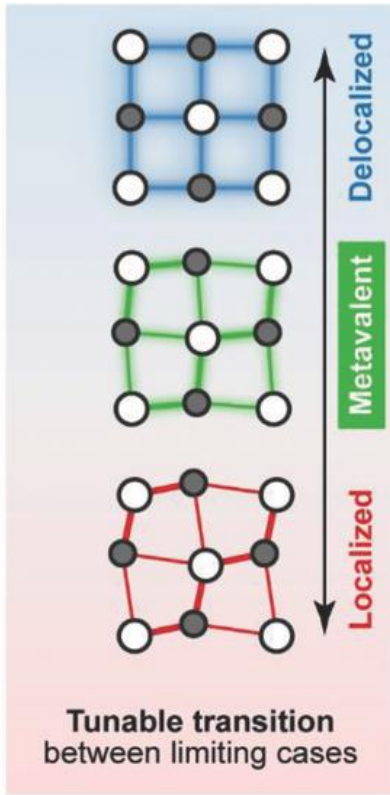
*Response properties
(involve excited states)*

❑ Almost metal-like conductivity

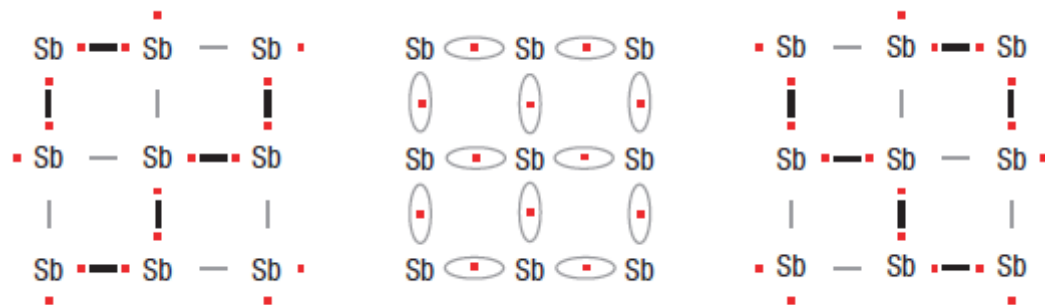
❑ Vibrational properties are largely affected, with unusual phonon softening
Huge mode-specific Grüneisen parameter for transverse optical phonons

❑ Unusual bond breaking mechanism in laser-assisted atom probe tomography

*Response property to an external,
very large, destroying stimulus*



$\text{Ge}_2\text{Sb}_2\text{Te}_5$ (GST)



c-GST slightly distorted cubic, 1c-2e, more delocalized

a-GST short and long nnb distances, 2c-2e more localized. Closer to 8-N ZK rule

Localization and delocalization indices should give an unbiased answer



Domain overlap matrices from plane-wave-based methods of electronic structure calculation

Pavlo Golub¹ and Alexey I. Baranov^{1,2,a)}¹Department of Chemistry and Food Chemistry, Technical University of Dresden, Bergstrasse 66, 01062 Dresden, Germany²Max Planck Institute for Chemical Physics of Solids, Nöthnitzer Strasse, 40, 01187 Dresden, Germany

Plane waves are one of the most popular and efficient basis sets for electronic structure calculations of solids; however, their delocalized nature makes it difficult to employ for them classical orbital-based methods of chemical bonding analysis. The quantum chemical topology approach, introducing chemical concepts via partitioning of real space into chemically meaningful domains, has no difficulties with plane-wave-based basis sets. Many popular tools employed within this approach, for instance delocalization indices, need overlap integrals over these domains—the elements of the so called domain overlap matrices. This article reports an efficient algorithm for evaluation of domain overlap matrix elements for plane-wave-based calculations as well as evaluation of its implementation for one of the most popular projector augmented wave (PAW) methods on the small set of simple and complex solids. The stability of the obtained results with respect to PAW calculation parameters has been investigated, and the comparison of the results with the results from other calculation methods has also been made. *Published by AIP Publishing.* [<http://dx.doi.org/10.1063/1.4964760>]

Domain-averaged Fermi-hole analysis for solids

Alexey I. Baranov,^{1,a)} Robert Ponec,² and Miroslav Kohout¹¹Max Planck Institute for Chemical Physics of Solids, Nöthnitzer Strasse 40, 01187 Dresden, Germany²Institute of Chemical Process Fundamentals, Academy of Sciences of the Czech Republic v.v.i., Rozvojová 135, 165 02 Prague 6, Czech Republic

(Received 13 August 2012; accepted 31 October 2012; published online 6 December 2012)

$$\rho_2(\mathbf{r}_1, \mathbf{r}_2) = \frac{1}{2} [\rho(\mathbf{r}_1)\rho(\mathbf{r}_2) - \rho_{2,xc}(\mathbf{r}_1, \mathbf{r}_2)]$$

$$LI(A) = \lambda(A) = \int \int_A \rho_{2,xc}(\mathbf{r}_1, \mathbf{r}_2) d\mathbf{r}_1 d\mathbf{r}_2$$

Half N. of e pairs fully localised in A

$$DI(A,B) = \delta(A,B) = 2 \cdot \int \int_{A,B} \rho_{2,xc}(\mathbf{r}_1, \mathbf{r}_2) d\mathbf{r}_1 d\mathbf{r}_2$$

N. of e pairs shared between A and B

$$\sum_A \left[\lambda(A) + \frac{1}{2} \sum_{B \neq A} \delta(A,B) \right] = N$$

For HF (and SD wfs ansatz) \Rightarrow

$$\rho_{2,xc}(\mathbf{r}_1, \mathbf{r}_2) = \sum_{i,j=1}^{M=N/2} 2 [\phi_i(\mathbf{r}_2)\phi_i^*(\mathbf{r}_1)\phi_j(\mathbf{r}_1)\phi_j^*(\mathbf{r}_2)]$$

$$\lambda(\Omega_1) = 2 \cdot \sum_{i,j=1}^{M=N/2} \int \int_{\Omega_1} \phi_i(\mathbf{r}_2)\phi_i^*(\mathbf{r}_1)\phi_j(\mathbf{r}_1)\phi_j^*(\mathbf{r}_2) d\mathbf{r}_1 d\mathbf{r}_2 = 2 \cdot \sum_{i,j=1}^{M=N/2} (S_{ij}^{\Omega_1})^2$$

$$\delta(\Omega_1, \Omega_2) = 4 \cdot \sum_{i,j=1}^{M=N/2} \int \int_{\Omega_1, \Omega_2} \phi_i(\mathbf{r}_2)\phi_i^*(\mathbf{r}_1)\phi_j(\mathbf{r}_1)\phi_j^*(\mathbf{r}_2) d\mathbf{r}_1 d\mathbf{r}_2 = 4 \cdot \sum_{i,j=1}^{M=N/2} S_{ij}^{\Omega_1} S_{ij}^{\Omega_2}$$

Quantitative Electron Delocalization in Solids from Maximally Localized Wannier Functions

A. Otero-de-la-Roza,^{*,†} Ángel Martín Pendás,[†] and Erin R. Johnson[‡][†]Departamento de Química Física y Analítica, Facultad de Química, Universidad de Oviedo, 33006 Oviedo, Spain[‡]Department of Chemistry, Dalhousie University, 6274 Coburg Road, Halifax, Nova Scotia, Canada B3H 4R2

$$S_{ij}^{\Omega_k} = \int_{\Omega_k} \phi_i^*(\mathbf{r}_1)\phi_j(\mathbf{r}_1) d\mathbf{r}_1$$

↑
DOM

DOM from plane wave calculations

$$\tilde{\psi}_{j\vec{k}}(\vec{r}) = \sum_{\vec{G}} c_{j\vec{k}}(\vec{G}) e^{i(\vec{k}+\vec{G})\vec{r}}$$

IR : Bloch states with band index j and k -vector \vec{k} , expanded in PWs
 Σ over the reciprocal lattice vectors \vec{G}

$$S_{j\vec{k};j'\vec{k}'}(\Omega) = \int d\vec{r} \tilde{\psi}_{j\vec{k}}^*(\vec{r}) w^\Omega(\vec{r}) \chi_{IR}(\vec{r}) \tilde{\psi}_{j'\vec{k}'}(\vec{r})$$

$$+ \sum_a \int d\vec{r} \psi_{j\vec{k}}^{a*}(\vec{r}) w^\Omega(\vec{r}) \psi_{j'\vec{k}'}^a(\vec{r}).$$

Atomic spheres contribution

Augmented Plane Wave (APW) or Projector Augmented wave (PAW) methods:

- Interstitial region (IR)
- +
- Non overlapping atomic or muffin-tin (MT) spheres

IR PW contribution
 $\chi_{IR}=1$ in IR and 0 elsewhere

THE JOURNAL OF CHEMICAL PHYSICS 145, 154107 (2016)



Domain overlap matrices from plane-wave-based methods of electronic structure calculation

Pavlo Golub¹ and Alexey I. Baranov^{1,2,a)}

¹Department of Chemistry and Food Chemistry, Technical University of Dresden, Bergstrasse 66, 01062 Dresden, Germany

²Max Planck Institute for Chemical Physics of Solids, Nöthnitzer Strasse, 40, 01187 Dresden, Germany

DOM calculation implemented for the PAW method as a general purpose module of the program DGRID interfaced to the output of the ABINIT code. DOM evaluated for QTAIM basins



A Quantum-Mechanical Map for Bonding and Properties in Solids

*Jean-Yves Raty, Mathias Schumacher, Pavlo Golub, Volker L. Deringer, Carlo Gatti, and Matthias Wuttig**

- Combine the quantum mechanically based (1e and 2e distributions) and the property-based perspective to derive a holistic view of bonding in solids
- Do “metavalent” solids exhibit special DI and LI features, besides their 5 “fingerprints properties” ?

For conductivity and coordination numbers, “metavalent” solids are located between the covalent and metallic regimes

They are, however, distinctly different from both because they show

- anomalously large response properties
- a unique APT (Atom Probe Tomography) bond-breaking mechanism not observed in either covalent or metallic solids

Definition based on a set of observable properties has led to a revision of “resonant” bonding model, previously widely used to describe bonding in PCMs. **Response** properties of PCMs are fundamentally different from those of resonantly bonded benzene and graphite

Structure

Elements:

Al	$Fm\bar{3}m$
Ag	$Fm\bar{3}m$
Sn ^α	$Fd\bar{3}m$
Pb	$Fm\bar{3}m$
Si	$Fd\bar{3}m$
Ge	$Fd\bar{3}m$
Na	$Im\bar{3}m$
Mg	$P6_3/mmc$
Ca*	$P6_3/mmc$
C ^{diamond}	$Fd\bar{3}m$
C ^{graphite}	$P6_3/mmc$

Intermetallics:

NiAl	$Pm\bar{3}m$
TiAl	$P4/mmm$

11 elemental phases
 74 binary phases of main-group elements
 11 binary phases of IIB transition metals
 2 Intermetallics
 3 Ternary phases
 + metastable phases of PCM

IIIA-VA compounds:

AlN	$P6_3mc$
AlP	$F\bar{4}3m$
AlAs	$F\bar{4}3m$
AlSb	$F\bar{4}3m$
AlBi	$F\bar{4}3m$
GaN	$P6_3mc$
GaP	$F\bar{4}3m$
GaAs	$F\bar{4}3m$
GaSb	$F\bar{4}3m$
InN*	$F\bar{4}3m$
InP	$F\bar{4}3m$
InAs	$F\bar{4}3m$
InSb	$F\bar{4}3m$

IA-VIIA compounds:

NaCl	$Fm\bar{3}m$
NaF	$Fm\bar{3}m$
KF	$Fm\bar{3}m$
KCl	$Fm\bar{3}m$
KBr	$Fm\bar{3}m$
KI	$Fm\bar{3}m$
RbCl	$Fm\bar{3}m$
RbBr	$Fm\bar{3}m$
RbBr ^{$Pm\bar{3}m$*}	$Pm\bar{3}m$
CsF	$Fm\bar{3}m$
CsF ^{$Pm\bar{3}m$*}	$Pm\bar{3}m$

Ternary compounds:

AgBiSe ₂
AgBiTe ₂
AgSbTe ₂

IIA-VIA compounds:

BeO	$P6_3mc$
BeS	$F\bar{4}3m$
BeSe	$F\bar{4}3m$
BeTe	$F\bar{4}3m$
MgO	$Fm\bar{3}m$
MgS	$Fm\bar{3}m$
MgSe*	$F\bar{4}3m$
MgTe	$F\bar{4}3m$
CaO	$Fm\bar{3}m$
CaS	$Fm\bar{3}m$
CaSe	$Fm\bar{3}m$
CaTe	$Fm\bar{3}m$
SrO	$Fm\bar{3}m$
SrS	$Fm\bar{3}m$
SrSe	$Fm\bar{3}m$
SrTe	$Fm\bar{3}m$
BaS	$Fm\bar{3}m$
BaSe	$Fm\bar{3}m$
BaTe	$Fm\bar{3}m$

IIB-VIA compounds:

ZnO*	$F\bar{4}3m$
ZnS	$F\bar{4}3m$
ZnS ^{Wurtzite*}	$P6_3mc$
ZnSe	$F\bar{4}3m$
ZnTe	$F\bar{4}3m$
CdS	$F\bar{4}3m$
CdSe	$F\bar{4}3m$
CdTe	$F\bar{4}3m$
HgS	$F\bar{4}3m$
HgSe	$F\bar{4}3m$
HgTe	$F\bar{4}3m$

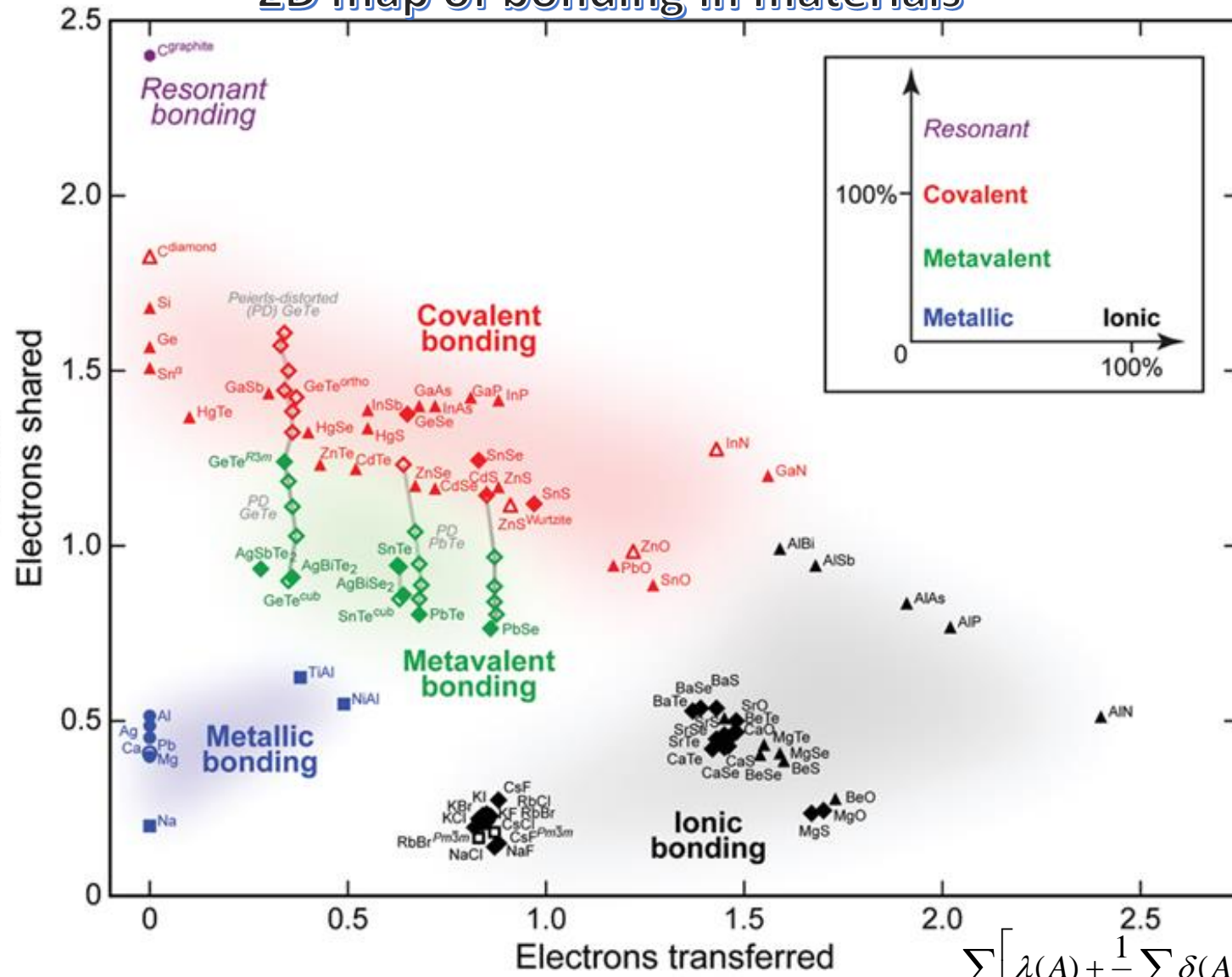
IVA-VIA compounds:

GeSe	$Pnma$
GeTe ^{220u*}	$R3m, dist.$
GeTe ^{221u*}	$R3m, dist.$
GeTe ^{224u*}	$R3m, dist.$
GeTe ^{227u*}	$R3m, dist.$
GeTe ^{ortho*}	$Pnma$
GeTe ^{230u*}	$R3m, dist.$
GeTe ^{233u*}	$R3m, dist.$
GeTe ^{R3m}	$R3m$
GeTe ^{239u*}	$R3m, dist.$
GeTe ^{242u*}	$R3m, dist.$
GeTe ^{245u*}	$R3m, dist.$
GeTe ^{cub*}	$Fm\bar{3}m$
SnO	$P4/nmm$
SnS	$Pnma$
SnSe	$Pnma$
SnTe	$R3m, dist.$
SnTe ^{cub*}	$Fm\bar{3}m$
PbO	$P4/nmm$
PbSe ^{u2300*}	$R3m, dist.$
PbSe ^{u2400*}	$R3m, dist.$
PbSe ^{u2440*}	$R3m, dist.$
PbSe ^{u2464*}	$R3m, dist.$
PbSe ^{u2482*}	$R3m, dist.$
PbSe	$Fm\bar{3}m$
PbTe ^{u2300*}	$R3m, dist.$
PbTe ^{u2400*}	$R3m, dist.$
PbTe ^{u2440*}	$R3m, dist.$
PbTe ^{u2464*}	$R3m, dist.$
PbTe ^{u2482*}	$R3m, dist.$
PbTe	$Fm\bar{3}m$

* indicates metastable phases; the label "dist." signifies gradual Peierls distortions



2D map of bonding in materials



- \triangle sp^3 tetrahedrally bonded solids
- \diamond Distorted and ideal rocksalt types (octahedrally coordinated)
- \square Body-centered
- \circ Closed-packed metal structures

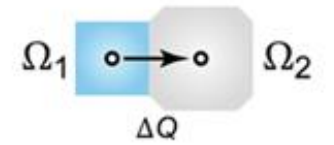
Filled symbols: thermodynamically stable phases ($T=0$)

Open symbols: metastable phases

GeTe, SnTe, PbTe, PbSe : additional structural intermediates along the Peierls distortion coordinate (gray line, as guide for the eye)

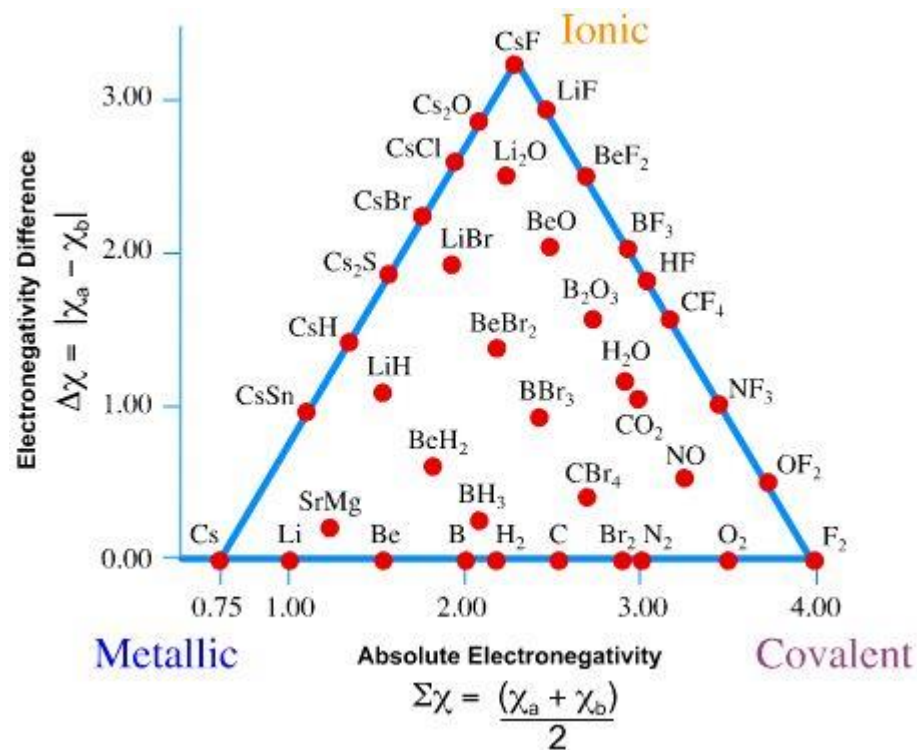
Archetypes of ionic, covalent, and metallic bonding lie in distinctly different, physically meaningful regions

$$\sum_A \left[\lambda(A) + \frac{1}{2} \sum_{B \neq A} \delta(A, B) \right] = N \quad \rightarrow \quad \text{Explains departure from perfect covalency with increasing polarity}$$



Central region of the map which lies between the 3 archetypical mechanisms, without belonging to one of them, and is populated by materials as well

van Arkel–Ketelaar triangles



Arkel, A. E. V. *Molecules and Crystals in Inorganic Chemistry*; Interscience: New York, 1956.
 Ketelaar, J. A. A. *Chemical Constitution: An Introduction to the Theory of Chemical Bond*, 2nd ed.; Elsevier: New York, 1958.

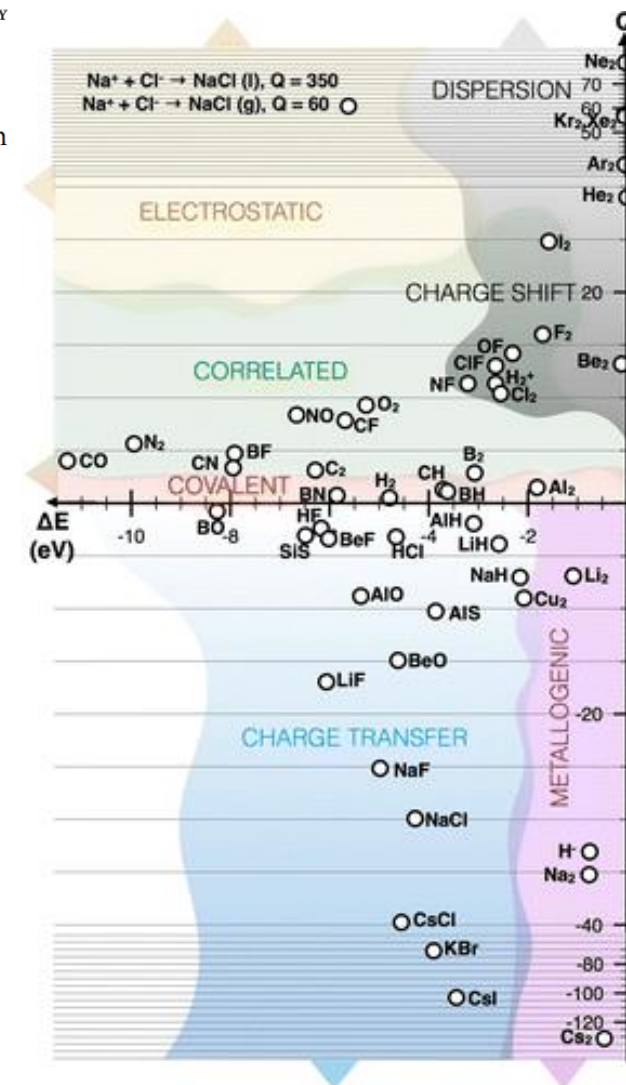
Distinguishing Bonds

Martin Rahm* and Roald Hoffmann

A Classification of Covalent, Ionic, and Metallic Solids Based on the Electron Density

P. Mori-Sanchez, A. Martin Pendas, V. Luana,
J. Am. Chem. Soc. **124**, 14721 (2002)

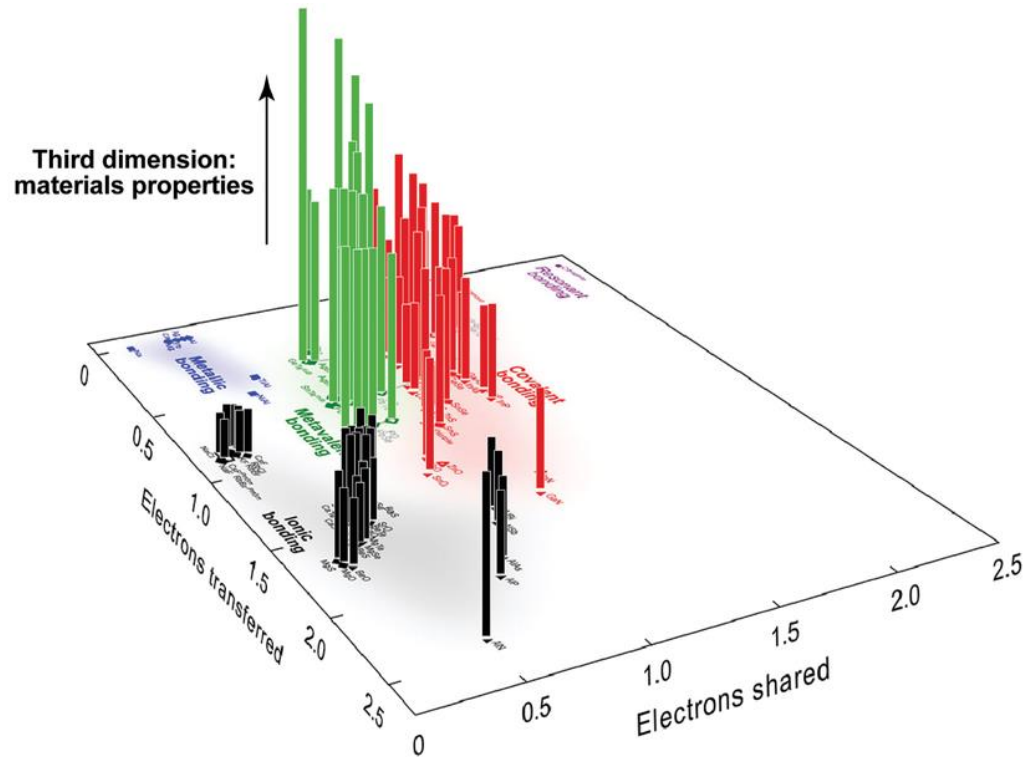
The 3 indices, flatness, CT, and molecularity, easily obtained from the ED give rise to a classification in close resemblance to the classical van Arkel-Ketelaar diagrams



The Q-scale plotted against the bond dissociation energy ΔE in a range of diatomics reveals familiar groups of chemical interactions

- ❑ Missing aspect: a rigorous link between a compound's location in the 2D map and its physical properties (as relevant for applications)
- ❑ Such a link would make it possible not only to classify bonding in materials, but to exploit the quantitative bonding information for materials design.

a



3D maps defining design rules for materials with desired properties

The base plane is defined as in the 2D map

Extending this map in the third dimension three response properties are quantified:

(b) Born effective charges, Z^* (averaged over atoms)

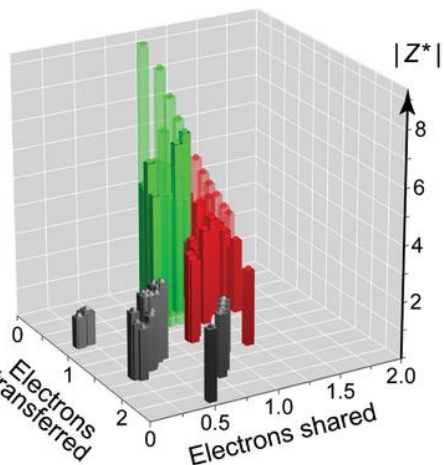
(c) optical dielectric constants, ϵ_∞

(d) absolute transverse optical (TO) mode Grüneisen parameters, $|\gamma_{TO}|$ for binary compounds

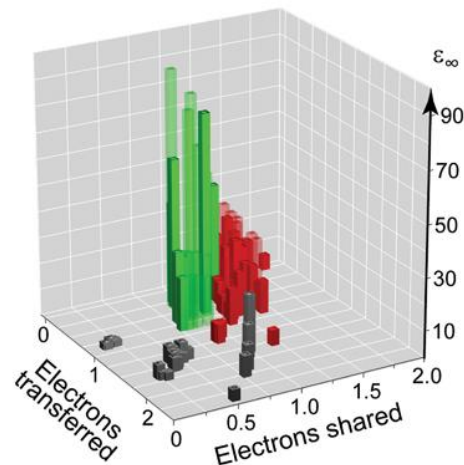
Ionic materials (**Black**), Covalent (**red**) Metavalent (**green**) (structural intermediates as semitransparent bars)

“Metavalent” bonding is characterized by unusually high values of all three indicators (**green bars**).

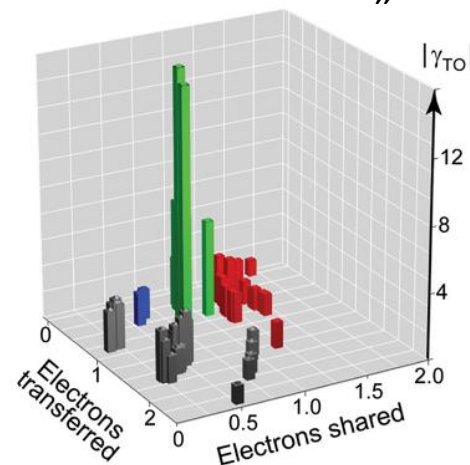
b Born effective charges (bond polarizability)



c Optical dielectric constants (optical identifier)

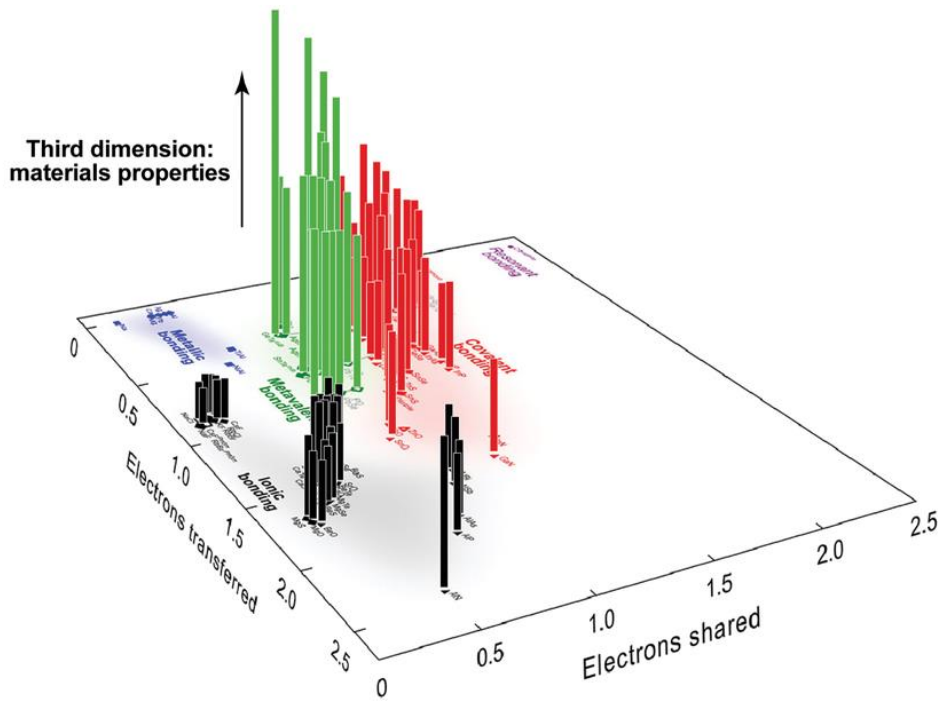


d Grüneisen parameters (anharmonicity identifier)



H-bonds may have vdW, ionic, covalent contributions with weights depending from D to A distance. However their properties (e.g OH stretching frequency) vary smoothly with R_{DA}

“Metavalent” bonding is not intermediate, in terms of properties, between covalent and metallic bonding

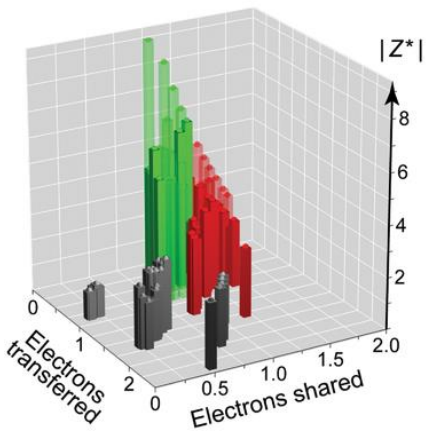
a

The 3D map suggests a blueprint to tailor the properties of a MVB material.

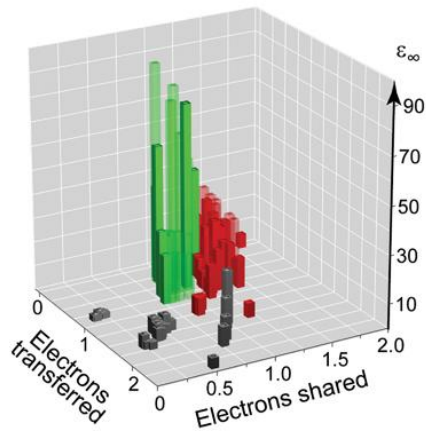
Bonding in chalcogenides was suggested to be closely interwoven with a lattice instability, leading to large Gruneisen parameters (S. Lee et al. *Nat. Comm.* **5**, 3525, 2014)

Our 3D plot (d) shows that this anomaly is uniquely linked to MVB. More specifically, to the border between MVB and metallic bonding

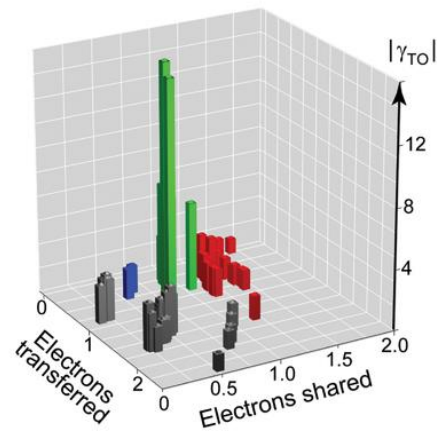
b Born effective charges (bond polarizability)



c Optical dielectric constants (optical identifier)



d Grüneisen parameters (anharmonicity identifier)

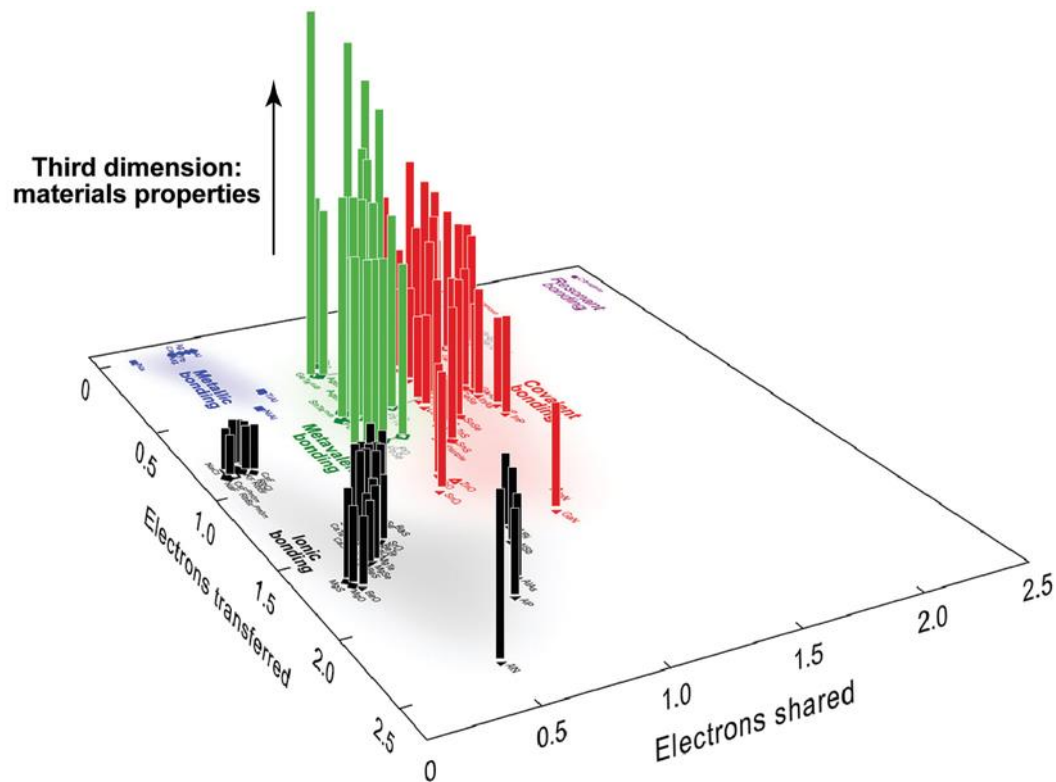


Search for thermoelectric good candidates



Move on the 2D map to MVB materials that border on metals, at around ≈ 0.8 e (0.4 e pair) shared

M. Cagnoni, D. Fehren, M. Wuttig
Adv. Mater. 2018, 30, 1801787

a

My view: No special need to introduce a new bonding type

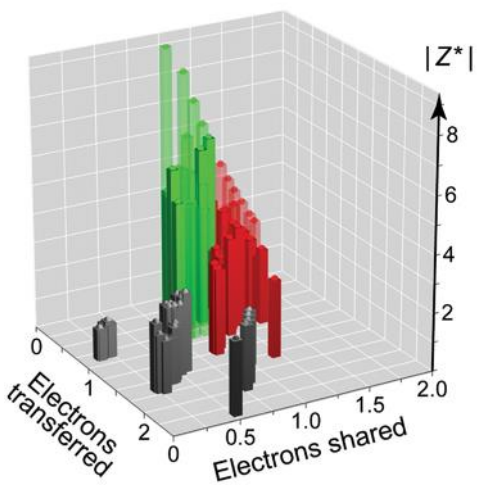
But recognize that specific *electron-deficient* covalent bonds may lead to a rapid change and anomalously large values for (three) independent response properties.

So the question again is what we mean for bonding...

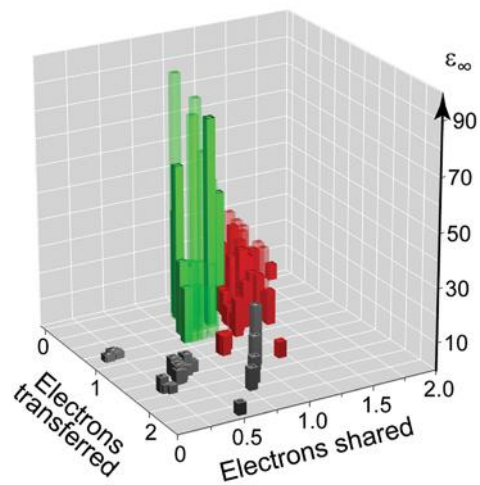
And the message is : look at bonding also upon an external stimulus...

MVB reveals itself only when a dynamic picture of bonding and of its properties is probed and exploited.

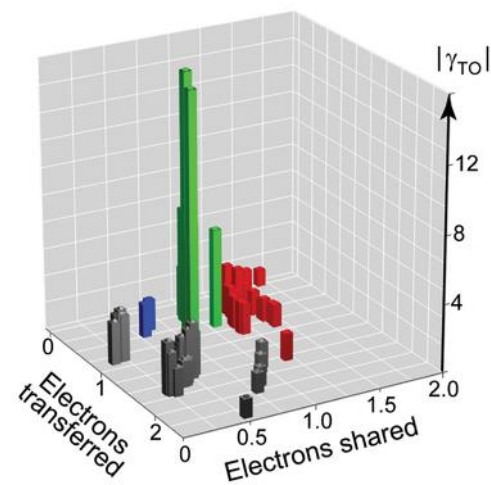
b Born effective charges (bond polarizability)



c Optical dielectric constants (optical identifier)



d Grüneisen parameters (anharmonicity identifier)



Spatially resolved characterization of electron localization and delocalization in molecules: Extending the Kohn-Resta approach

Andrey A. Astakhov | Vladimir G. Tsirelson 

A study on the electron organization of many-electron systems in the context of *linear response theory*

It highlights the *profound connection* between the variances of the local electron position and momentum operators and the optical conductivity tensor, hence between **electron localization/delocalization in position and momentum space and the observed spectroscopic and conductivity properties**.

Our study seem to emphasizes the dramatic role such connections may play in a peculiar case of bonding, namely, MVB

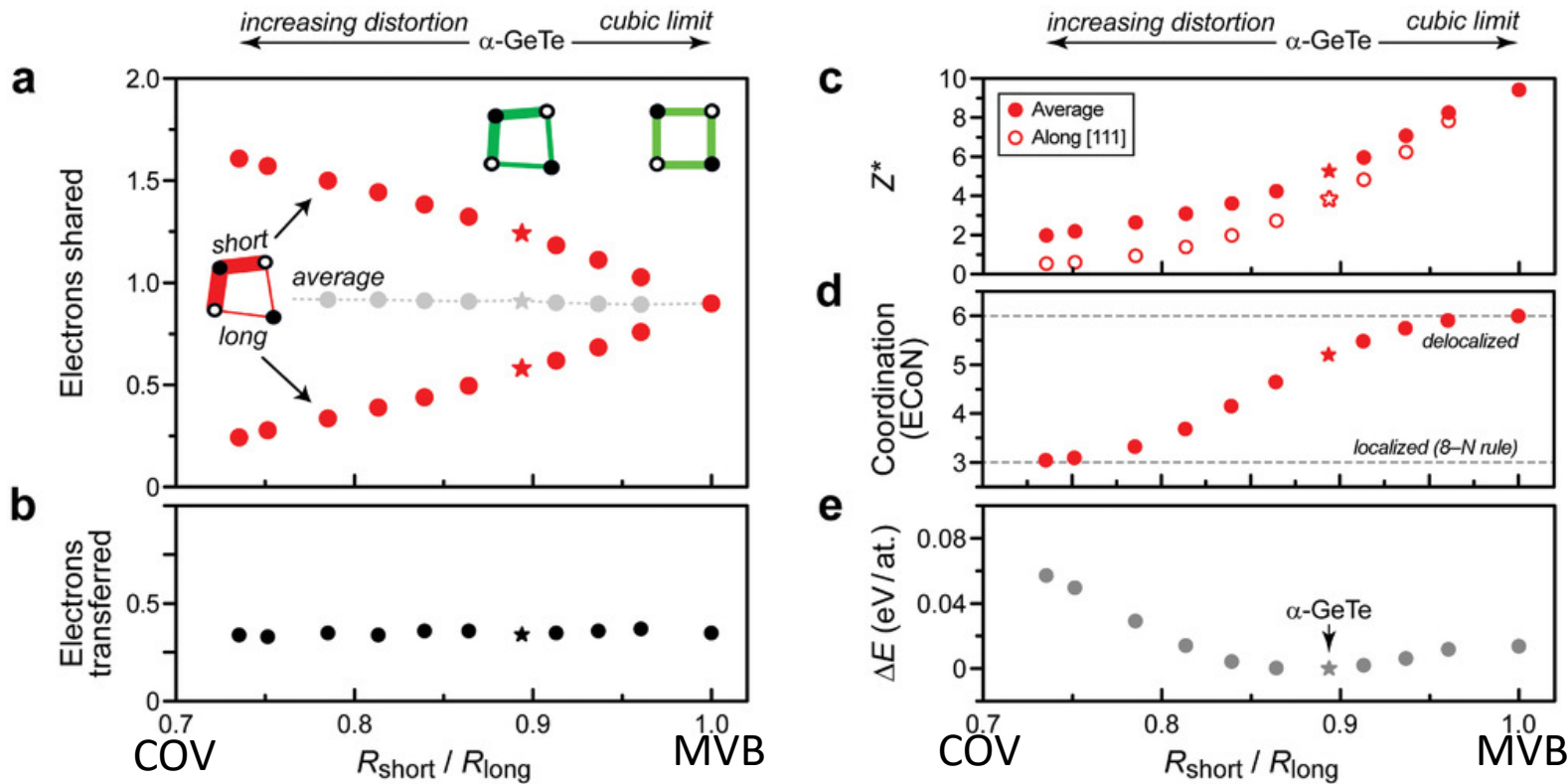
Tsirelson's study shows that electron localization and delocalization phenomena in atoms and molecules can be probed by external electric field.



The approach provides new electronic descriptors distinguishing and quantifying chemical bonds of different types.

More insights in the property changes upon Peierls distortion

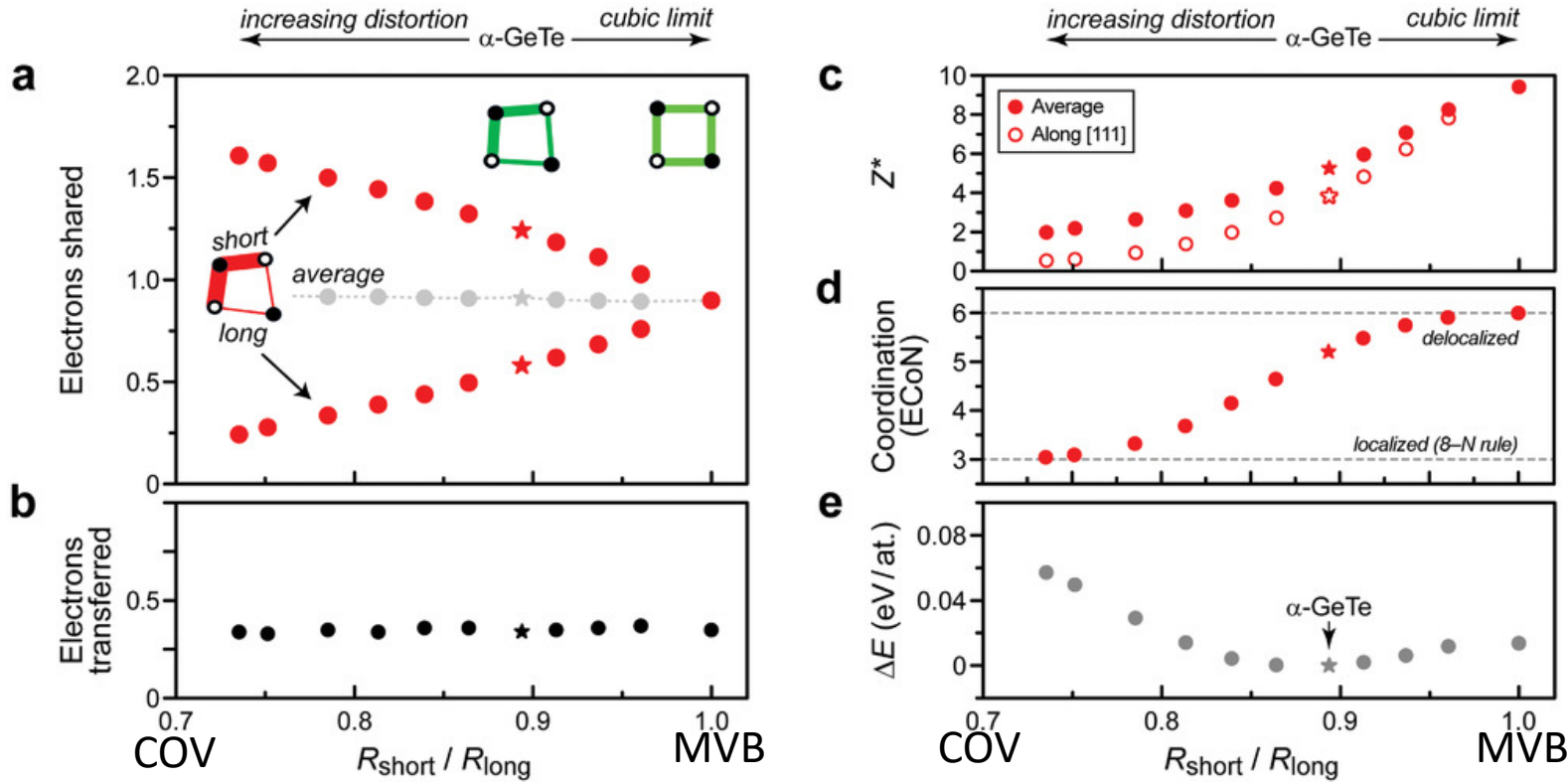
Long-standing issue in the structural study of MVB materials



Many of them crystallize in the rocksalt type with ideal O_h coordination of atoms but some, prominently GeTe, show a small distortion, 3 shorter and 3 longer bonds (referred to as a Peierls distortion, PD)

- The progressive PD induces a redistribution of electrons between short and long GeTE bonds which become (a) respectively stronger and weaker, but the *average* amount of electrons shared is almost invariant (b)
- (c) Z^* , a measurable indicator for the onset of MVB (● average; ○ projected along [111] where the effect of distortion is >)
- (d) ECon, quantifies the gradual departure from the 8-N rule
- (e) the energy cost associated with the distortion relative to GeTe (very small overall)

More insights in the property changes upon Peierls distortion



In the amorphous phases of PCMs the PD becomes extremely large and directionally blurred. Anomalous properties are lost, thus creating the electronic and optical property contrast exploited in device applications

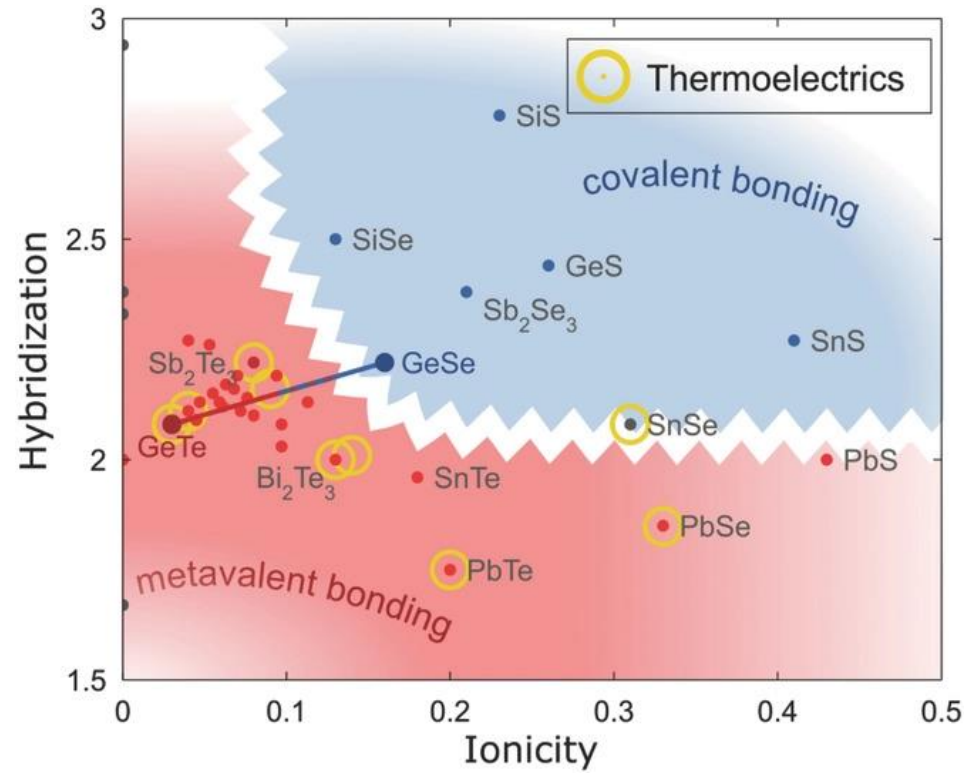
Trends in the figures suggest a route toward the design of properties and thereby of “tailored” MVB materials if one achieves control over the PD. This could be done by strain, alloying, creating defects, or nanostructuring (moving along the horizontal axis in the Figure and modifying the ECoN), and this directly allows to tune the properties.

A Quantum-Mechanical Map for Bonding and Properties in Solids

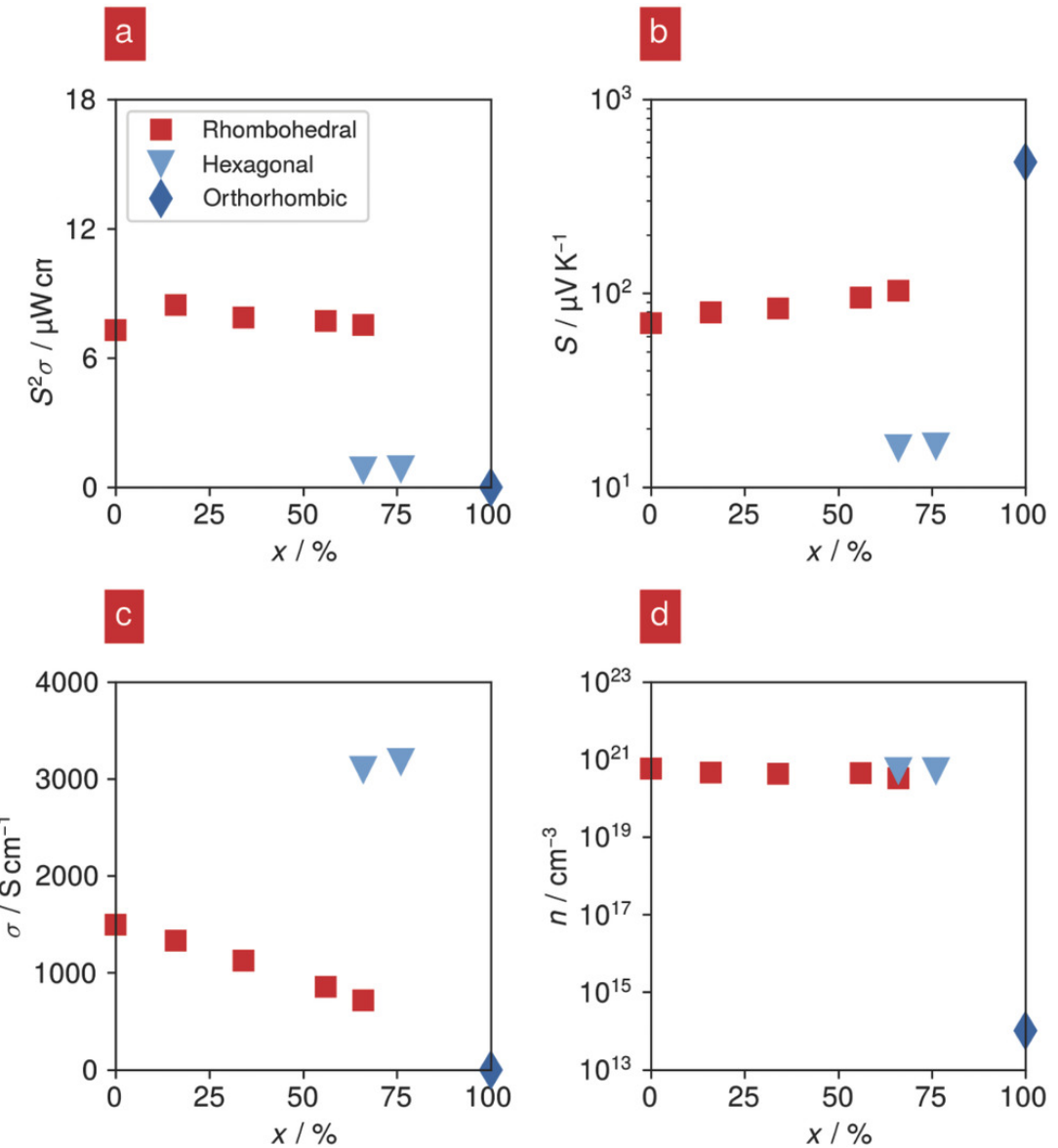
- It opens up a conceptually new avenue for materials design:
- 1) search for desired properties in a 3D space
 - 2) map this back onto the 2D plane of bonding, navigating structural and composition spaces and identifying highly promising target materials.

Thermoelectric Performance of IV–VI Compounds with Octahedral-Like Coordination: A Chemical-Bonding Perspective

Matteo Cagnoni, Daniel Führen, and Matthias Wuttig*



Moving along the GeTe_{1-x}Se_x pseudo-binary line



Electronic transport properties in crystalline GeSe_xTe_{1-x} alloys



SHARE Editors' Choice

Science 11 Jan 2019:
Vol. 363, Issue 6423, pp. 138

Article

Info & Metrics

eLetters



Science

Vol 363, Issue 6423
11 January 2019[Table of Contents](#)
[Print Table of Contents](#)
[Advertising \(PDF\)](#)
[Classified \(PDF\)](#)

FUNCTIONAL MATERIALS

A functional materials map

Brent Grocholski

Chemical bonding is important for understanding and designing new functional materials. In two papers, Wuttig *et al.* and Raty *et al.* propose a bonding type they term “metavalent.” Metavalent materials lie between covalently and metallically bound ones but are distinctly different from both. Several of the compounds that plot in the metavalent field have unique and important physical properties that make for good thermoelectric, phase-change, and other functional materials. The new bonding category potentially provides a guide for the development of interesting new materials.

Adv. Mater. 10.1002/adma.201803777, 10.1002/adma.201806280 (2018).

From Chemistry World

NEWS

Bonding rethink called for as new metavalent bond proposed



BY PHILIP BALL | 19 DECEMBER 2018

One of the most basic facts that chemistry students learn is the distinct types of chemical bond in solid-state materials: covalent, ionic and metallic, as well as curiosities such as hydrogen bonding. But if a proposal in two recent papers holds up, they will soon need to be taught about another class: the metavalent bond.

Would we have been *reported* if the term *metavalent* had not been used and a new bonding type had not been claimed?



Thanks:



Mathias Schumcher

Pavlo Golub

Volker L. Deringer

Matthias Wuttig

RWTH, Physics Dept,
Aachen, Germany

Jean-Yves Raty

Dept. of Physics of Solids Interfaces and
Nanostructures Université de Liège, Belgium

To DNRF for funding through



...and to all of you for your attention and
patience...

